On Joint Mode/Relay Selection for Covert Relay Communications

by

Yan Liu

A dissertation submitted in partial fulfillment
of the requirements for the degree of
Doctor of Philosophy
(The School of Systems Information Science)
in Future University Hakodate
September 2024

To my family

ACKNOWLEDGEMENTS

During my doctoral studies at Future University Hakodate, I would like to express my heartfelt gratitude to all the people who have supported and assisted me. Without their help, it would not have been possible to complete this thesis. First and foremost, I would like to express my deepest gratitude to my advisor, Professor Xiaohong Jiang, who has not only provided continuous guidance and support in my research but also been a mentor and friend in my life, teaching me many valuable lessons. It has been an honor to be one of his students and I have learned a great deal from him, which is very helpful for me to navigate life's challenges. I appreciate all his contributions of time and ideas that made my Ph.D. experience both productive and exciting. He has been intentional in teaching me the essential skills required to be a good researcher, as well as the admirable traits that contribute to becoming a better person. I would also like to express my heartfelt gratitude to Professor Jiang's wife, Mrs. Li, for her countless care.

Besides my advisor, I would like to thank the rest of my thesis committee: Professor Hiroshi Inamura, Professor Masaaki Wada, Professor Ayahiko Niimi and Professor Shigemi Ishida for their invaluable comments and insights, which not only helped me significantly improve this thesis but also inspired me to broaden my future research areas.

I would also like to give my sincere gratitude to Huihui Wu of Tsinghua University, China, who greatly helped me improve both the quality and clarity of my dissertation research. She showed me the way to be an excellent researcher.

My sincere thanks also go to the other members in our laboratory Guozhu Zhao, Wenhao Zhang, Xinzhe Pi, He Zhu, Zhen Jia, Jiaqing Bai, Zewei Guo, Meiyun Xie, Xin Guo, Yu Zhang and Jianing Wang for their contributions in some way to this thesis.

Last but not least, I would like to thank my parents and other family members. I especially want to thank my boyfriend for his unwavering support and encouragement. Words cannot express how grateful I am to them for all the sacrifices they have made for me.

ABSTRACT

On Joint Mode/Relay Selection for Covert Relay Communications

by

Yan Liu

Covert relay communications, which aim to hide the existence of the wireless transmission process between legitimate users via a relay, have recently been regarded as an advanced secure communication paradigm to protect sensitive and confidential information for wireless communications. It is notable that the mode (i.e., transmission mode and forwarding mode) selection and relay selection techniques for covert relay communications play a crucial role in improving performance and efficiency. However, the joint transmission/forwarding mode selection and joint mode/relay selection for efficient covert relay communications in wireless systems remain unexplored issues. We first consider covert relay communication in a single-relay system, and develop theoretical models to show the system covert throughput performance under different combinations between transmission modes of full-duplex (FD)/half-duplex (HD) and forwarding modes of amplify-and-forward (AF)/decode-and-forward (DF). Based on these models, we propose a joint transmission/forwarding mode selection scheme to achieve the maximum covert throughput (MCT) in the system. We then consider covert relay communication in a multi-relay system with AF forwarding mode. For

the scenarios when all relays operate in either fixed HD or FD transmission mode, we develop the corresponding relay selection schemes for covert relay communication in the system. For the scenario when all relays operate in the hybrid HD/FD mode where each relay can switch between HD and FD transmission modes, we propose a joint mode/relay selection scheme for covert relay communication in the system. Under either scheme, we develop related theoretical models for performance analysis, and also explore the optimal designs of transmit power, jamming power and target transmission rate for covert throughput maximization. We further consider covert relay communication in a buffer-aided multi-relay system with DF forwarding mode, where each relay is equipped with an infinite buffer. For the scenarios when all relays operate in either fixed HD or FD transmission mode, we develop the corresponding relay selection schemes for covert relay communication in the system. For the scenario when all relays operate in the hybrid HD/FD mode, we propose a joint mode/relay selection scheme for covert relay communication in the system. We also develop related theoretical models for performance analysis under each scheme, and explore the optimal designs of transmit power, jamming power and target transmission rate for covert throughput maximization. Extensive numerical results are provided in this thesis to illustrate the impacts of joint transmission/forwarding mode selection and joint mode/relay selection on covert relay communications in different wireless relay systems. It is expected that the work in this dissertation can shed light on performance enhancement in future covert wireless communications.

TABLE OF CONTENTS

LIST OF FIGURES

Figure

LIST OF TABLES

Table

CHAPTER I

Introduction

In this chapter, we first introduce the background of wireless communication systems. Then, we provide a systematic introduction and analysis of covert relay communications. We further present the objectives and main contributions of this thesis. Finally, we give the outline and main notations of this thesis.

1.1 Background

1.1.1 Wireless Communication Systems

Wireless communication systems refer to communication systems that use radio waves and other wireless signals for information transmission. These systems do not require wired connections and support various functions such as mobile communication, remote control, and sensor networks. For example, in smart homes, wireless communication systems realize remote control and intelligent management by connecting smart door locks, cameras, and various smart appliances [1]. In telemedicine, wireless communication systems are also pivotal for the real-time transmission of health data from wearable devices, ensuring that doctors are able to provide timely medical advice and emergency treatment [2]. In addition, the system can also be used in sensor networks to transmit and process various sensor data through wire-

less communication technology to meet the needs of environmental monitoring and security monitoring. In conclusion, wireless communication systems, as the foundational technology for modern communication, have a wide range of applications and significant potential for future development.

1.1.2 Security in Wireless Communication Systems

As wireless communication systems become integral to modern infrastructure, their security has become a critical concern [3]. The openness of wireless communications allows any compatible device to receive signals, which makes it prone to various security threats such as unauthorized access, eavesdropping, and data leakage, posing a serious challenge to the security of wireless communication systems [4]. In 2017, Belgian researcher Mathy Vanhoef exposed Key Reinstallation AttaCKs (KRACK), which exploited weaknesses in the Wi-Fi Protected Access 2 (WPA2) protocol to decrypt network traffic and steal sensitive information. In 2020, researchers at ESET discovered Kr00k, a vulnerability affecting hundreds of millions of devices equipped with Broadcom and Cypress Wi-Fi chips, facilitating the unauthorized decryption of wireless network traffic and potentially allowing access to sensitive data during transmission. GlobalData's report indicated that even network operators with advanced fifth-generation (5G) technologies face security risks. For example, the American telecommunications operator AT&T notified its customers of a data breach in 2023, where attackers accessed the personal information of about 9 million users. Furthermore, a survey conducted in 2023 showed that the number of active mobile broadband users had reached 7 billion globally. The activities of these users span a wide range of critical infrastructure areas, including healthcare, transportation, and home automation, highlighting the widespread application of wireless communication systems. As a result, the demand for security in wireless communication system is becoming increasingly stringent.

1.1.3 Security Methods in Wireless Communication Systems

Many effective methods have been proposed to solve security problems in wireless communication systems. These methods aim to develop mechanisms that guarantee only the intended recipients know the content of the transmitted information. In this context, cryptographic methods utilize complex encryption algorithms to transform the message into a ciphertext that ensures the recipients who possess the corresponding keys can decode it, thereby effectively preventing unintended recipients from accessing the content of the message [5, 6]. From another perspective, physical layer security methods exploit the inherent properties and uncertainties of wireless channels (e.g., thermal noise and signal interference) to enhance the security and privacy of communications [7–9]. It is worth noting that the available security methods, such as cryptography and physical-layer security (PLS) methods, mainly protect the transmitted content from eavesdropping. Covert communications, which aim to hide the existence of the wireless transmission process between legitimate users (i.e., guaranteeing a low probability of being detected by the warden), are emerging as an advanced secure communication technique for wireless communications [10, 11]. Covert communications offer an enhanced level of security for various critical application scenarios, including the Internet-of-Things (IoT) [12, 13], device-to-device (D2D) [14–16], unmanned aerial vehicle (UAV) communications [17–19], etc.

1.2 Covert Relay Communications

1.2.1 Why Covert Relay Communications

Covert relay communications, also known as relay-assisted covert communications, involve covert communications in a relay system where a source sends covert messages to a destination with the assistance of relay(s), subject to the detection of detector(s). Covert relay communications offer several advantages in improving the performance

of wireless systems. First, relay nodes can effectively expand the coverage area to address challenges such as long-distance communication and signal attenuation, thus providing a new way for covert communications with low transmit power [18, 20]. Second, the diverse designs of the relays can enrich the covert strategies, which not only assists the system in achieving covert communications but also enhances the overall covert performance of the system [21, 22]. Third, the locations and number of relays can be dynamically controlled, which enables a flexible relay system to be constructed for covert communications based on specific communication conditions and requirements, and ensures that the systems can adapt to diverse communication environments and scenarios [23, 24]. In essence, covert relay communications play a key role in enhancing both the covertness and reliability of communications and provide strong support for effective covert communications across various system settings.

1.2.2 Challenges for Covert Relay Communications

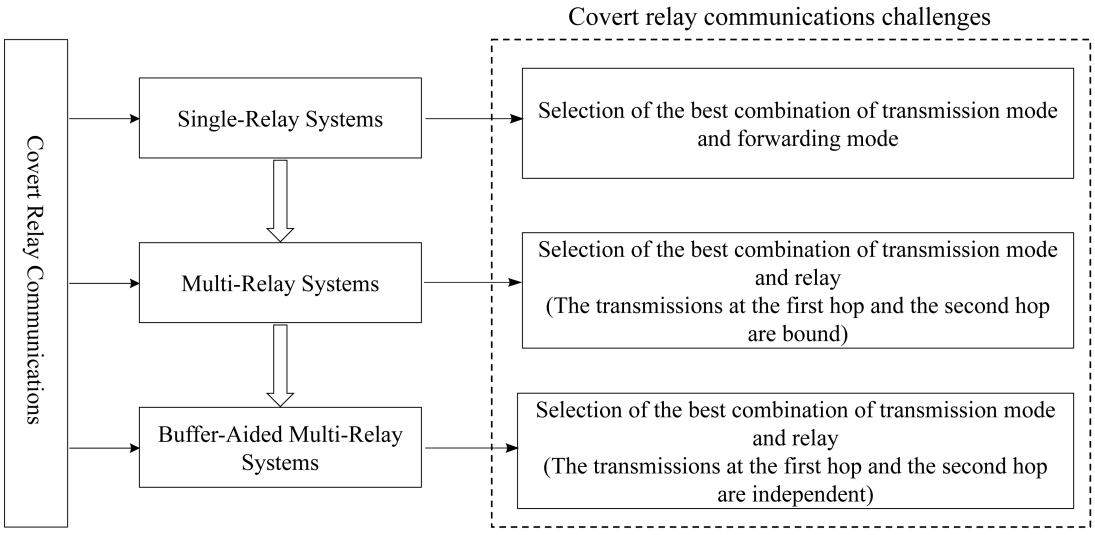

Figure 1.1: Challenges for covert relay communications.

This thesis investigates covert relay communications in single-relay systems, multi-relay systems and buffer-aided multi-relay systems, as illustrated in Fig. 1.1. In single-

relay systems, existing research examines aspects such as transmit power control [22, 25, 26], untrusted relay [27–29], and varying channel state information [29, 30]. Additionally, we have found that the transmission mode and forwarding mode of the relay also impact the effectiveness of covert relay communications. It is worth noting that many studies are conducted under a fixed combination between transmission modes of full-duplex (FD)/half-duplex (HD) and forwarding modes of amplify-and-forward (AF)/decode-and-forward (DF), and how to determine the optimal mode combination to maximize covert performance is a critical unexplored issue. Therefore, the relay needs to be able to flexibly adjust its transmission and forwarding modes in response to changes in the communication environment. In multi-relay systems, the relay selection technique for covert relay communication is significant [13, 31–33]. Relay selection usually involves the selection of one proper relay to assist the covert communication between a source and a destination according to the current link conditions. When choosing a relay for communication, a balance between covertness and communication performance (i.e., overemphasizing covertness can reduce communication efficiency, while ignoring covertness may increase the risk of detection by an adversary) should be carefully considered. This selection process often involves complex optimization problems to maximize covert throughput. We find that existing research has concentrated separately on mode selection and relay selection for covert relay communications. Therefore, jointly considering transmission modes and relay selection to identify the optimal relay for maximizing covert relay communication performance remains an unresolved issue. In buffer-aided multi-relay systems, relays equipped with buffers not only add considerations of data storage, transmission time, and buffer overflow but also increase the complexity of relay selection and scheduling strategies. Therefore, the joint transmission mode and relay selection to maximize the throughput of covert relay communication in such systems emerges as a critical issue.

1.3 Objectives and Main Contributions

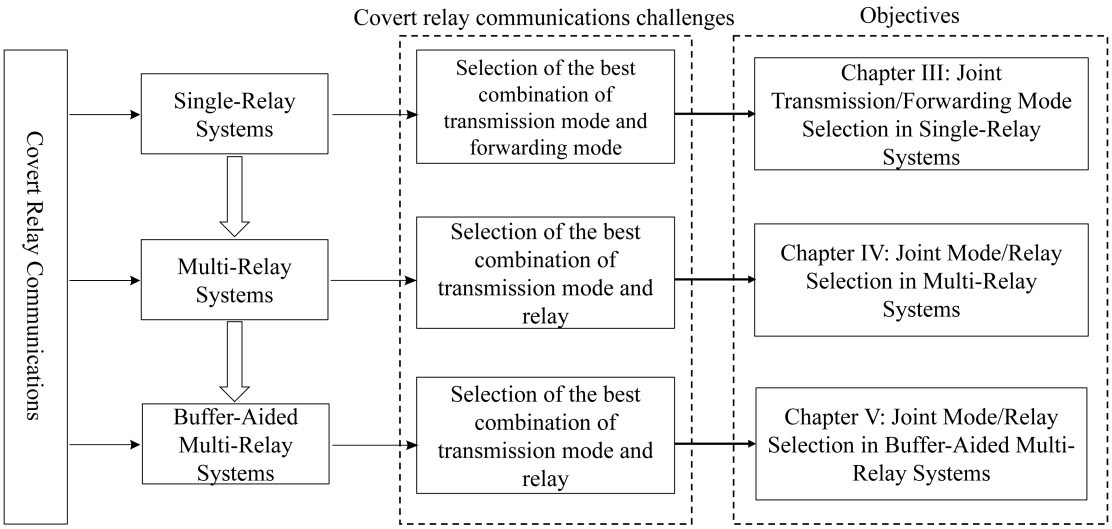

Figure 1.2: Objectives and main contributions of this thesis.

This thesis focuses on the fundamental research in wireless communication security, which is of great importance for the development of information security and privacy. As shown in Fig. 1.2, we establish various selection schemes for covert communication to overcome the challenges posed by the three relay systems. Towards this end, we first consider covert relay communication in a single-relay system, and develop theoretical models to show the covert throughput performance under different combinations between transmission modes and forwarding modes. Based on these models, we propose a joint transmission/forwarding mode selection scheme to achieve the maximum covert throughput in the system. We then consider covert relay communication in a multi-relay system with AF forwarding mode. For the scenarios when all relays operate in either HD, FD, or hybrid HD/FD transmission mode, we develop the corresponding relay selection schemes for covert relay communication in the system. Under either scheme, we develop related theoretical models for performance analysis, and also explore the optimal designs of transmit power, jamming power and target transmission rate for covert throughput maximization. We further

consider covert relay communication in a buffer-aided multi-relay system with DF forwarding mode, where each relay is equipped with an infinite buffer. For the scenarios when all relays operate in either HD, FD, or hybrid HD/FD transmission mode, we develop the corresponding relay selection schemes for covert relay communication in the system. We also develop related theoretical models for performance analysis under each scheme, and explore the optimal designs of transmit power, jamming power and target transmission rate for covert throughput maximization. The main works and contributions of this thesis are summarized in the following subsections.

1.3.1 Joint Transmission/Forwarding Mode Selection in Single-Relay Systems

Recent research has focused on covert relay communications in single-relay systems [22, 27, 28, 30, 34–36]. These works enhance our understanding of covert relay communications, but they usually focus on a specified combination of transmission mode and forwarding mode. It is important to note that the performance of covert relay communications can be flexibly controlled through a proper selection of transmission modes (i.e., FD [37] or HD [38]) and forwarding modes (i.e., AF [39] or DF [40]).

It is notable, however, that each mode in transmission mode and forwarding mode owns its distinctive advantages and disadvantages. Regarding transmission modes, the FD mode allows simultaneous receiving and forwarding operations to improve the spectrum efficiency but suffers from the self-interference problem, while the HD mode is free of self-interference but leads to a reduced covert throughput. As for forwarding mode, the simple AF amplifies both the signal and noise before forwarding so it results in a degraded signal-to-interference-plus-noise-ratio (SINR) at the receiver, while the complex DF can perform signal decoding to improve signal forwarding performance but requires high computation and hardware complexity. However, by

now it still lacks a solid performance comparison among four possible combinations of transmission mode and forwarding mode. Also, for a given relay system, how to choose a proper combination of transmission mode and forwarding mode to achieve the optimal covert relay communication performance remains an unexplored issue. To address these issues, this work develops solid theoretical models to facilitate the performance comparison and joint mode selection among FD/HD and AF/DF. The main contributions of this work are summarized as follows.

- We consider covert relay communication in a single-relay system, where the relay can flexibly select between the transmission modes of FD and HD as well as between the forwarding modes of AF and DF. Under each combination of transmission mode and forwarding mode, we first provide the theoretical modeling of three fundamental metrics to depict the performance of the covert relay communication in the system, including detection error probability (DEP), i.e., the probability that the warden cannot detect the transmission, transmission outage probability (TOP), i.e., the probability that messages cannot be transmitted reliably, and covert throughput (CT), i.e., the average throughput of the transmitted covert messages.

- Under each combination of transmission modes and forwarding modes (i.e., FD-AF, FD-DF, HD-AF, and HD-DF), we further provide optimization problem formulations to identify the optimal designs of the target transmission rate and the relay transmit power for covert throughput maximization, subjecting to the constraints of DEP and upper bound on relay transmit power.

- We provide extensive simulations and numerical results to illustrate the performance comparison among different transmission modes and forwarding modes, as well as how to jointly select a proper combination of transmission mode and forwarding mode to achieve the maximum covert throughput (MCT) in

the single-relay system with given settings of the target transmission rate, the self-interference coefficient of FD, constraints of DEP, and the upper bound on relay transmit power.

1.3.2 Joint Mode/Relay Selection in Multi-Relay Systems

Extensive works are devoted to the study of covert relay communications in wireless relay systems [13, 22, 27–34, 36, 41–43], which demonstrates the great applications of wireless relay systems in supporting covert communications. The systems concerned in these works can be classified into the ones with single relay and the ones with multiple relays. Compared to the single-relay systems, multi-relay systems have drawn significant attention due to their potentials in improving the covertness and throughput performance through flexible relay selection.

The available works on multi-relay systems mainly focus on designing relay selection schemes for DF relay systems under fixed HD or FD transmission mode. Notice that the work in [34] on single-relay systems indicates that a flexible transmission mode selection between HD or FD can bring benefits in improving the covert relay communication performance. Also, AF, which forwards the received signal without hard decoding, serves as another crucial and widely used forwarding mode [44]. However, how to conduct a joint transmission mode and relay selection for efficient covert relay communication in an AF multi-relay system remains an unexplored issue. Thus, this work is devoted to the study of covert relay communication with mode and relay selection in an AF relay system consisting of one source, multiple relays, one destination, one friendly jammer, and one warden, where each relay can switch between the HD and FD transmission modes. The main contributions of this work are summarized as follows.

- We first consider the two special scenarios where all relays in the system adopt the fixed HD or the fixed FD transmission mode. Under either scenario, we de-

velop the corresponding relay selection scheme, establish the theoretical models for the DEP and TOP, and also explore the evaluation of the MCT.

- We then consider the general scenario where each relay can switch between the HD and FD transmission modes, and develop the corresponding scheme for the joint selections of transmission mode and relay. The related issues of theoretical performance modeling and MCT evaluation under the joint selection scheme are addressed as well.

- Finally, we provide extensive numerical results to illustrate the achievable covert communication performance in an AF multi-relay system with only relay selection and how the joint transmission mode and relay selection can further lead to a performance enhancement in such a system.

1.3.3 Joint Mode/Relay Selection in Buffer-Aided Multi-Relay Systems

For multi-relay systems, relay selection has been introduced as an efficient cooperative technique. Specifically, as described in subsection 1.3.2, the transmissions at the first hop and the second hop are bound together, which may not allow for the simultaneous exploitation of the best available source-relay (S-R) channel and the best available relay-destination (R-D) channel, since the selected relay does not necessarily experience the best S-R channel and the best R-D channel at the same time. In order to overcome the limitations, we propose employing buffer-aided relays to achieve covert relay communication in a multi-relay system. If the relays are equipped with buffers, the relays with the best S-R channel and the best R-D channel can be selected for reception and transmission, respectively. This is because the selected relay can store the received signal in its buffer and retransmit it at a later time when it is selected for transmission. In addition, the relay selected for transmission may transmit the first signal in its buffer queue that it has previously received from a

source. This work is devoted to the study of covert relay communication with mode and relay selection in a buffer-aided multi-relay system with DF forwarding mode, which is consisted of one source, multiple relays, one destination, one friendly jammer, and one warden, where each relay can switch between the HD and FD transmission modes. The main contributions of this work are summarized as follows.

- We first consider the two special scenarios where all relays in the system adopt the fixed HD or the fixed FD transmission modes. Under either scenario, we develop the corresponding relay selection scheme, establish the theoretical models for the DEP and TOP, and also explore the optimal designs of transmit power, jamming power and target transmission rate for covert throughput maximization, subjecting to the constraints of covertness requirement, transmit power and jamming power.

- We then consider the general scenario where each relay can switch between the HD and FD transmission modes, and propose a joint mode/relay selection scheme for covert relay communication in the system. The related issues of theoretical performance modeling and MCT evaluation under the joint selection scheme are addressed as well.

- Finally, we provide extensive numerical results to illustrate the achievable covert communication performance in a DF multi-relay system with only relay selection and how the joint transmission mode and relay selection can further lead to a performance enhancement in such a system.

1.4 Thesis Outline

The remainder of this thesis is outlined as follows. Chapter II introduces the related works of this thesis. In Chapter III, we introduce our work regarding joint

transmission/forwarding mode selection in a single-relay system. In Chapter IV we present the work on joint mode/relay selection in a multi-relay system and in Chapter V we focus on the work of joint mode/relay selection in a buffer-aided multi-relay system. Finally, we conclude this thesis in Chapter VI.

1.5 Notations

The main notations of this thesis are summarized in Table 1.1.

Table 1.1: Main notations

Symbol	Definition
S	Source node
D	Destination node
W	Warden
K	Number of relays
R_k	The k-th relay
R^*	The selected relay
n	Number of channel uses
τ	Detection threshold
$\|h_{AB}\|^2$	Coefficient of the channel from A to B
p_{FA}	False alarm probability
p_{MD}	Missed detection probability
ξ	Detection error probability
ϵ	Covertness requirement
$\mathbb{P}(\cdot)$	Probability operator
$\mathbb{E}(\cdot)$	Expectation operator
γ	Signal to interference plus noise ratio (SINR)
p_{to}	Transmission outage probability

r_t	Target transmission rate
C	Channel capacity
T^*	Maximum covert throughput
σ^2	Power of noise
χ^2_{2n}	Chi-squared random variable with $2n$ degrees of freedom
$K_{-1}(\cdot)$	Modified Bessel function of the second kind with the -1-th order
$f(\cdot)$	Probability density function (PDF)
P	Transmit power

CHAPTER II

Related Works

This chapter introduces the existing works related to our study, including works on covert communications in one-hop systems and covert relay communications in two-hop systems.

2.1 Covert Communications in One-Hop Systems

By now, extensive pioneer works have been devoted to the study of covert communications. For the one-hop systems, the authors in [10] demonstrate that a square root law for covert communications on the additive white Gaussian noise (AWGN) channel, which states that no more than $O(\sqrt{n})$ bits information can be transmitted reliably and covertly in n channel uses. Based on this work, the square root law has been further extended to binary symmetric channels (BSCs) [45], discrete memoryless channels (DMCs) [46] and multiple access channels (MACs) [47]. The authors in [11, 48–66] prove that a positive rate in one-hop covert communications can be achieved by considering the uncertainty of prior knowledge at the warden, such as the uncertain time slot of communications [48, 49], the imperfect channel state information (CSI) [50–54], the background noise uncertainty [55–57], the optimized transmit power of transmitter [58, 59], and the random transmit power of jamming signals from a full-duplex receiver [60–62] or from external jammers [11, 63–66]. Fur-

thermore, the authors in [67–69] focus on an attractive communication scenario with two kinds of hostile attacks (i.e., overhearing the broadcast data and detecting the presence of data communication) and explore the communication performance under this scenario by considering both the secrecy and covertness requirements.

2.2 Covert Relay Communications in Two-Hop Systems

Extensive works are devoted to the study of covert relay communications in two-hop wireless systems [13, 22, 27–34, 36, 41–43], highlighting the significant applications of relay systems in supporting covert communications. The systems concerned in these works can be classified into the ones with a single relay and the ones with multiple relays.

2.2.1 Covert Relay Communications with Single Relay

The works in [22, 27–30, 34, 36, 41–43] focus on covert relay communications in single-relay systems. In [36], an adaptive mechanism for covert relay communication is proposed, where the relay can flexibly switch among different covert strategies based on the priori knowledge of legitimate users and warden. By exploiting the benefits of the multi-antenna technique, different beamforming schemes for covert relay communication are suggested in [22] and [41]. Specially, in [41], both the direct link between the transmitter and the receiver as well as the relay links from the transmitter to relay and from the relay to the receiver are jointly considered in the design of the covert relay communication scheme. The authors in [30] and [34] explore the channel uncertainty or artificial noise (AN) for covert communications with the help of a trusted relay. The works in [27, 29, 42] deal with the impact of power allocation, energy harvesting techniques, and outdated CSI on the achievable covert performance in a wireless greedy relay system, where the relay not only helps to forward the message of the transmitter but also covertly transmits its message to

the receiver. Furthermore, how to implement the covert relay communication in a two-hop untrusted relay system is studied in [28, 43], where the relay tries to eavesdrop on the contents of the transmission and the warden attempts to detect the existence of transmission. The authors in [28] propose a transmission and jamming power allocation strategy to satisfy both covertness and security requirements in an untrusted relay system, while the authors in [43] derived minimum DEP and average covert/secrecy rate in an untrusted relay-assisted D2D system under underlay and overlay modes, respectively.

2.2.2 Covert Relay Communications with Multiple Relays

The works [13, 31–33] focus on covert relay communications in multi-relay systems. The work in [31] provides a theoretical analysis of DEP and the average covert rate, demonstrating that the diversity gain for covert relay communication can be improved in a multi-relay system through proper relay selection. In [13], two relay selection schemes (i.e., random selection and superior-link selection schemes) are proposed for covert relay communication in a multi-relay system, and it is demonstrated that the superior-link selection scheme always outperforms the random selection scheme in terms of covert capacity. The works in [32] and [33] deal with the joint designs of jamming and relay selection for covert relay communication in multi-relay systems. In [32], the relay node with the largest channel gain to the receiver is selected for relaying the covert message while the relay node with the minimal channel gain to the receiver is selected as a jammer to confuse the warden, and the transmit power of the selected relay node is further optimized to improve the covert rate in the system. The work in [33] suggests a relay selection scheme and a jammer selection scheme, where the relay node with the largest channel gain to the receiver is selected for relaying the covert message, but all relay nodes with the channel gain to the receiver smaller than a given threshold are selected as jammers. The joint optimal transmit

power designs of both the transmitter and the relay are also explored in [33] for covert rate maximization.

CHAPTER III

Joint Transmission/Forwarding Mode Selection in Single-Relay Systems

This chapter focuses on covert relay communication in a single-relay system consisting of a source, a relay, a destination and a warden, where the relay can flexibly select between the transmission modes of full-duplex (FD)/half-duplex (HD) as well as between the forwarding modes of amplify-and-forward (AF)/decode-and-forward (DF). For a given combination of transmission mode and forwarding mode, we first develop theoretical models for the detection error probability (DEP) and transmission outage probability (TOP) and covert throughput (CT), and also explore the optimal designs of the relay transmit power and the target transmission rate for CT maximization under the mode combination, subjecting to the constraints of covertness requirement and the upper bound on relay transmit power. Based on these models, we further propose a joint transmission/forwarding mode selection scheme to achieve the maximal CT among all mode combinations in the system. Finally, we provide extensive numerical results to illustrate and compare the performance among different combinations of transmission modes and forwarding modes, and how to jointly select a proper combination of transmission mode and forwarding mode to achieve the maximal CT in the system.

3.1 System Model and Performance Metrics

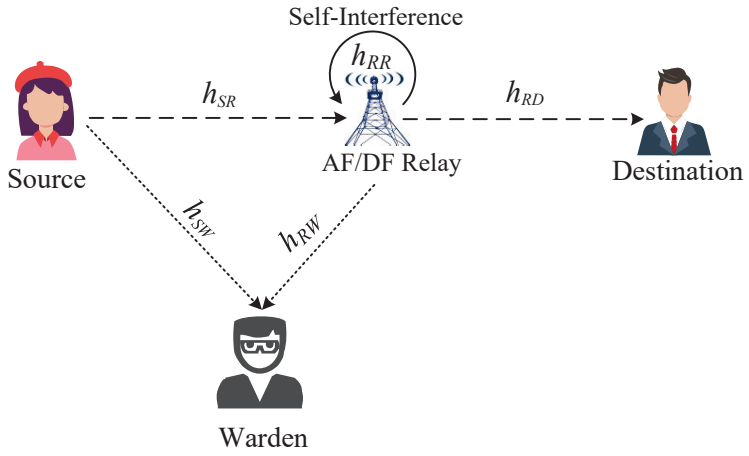

(a) FD relay in one time slot with self-interference

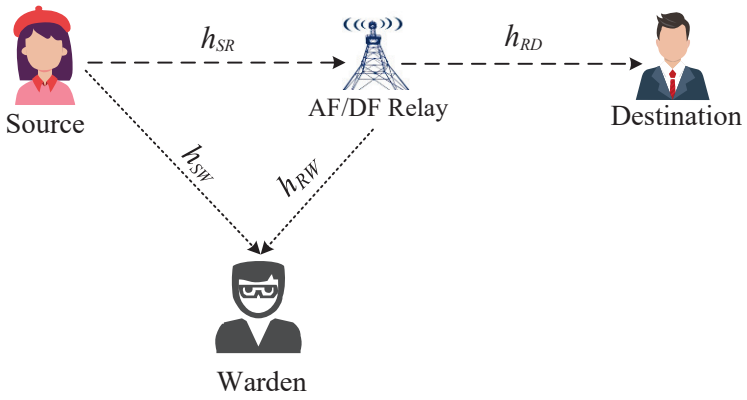

(b) HD relay in two time slots without self-interference

Figure 3.1: Covert relay communication with a relay that operates in FD/HD transmission mode and AF/DF forwarding mode.

3.1.1 Communication Scenario and Assumptions

As depicted in Fig. 3.1, we consider a two-hop single-relay system consisting of a source S, a relay R, a destination D, and a warden W. S desires to transmit covert messages to D with the aid of R in the presence of W, who silently observes the communication in all time slots and tries to detect whether S has transmitted messages to D or not. When S does not transmit messages, R acts as a jammer J

and sends Gaussian jamming signals to confuse W's detection. To further avoid W's detection, we follow the common assumption that S uses a secret Gaussian codebook pre-shared with D, which is unknown to W. We assume that each of S, D and W has a single antenna, while R is equipped with two independent antennas for reception and transmission, respectively. Thus, S, D and W only operate in the HD mode, while R can operate in either FD or HD mode. In FD mode, R receives and forwards information simultaneously on the same frequency, which causes self-interference to the communication. In HD mode, R receives and then forwards information to D without self-interference, but the transmission requires two time slots.

We assume all links follow the quasi-static Rayleigh fading channel model, where the channel coefficients remain constant in one slot and change independently and randomly from one slot to another. We use h_{AB} to denote the channel from node A to B, which is a zero-mean circularly symmetric complex Gaussian random variable with variance $E[|h_{AB}|^2] = \lambda_{AB}$. Here, $AB \in \{SR, SW, RD, RR, RW\}$ and $\lambda = 1$. Thus, the corresponding channel gain is denoted as $|h_{AB}|^2$. Following the common assumptions in [63, 68], we assume that S knows the statistical characterization of h_{SR}, the relay knows the statistical characterizations of both h_{RD} and h_{RR}, and W knows the statistical characterizations of both h_{SW} and h_{RW}.

3.1.2 Transmission Process

3.1.2.1 FD-AF Scenario

Under the FD-AF scenario, S randomly selects one time slot to send messages to R, and R amplifies and forwards the received messages to D simultaneously. Let $x_S(i)$ $(i = 1, 2, \ldots, n)$ denote the i-th symbol transmitted from S to R. Here, $x_S(i)$ satisfies the unit power constraint of $E[|x_S(i)|^2] = 1$ and $E[\cdot]$ denotes the expected value of a random variable. Thus, under the FD-AF scenario, the received signal

$y_R(i)$ for the i-th channel use at R is given by

$$y_R(i) = \sqrt{P_S} h_{SR} x_S(i) + \sqrt{P_R} h_{RR} x_R(i) + n_R(i), \tag{3.1}$$

where P_S and P_R are the transmit powers of S and R, respectively, and P_R is subject to the maximum transmit power constraint of $P_R^{\max}$. $x_R(i)$ is the i-th symbol with the unit power transmitted from R, i.e., $E[|x_R(i)|^2] = 1$. $n_R(i)$ is the AWGN at R with zero mean and variance σ_R^2, i.e., $n_R(i) \sim \mathcal{CN}(0, \sigma_R^2)$.

To normalize the transmit power of R in the AF mode, R first amplifies its received signal by an amplification factor $G_{FD} > 0$ and then forwards it to D. Thus, the signal transmitted from R is given by

$$x_R(i) = G_{FD} y_R(i). \tag{3.2}$$

Notice that the received power at R is given by

$$E[|y_R(i)|^2] = P_S |h_{SR}|^2 + P_R |h_{RR}|^2 + \sigma_R^2. \tag{3.3}$$

Then the amplification factor G_{FD} is determined as

$$G_{FD} = \sqrt{\frac{1}{P_S |h_{SR}|^2 + P_R |h_{RR}|^2 + \sigma_R^2}}. \tag{3.4}$$

Finally, the signal $y_D(i)$ received at D in the i-th channel use is given by

$$y_D(i) = \sqrt{P_R} h_{RD} x_R(i) + n_D(i), \tag{3.5}$$

where $n_D(i)$ is the AWGN at D with zero mean and variance σ_D^2, i.e., $n_D(i) \sim \mathcal{CN}(0, \sigma_D^2)$.

3.1.2.2 FD-DF Scenario

Under the FD-DF scenario, S randomly selects one time slot to send messages to R, and R concurrently decodes the received signal $y_R(i)$ and forwards the re-encoded signal $x_R(i)$ on the same frequency. In this case, the expression of the received signal at the relay is the same as the formula in (3.1).

With the DF forwarding mode, R decodes and regenerates the original signal transmitted from S. Then the signal from R can be expressed as

$$x_R(i) = \sqrt{\frac{1}{P_S}} t_R(i), \tag{3.6}$$

where $t_R(i) = \sqrt{P_S} x_S(i)$ represents the total signal received from S.

The expression of the received signal at D in the i-th channel use is the same as the formula in (3.5).

3.1.2.3 HD-AF Scenario

Under the HD-AF scenario, the communication between S and D is spread over two orthogonal time slots to eliminate the self-interference caused in the FD mode. S transmits signals to R in the first time slot, and then R forwards a linearly amplified version of the received signals to D in the next time slot. As such, the received signal $y_R^{(1)}(i)$ for the i-th channel use at R is given by

$$y_R^{(1)}(i) = \sqrt{P_S} h_{SR} x_S(i) + n_R(i). \tag{3.7}$$

In the second time slot, the received signal at D under the HD-AF scenario is given by

$$y_D^{(2)}(i) = \sqrt{P_R} h_{RD} x_R(i) + n_D(i), \tag{3.8}$$

where $x_R(i)$ in HD mode is similar to the notion $x_R(i)$ in FD mode. Thus, the

transmit signal of the relay is given by

$$x_R(i) = G_{HD} y_R^{(1)}(i), \tag{3.9}$$

where the amplification factor G_{HD} is determined as

$$G_{HD} = \sqrt{\frac{1}{P_S |h_{SR}|^2 + \sigma_R^2}}. \tag{3.10}$$

3.1.2.4 HD-DF Scenario

Under the HD-DF scenario, S transmits its signals to R by n channel uses in the first time slot, and then R decodes the received signal $y_R^{(1)}(i)$ and forwards the re-encoded signal $x_R(i)$ in the next time slot. Under this scenario, the expressions of the received signals at R and D in the i-th channel use are the same as the formulae in (3.7) and (3.8), respectively.

According to the transmit signal at R under the FD-DF and HD-AF scenarios in (3.6) and (3.9), the transmit signal at R under the HD-DF scenario is

$$x_R(i) = \sqrt{\frac{1}{P_S}} t_R(i), \tag{3.11}$$

where $t_R(i) = \sqrt{P_S} x_S(i)$ is the total signal received from S in the first time slot.

3.1.3 Detection at Warden

Regarding the detection of covert communication, we apply the common assumption that W adopts a radiometer (i.e., power detector) as its detector [11, 61]. W faces a binary hypothesis testing problem where it needs to make a judgment on whether S or R has transmitted data to D or not. There are two hypotheses in hypothesis testing: the null hypothesis $\mathcal{H}_0$ means that S or R does not conduct the transmission, while the alternative hypothesis $\mathcal{H}_1$ denotes that they conduct the transmission.

3.1.3.1 Warden's Detection in FD Mode

In the FD-AF relay system, when W receives only the jamming signal $x_J(i)\,(i = 1, 2, \ldots, n)$ from R with $E[|x_J(i)|^2] = 1$, $\mathcal{H}_0$ is true. When W receives both the signal from S and the amplified signal from R in one time slot, $\mathcal{H}_1$ is true. Thus, we have

$$y_W(i) = \begin{cases} \sqrt{P_R} h_{RW} x_J(i) + n_W(i), & \mathcal{H}_0, \\ \sqrt{P_S} h_{SW} x_S(i) + \sqrt{P_R} h_{RW} x_R(i) + n_W(i), & \mathcal{H}_1. \end{cases} \tag{3.12}$$

where $n_W(i)$ is the AWGN at W with zero mean and variance σ_W^2, i.e., $n_W(i) \sim \mathcal{CN}(0, \sigma_W^2)$.

Remark 1 *Notice that the detection model (3.12) of the two-hop FD relaying system is consistent with the one of a single-hop Rayleigh fading system with a jammer [62, 65]. However, compared with the single-hop system, the two-hop relay system concerned in this work leads to a different definition and thus a different evaluation method for the DEP and TOP, as well as a different formulation for the CT optimization problem (see Subsections 3.1.4 and 3.2.1.1).*

3.1.3.2 Warden's Detection in HD Mode

In the HD-AF relay system, the transmission of one symbol is spread over two orthogonal time slots. In the first time slot, when R sends only the jamming signal with power P_R to confuse W, $\mathcal{H}_0$ is true. When W receives the signal from S, $\mathcal{H}_1$ is true. Thus, in the first time slot, we have

$$y_W^{(1)}(i) = \begin{cases} \sqrt{P_R} h_{RW} x_J(i) + n_W(i), & \mathcal{H}_0, \\ \sqrt{P_S} h_{SW} x_S(i) + n_W(i), & \mathcal{H}_1. \end{cases} \tag{3.13}$$

In the second time slot, when W receives only the jamming signal from R, $\mathcal{H}_0$ is

true. When W receives the re-encoded signal from R, $\mathcal{H}_1$ is true. Thus, in the second time slot, we have

$$y_W^{(2)}(i) = \begin{cases} \sqrt{P_R} h_{RW} x_J(i) + n_W(i), & \mathcal{H}_0, \\ \sqrt{P_R} h_{RW} x_R(i) + n_W(i), & \mathcal{H}_1. \end{cases} \tag{3.14}$$

3.1.3.3 Warden's Detection Strategy

Owing to the assumption that W knows the statistical characteristics rather than the instantaneous values of h_{SW} and h_{RW}, it decides whether the communication exists or not according to the received signal power measured by the power detector. Thus, the decision rule in one time slot is given by

$$\bar{P}_W \triangleq \frac{1}{n} \sum_{i=1}^{n} |y_W(i)|^2 \underset{\mathcal{D}_0}{\overset{\mathcal{D}_1}{\gtrless}} \tau, \tag{3.15}$$

where $\bar{P}_W$ is the average power of received signals, τ is the detection threshold, $\mathcal{D}_0$ and $\mathcal{D}_1$ denote that W makes a decision when it accepts $\mathcal{H}_0$ and $\mathcal{H}_1$, respectively. Notice that the equation (3.15) refers to the detection in one time slot, but the detection under the HD mode involves two consecutive time slots. Thus, under the HD mode, we can first apply equation (3.15) to get the detection result for each time slot and then combine the detection results of these two time slots to obtain the overall detection result (see Subsection 3.2.3.1).

3.1.4 Performance Metrics

In this subsection, we introduce DEP, TOP, and CT to depict the covert performance, transmission performance, and overall system performance, respectively.

To depict the detection performance, two types of detection errors are concerned. One is a false alarm (FA), which means W accepts $\mathcal{H}_1$ while the transmission does

not exist. The other is missed detection (MD), which means W accepts $\mathcal{H}_0$ while the transmission exists. Thus, the DEP ξ is given by

$$\xi = p_{FA} + p_{MD}. \tag{3.16}$$

When the target transmission rate r_t between S and D is greater than the channel capacity C [37], a transmission outage happens in the sense that D cannot recover the messages reliably. The TOP p_{to} is defined as the probability that such a transmission outage happens [61], which is determined as

$$p_{to} = \mathbb{P}\left\{C < r_t\right\}. \tag{3.17}$$

Note that the capacity C depends on either SINR or signal-to-noise ratio (SNR) from S to D, so the capacities C in different modes are

$$C = \begin{cases} \log_2(1 + \mathrm{SINR}_{FD}), & \text{FD}, \\ \frac{1}{2}\log_2(1 + \mathrm{SNR}_{HD}), & \text{HD}. \end{cases} \tag{3.18}$$

Based on (3.17) and (3.18), p_{to} can be rewritten as

$$p_{to} = \begin{cases} \mathbb{P}\left\{\mathrm{SINR}_{FD} < \gamma_{th}^{FD}\right\}, & \text{FD}, \\ \mathbb{P}\left\{\mathrm{SNR}_{HD} < \gamma_{th}^{HD}\right\}, & \text{HD}, \end{cases} \tag{3.19}$$

where the SINR threshold is $\gamma_{th}^{FD} = 2^{r_t} - 1$ in FD mode and the SNR threshold is $\gamma_{th}^{HD} = 2^{2r_t} - 1$ in HD mode.

We define the CT T as the achievable throughput $r_t(1 - p_{to})$, subject to the covertness constraint on ξ and maximum power constraint on relay transmit power

P_R. Thus, T is formulated as

$$T = r_t\,(1 - p_{to}\,), \tag{3.20a}$$

$$\text{s.t. } P_R \le P_R^{\max}, \tag{3.20b}$$

$$\xi \ge 1 - \epsilon, \tag{3.20c}$$

where $P_R^{\max}$ denotes the maximum transmit power of R, and ϵ (with $0 < \epsilon < 1$) is an arbitrary small constant denoting the covert requirement.

3.2 Covert Performance under Fixed Mode Combination

3.2.1 FD-AF Scenario

3.2.1.1 DEP Analysis

When S does not conduct transmission, W only receives jamming signals and noise. Based on the detection mechanism of W in (3.15), if $\bar{P}_W \ge \tau$ in this case, W still accepts the hypothesis $\mathcal{H}_1$ while the transmission does not exist, leading to a false alarm. Thus, the probability p_{FA} of FA is given by

$$\begin{aligned} p_{FA} &= \mathbb{P}\{(P_R|h_{RW}|^2 + \sigma_W^2)\frac{\chi_{2n}^2}{n} \ge \tau \,|\, \mathcal{H}_0\} \\ &= \mathbb{P}\{(P_R|h_{RW}|^2 + \sigma_W^2) \ge \tau \,|\, \mathcal{H}_0\} \\ &= \begin{cases} e^{-\frac{(\tau - \sigma_W^2)}{P_R}}, & \sigma_W^2 < \tau, \\ 1, & \sigma_W^2 \ge \tau, \end{cases} \end{aligned} \tag{3.21}$$

where χ_{2n}^n represents a chi-squared random variable with $2n$ degrees of freedom [70]. By the Strong Law of Large Numbers, $\frac{\chi_{2n}^n}{n}$ converges in probability to 1 when $n \to \infty$.

When S conducts transmission, W receives signals from S, jamming signals and noise. Based on the detection mechanism of W in (3.15), if $\bar{P}_W < \tau$ in this case,

W still accepts the hypothesis $\mathcal{H}_0$ while the transmission exists, leading to a missed detection. Thus, the probability p_{MD} of MD is given by

$$\begin{aligned} p_{MD} &= \mathbb{P}\{(P_S|h_{SW}|^2 + P_R|h_{RW}|^2 + \sigma_W^2) < \tau \,|\, \mathcal{H}_1\} \\ &= \begin{cases} 1 + \frac{P_S e^{-\frac{(\tau-\sigma_W^2)}{P_S}} - P_R e^{-\frac{(\tau-\sigma_W^2)}{P_R}}}{P_R - P_S}, & \sigma_W^2 < \tau, \\ 0, & \sigma_W^2 \geq \tau. \end{cases} \end{aligned} \tag{3.22}$$

Substituting p_{FA} in (3.21) and p_{MD} in (3.22) into ξ in (3.16), we obtain the DEP in the FD-AF relay system as

$$\xi_{FD-AF}(\tau) = \begin{cases} 1 + \frac{P_S(e^{-\frac{(\tau-\sigma_W^2)}{P_S}} - e^{-\frac{(\tau-\sigma_W^2)}{P_R}})}{P_R - P_S}, & \sigma_W^2 < \tau, \\ 1, & \sigma_W^2 \geq \tau. \end{cases} \tag{3.23}$$

Then, we have the following theorem regarding the minimum DEP.

Theorem III.1 *For the concerned relay system with transmit power P_S for S and transmit power P_R for R, the minimum DEP ξ_{FD-AF}^* under the FD-AF scenario is determined as*

$$\xi_{FD-AF}^* = 1 - (\frac{P_S}{P_R})^{-\frac{P_R}{P_S - P_R}}. \tag{3.24}$$

Proof 1 *Following a similar analysis to the proof of Proposition 1 in [62], the optimal detection threshold τ^* under the FD-AF scenario can be derived as*

$$\tau^* = \frac{P_S P_R(\ln \frac{1}{P_S} - \ln \frac{1}{P_R})}{P_R - P_S} + \sigma_W^2. \tag{3.25}$$

Also, by following a proof similar to that of Proposition 1 in [62], we can prove that ξ_{FD-AF} decreases with τ when $\tau \in (\sigma_W^2, \tau^*)$, and ξ_{FD-AF} increases with τ when $\tau \in (\tau^*, \infty)$. Thus, the minimum DEP is achieved when $\tau = \tau^*$, so ξ_{FD-AF} is

determined as

$$\xi_{FD-AF} = 1 + \frac{P_S(e^{-\frac{(\tau^*-\sigma_W^2)}{P_S}} - e^{-\frac{(\tau^*-\sigma_W^2)}{P_R}})}{P_R - P_S} = 1 - (\frac{P_S}{P_R})^{-\frac{P_R}{P_S-P_R}}. \tag{3.26}$$

3.2.1.2 TOP Analysis

We denote the SINR at R and D as SINR_R and SINR_D, respectively. According to the received signals in (3.1) and (3.5), SINR_R and SINR_D are given by

$$\text{SINR}_R = \frac{P_S|h_{SR}|^2}{P_R|h_{RR}|^2 + \sigma_R^2}, \tag{3.27}$$

$$\text{SINR}_D = \frac{P_R|h_{RD}|^2}{\sigma_D^2}. \tag{3.28}$$

Compared with the single-hop system, the analysis of SINR for the two-hop system needs to consider SINR_R and SINR_D simultaneously. Thus, based on the formulae in (3.27) and (3.28), the SINR from S to D under the FD-AF scenario [71] is given by

$$\begin{aligned} \text{SINR}_{FD-AF} &= \frac{\text{SINR}_R\text{SINR}_D}{\text{SINR}_R + \text{SINR}_D + 1}, \\ &= \frac{\gamma_{SR}\gamma_{RD}}{\gamma_{SR} + (\gamma_{RD}+1)(\gamma_{RR}+1)}, \end{aligned} \tag{3.29}$$

where $\gamma_{AB} = \frac{P_A E[|h_{AB}|^2]}{\sigma_B^2}$, and the probability density function (PDF) of random variable γ_{AB} is $f_{\gamma_{AB}}(x) = \frac{1}{\gamma_{AB}} e^{-\frac{1}{\gamma_{AB}}x}$, for $AB \in \{SR, RR, RD\}$.

Then, we have the following theorem regarding the expression of TOP.

Theorem III.2 *For the concerned relay system with average SINR γ_{SR} between S and R, average SINR γ_{RD} between R and D, average SINR γ_{RR} for the self-interference and SINR threshold γ_{th}^{FD}, the TOP p_{to}^{FD-AF} under the FD-AF scenario is determined as*

$$p_{to}^{FD-AF} = 1 - \eta_1 \times K_{-1}(\zeta_1), \tag{3.30}$$

where $\eta_1 = 2(\frac{\gamma_{th}^{FD}(\gamma_{th}^{FD}+1)(\gamma_{RR}+1)}{\gamma_{SR}\gamma_{RD}})^{\frac{1}{2}} e^{-\frac{\gamma_{th}^{FD}(\gamma_{RD}(\gamma_{RR}+1)+\gamma_{SR})}{\gamma_{SR}\gamma_{RD}}}$ *and* $\zeta_1 = 2(\frac{\gamma_{th}^{FD}(\gamma_{th}^{FD}+1)(\gamma_{RR}+1)}{\gamma_{SR}\gamma_{RD}})^{\frac{1}{2}}$. $K_{-1}(\zeta_1) = \frac{1}{\zeta_1}\int_0^\infty exp(-(t+\frac{\zeta_1^2}{4t}))dt$ *is the modified Bessel function of the second kind with the -1-th order [72, 73].*

Proof 2 *The TOP of the FD-AF scenario can be derived as*

$$\begin{aligned} p_{to}^{FD-AF} &= \mathbb{P}\{\frac{\gamma_{SR}\gamma_{RD}}{\gamma_{SR}+(\gamma_{RD}+1)(\gamma_{RR}+1)} < \gamma_{th}^{FD}\} \\ &= \iint_{\gamma_{SD}<\gamma_{th}^{FD}} f_{(\gamma_{SR})} f_{(\gamma_{RD})} dxdy \\ &= \int_0^{\phi_1} \frac{1}{\gamma_{SR}} e^{-\frac{1}{\gamma_{SR}}x} dx \int_0^\infty \frac{1}{\gamma_{RD}} e^{-\frac{1}{\gamma_{RD}}y} dy + \int_{\phi_1}^\infty \frac{1}{\gamma_{SR}} e^{-\frac{1}{\gamma_{SR}}x} dx \int_0^{\psi_1} \frac{1}{\gamma_{RD}} e^{-\frac{1}{\gamma_{RD}}y} dy, \end{aligned} \tag{3.31}$$

where $\gamma_{SD} = \frac{\gamma_{SR}\gamma_{RD}}{\gamma_{SR}+(\gamma_{RD}+1)(\gamma_{RR}+1)}$, $\phi_1 = \gamma_{th}^{FD}(\gamma_{RR}+1)$, *and* $\psi_1 = \frac{\gamma_{th}^{FD}(x+\gamma_{RR}+1)}{x-\gamma_{th}^{FD}(\gamma_{RR}+1)}$. *We note that from (3.31), the* p_{to}^{FD-AF} *can be divided into two parts. The first part* Q_1 *can be expressed as*

$$\begin{aligned} Q_1 &= \int_0^{\phi_1} \frac{1}{\gamma_{SR}} e^{-\frac{1}{\gamma_{SR}}x} dx \int_0^\infty \frac{1}{\gamma_{RD}} e^{-\frac{1}{\gamma_{RD}}y} dy \\ &= 1 - e^{-\frac{\gamma_{th}^{FD}(\gamma_{RR}+1)}{\gamma_{SR}}}, \end{aligned} \tag{3.32}$$

and the second part Q_2 *can be written as*

$$\begin{aligned} Q_2 &= \int_{\phi_1}^\infty \frac{1}{\gamma_{SR}} e^{-\frac{1}{\gamma_{SR}}x} dx \int_0^{\psi_1} \frac{1}{\gamma_{RD}} e^{-\frac{1}{\gamma_{RD}}y} dy \\ &= e^{-\frac{\gamma_{th}^{FD}(\gamma_{RR}+1)}{\gamma_{SR}}} - \int_{\phi_1}^\infty \frac{1}{\gamma_{SR}} e^{-\frac{1}{\gamma_{SR}}x} e^{-\frac{\gamma_{th}^{FD}(x+\gamma_{RR}+1)}{\gamma_{RD}(x-\gamma_{th}^{FD}(\gamma_{RR}+1))}} dx \\ &= e^{-\frac{\gamma_{th}^{FD}(\gamma_{RR}+1)}{\gamma_{SR}}} - \eta_1 \times K_{-1}(\zeta_1), \end{aligned} \tag{3.33}$$

Finally, we can complete the derivation in (3.31) by combining Q_1 *in (3.32) and* Q_2 *in (3.33).*

3.2.1.3 CT Maximization

Our objective is to maximize the CT, which can be formulated as the following optimization problem

$$T^*_{FD-AF} = \max_{P_R, r_t} \; r_t \, \eta_1 K_1(\zeta_1), \tag{3.34a}$$

$$\text{s.t.} \;\; P_R \leq P_R^{\max}, \tag{3.34b}$$

$$\xi^*_{FD-AF} \geq 1 - \epsilon. \tag{3.34c}$$

According to the optimization problem defined in (3.34), we need to determine the optimal settings for target transmission rate r_t and relay transmit power P_R to obtain the maximal CT. To determine the optimal P_R, we first analyze the feasible region of P_R based on the constraints in (3.34b) and (3.34c). From (3.34b) we can easily see that $P_R \leq P_R^{\max}$. Based on the expression of (3.24) and a proof similar to that for the Proposition 3 in [62], we can prove that $P_R \geq \frac{P_S \ln \epsilon}{W_0(\epsilon \ln \epsilon)}$. Thus, $P_R \in [\frac{P_S \ln \epsilon}{W_0(\epsilon \ln \epsilon)}, P_R^{\max}]$.

To determine the maximal CT T^*_{FD-AF}, we need to solve the optimization problem in (3.34) to identify the optimal target transmission rate r_t^* and the optimal relay transmit power P_R^*. Here, we apply the Traversal Searching Algorithm to devise the following Algorithm 1 for solving the optimization problem in (3.34).

3.2.2 FD-DF Scenario

3.2.2.1 DEP Analysis

When the system adopts the FD-DF relay, the expression of the signal received at W is the same as the (3.12) in the FD-AF relay system. Thus, the formulae for the FA probability and MD probability in FD-DF relay system are the same as (3.21) and (3.22), respectively. Furthermore, the expression for DEP in Theorem III.1 also applies to this system.

Algorithm 1: Maximum Covert Throughput Traversal Searching Algorithm in the FD-AF Scenario

Input: Transmit power of S P_S, upper bound of relay transmit power $P_R^{\max}$, self-interference channel gain $|h_{RR}|^2$, covert requirement ϵ ;

Output: Maximum covert throughput T_{FD-AF}^*;

Initialize $r_t^1 = 0$, $T_{FD-AF}(P_R^*, r_t^1) = 0$ and $\epsilon = 0.1$;

Set the length L for r_t, the iteration index $m \in \{1, 2, \ldots, M\}$ and $r_t^{m+1} = r_t^m + L$;

Compute $\xi_{FD-AF}^{*,-1}$ according to (3.24) and obtain P_R^0;

if $P_R^0 \leq P_R \leq P_R^{\max}$ **then**

  Find out the P_R^* which makes the $T_{FD-AF}(P_R^*, r_t^{m+1})$ in (3.34a) obtain the maximum value;

end

if $T_{FD-AF}(P_R^{*,m}, r_t^m) \leq T_{FD-AF}(P_R^*, r_t^{m+1})$ **then**

  $m++$;

  Compute $T_{FD-AF}(P_R^*, r_t^{m+1})$ as 4th-8th rows;

else

  Return $T_{FD-AF} = T_{FD-AF}(P_R^*, r_t^m)$ and $r_t^* = r_t^m$;

end

3.2.2.2 TOP Analysis

With the FD-DF relay, the SINR_R and SINR_D are the same as in (3.27) and (3.28), respectively. Since the SINR in the FD-DF relay system is determined by the minimum of SINR_R and SINR_D, it can be expressed as

$$\text{SINR}_{FD-DF} = \min(\text{SINR}_R, \text{SINR}_D). \tag{3.35}$$

Substituting (3.35) into (3.19), the TOP in the FD-DF relay system is given by

$$\begin{aligned} p_{to}^{FD-DF} &= 1 - \left(1 - \int_0^{\gamma_{th}^{FD}(\gamma_{RR}+1)} \frac{1}{\gamma_{SR}} e^{-\frac{1}{\gamma_{SR}}x} dx\right)\left(1 - \int_0^{\gamma_{th}^{FD}} \frac{1}{\gamma_{RD}} e^{-\frac{1}{\gamma_{RD}}y} dy\right) \\ &= 1 - e^{-\frac{\gamma_{th}^{FD}(\gamma_{RD}(\gamma_{RR}+1)+\gamma_{SR})}{\gamma_{SR}\gamma_{RD}}}. \end{aligned} \tag{3.36}$$

3.2.2.3 CT Maximization

By substituting (3.36) into (3.20), the maximal CT T^*_{FD-DF} in the FD-DF relay system can be formulated as the following optimization problem

$$T^*_{FD-DF} = \max_{P_R, r_t} \; r_t \, e^{-\frac{\gamma^{FD}_{th}(\gamma_{RD}(\gamma_{RR}+1)+\gamma_{SR})}{\gamma_{SR}\gamma_{RD}}}, \tag{3.37a}$$

$$\text{s.t.} \;\; P_R \leq P_R^{\max}, \tag{3.37b}$$

$$\xi^*_{FD-DF} \geq 1-\epsilon. \tag{3.37c}$$

By substituting (3.37a) into the step 5 of Algorithm 1, we can then apply Algorithm 1 to solve this optimization problem.

3.2.3 HD-AF Scenario

3.2.3.1 DEP Analysis

The HD-AF relay system involves two time slots. In the second time slot, R sends either the normal signals by Gaussian codebooks or Gaussian jamming signals, both of them will lead to the same statistical signal structure at W. Thus, W cannot detect the existence of the signal transmission from R to D, so the detection performance of W is only determined by the transmission from S to R in the first time slot. Besides, we notice that the received power under hypothesis $\mathcal{H}_0$ in (3.13) is the same as that in (3.12), so the FA probability p_{FA} here is the same as that in (3.21). On the other hand, the MD probability p_{MD} of the HD-AF relay system can be determined as

$$\begin{aligned} p_{MD} &= \mathbb{P}\{(P_S|h_{SW}|^2+\sigma_W^2) < \tau \cap (P_R|h_{RW}|^2+\sigma_W^2) < \tau \,|\, \mathcal{H}_1\} \\ &= \begin{cases} (1-e^{-\frac{(\tau-\sigma_W^2)}{P_S}})(1-e^{-\frac{(\tau-\sigma_W^2)}{P_R}}), & \sigma_W^2 < \tau, \\ 0, & \sigma_W^2 \geq \tau. \end{cases} \end{aligned} \tag{3.38}$$

Substituting p_{FA} in (3.21) and p_{MD} in (3.38) into (3.16), the DEP with HD-AF relay is given by

$$\xi_{HD-AF}(\tau) = \begin{cases} 1 - e^{-\frac{(\tau-\sigma_W^2)}{P_S}} + e^{-\frac{(P_S+P_R)(\tau-\sigma_W^2)}{P_S P_R}}, & \sigma_W^2 < \tau, \\ 1, & \sigma_W^2 \geq \tau. \end{cases} \tag{3.39}$$

Theorem III.3 *For the concerned relay system with transmit power P_S for S and transmit power P_R for R, the minimum DEP ξ^*_{HD-AF} under the HD-AF scenario is determined as*

$$\xi^*_{HD-AF} = 1 - (\frac{P_S + P_R}{P_R})^{-\frac{P_R}{P_S}} + (\frac{P_S + P_R}{P_R})^{-\frac{P_S+P_R}{P_S}}. \tag{3.40}$$

Proof 3 *The proof for this theorem is similar to the proof of Theorem III.1, and the optimal detection threshold τ^* for W can be denoted by*

$$\tau^* = P_R \ln(\frac{P_S + P_R}{P_R}) + \sigma_W^2. \tag{3.41}$$

By substituting the optimal detection threshold into the formula in (3.39), we obtain the minimum DEP under the HD-AF scenario as

$$\xi_{HD-AF} = 1 - e^{-\frac{(\tau-\sigma_W^2)}{P_S}} + e^{-\frac{(P_S+P_R)(\tau-\sigma_W^2)}{P_S P_R}} = 1 - (\frac{P_S + P_R}{P_R})^{-\frac{P_R}{P_S}} + (\frac{P_S + P_R}{P_R})^{-\frac{P_S+P_R}{P_S}}. \tag{3.42}$$

3.2.3.2 TOP Analysis

We denote the SNR at R and D as SNR_R and SNR_D, respectively. According to the formulae of received signals in (3.7) and (3.8), SNR_R and SNR_D are given by

$$\text{SNR}_R = \frac{P_S |h_{SR}|^2}{\sigma_R^2}, \tag{3.43}$$

$$\mathrm{SNR}_D = \frac{P_R |h_{RD}|^2}{\sigma_D^2}. \tag{3.44}$$

Based on the formulae in (3.43) and (3.44), the SNR from S to D under the HD-AF scenario is given by

$$\begin{aligned} \mathrm{SNR}_{HD-AF} &= \frac{\mathrm{SNR}_R \mathrm{SNR}_D}{\mathrm{SNR}_R + \mathrm{SNR}_D + 1}, \\ &= \frac{\gamma_{SR}\gamma_{RD}}{\gamma_{SR} + \gamma_{RD} + 1}. \end{aligned} \tag{3.45}$$

Substituting (3.45) into (3.19), the TOP in the HD-AF scenario is determined as

$$\begin{aligned} p_{to}^{HD-AF} &= \mathbb{P}\{\frac{\gamma_{SR}\gamma_{RD}}{\gamma_{SR} + \gamma_{RD} + 1} < \gamma_{th}^{HD}\} \\ &= 1 - \eta_2 \times K_{-1}(\zeta_2), \end{aligned} \tag{3.46}$$

where $\eta_2 = 2(\frac{\gamma_{th}^{HD}(\gamma_{th}^{HD}+1)}{\gamma_{SR}\gamma_{RD}})^{\frac{1}{2}} e^{-\frac{\gamma_{th}^{HD}(\gamma_{RD}+\gamma_{SR})}{\gamma_{SR}\gamma_{RD}}}$, $\zeta_2 = 2(\frac{\gamma_{th}^{HD}(\gamma_{th}^{HD}+1)}{\gamma_{SR}\gamma_{RD}})^{\frac{1}{2}}$, and $K_{-1}(\zeta_2) = \frac{1}{\zeta_2}\int_0^\infty exp(-(t + \frac{\zeta_2^2}{4t}))dt$ is the modified Bessel function of the second kind and -1-th order.

3.2.3.3 CT Maximization

Based on (3.20) and (3.46), the maximal CT T_{HD-AF}^* in the HD-AF scenario can be formulated as the following optimization problem

$$T_{HD-AF}^* = \max_{P_R, r_t} \; r_t \, \eta_2 K_1(\zeta_2), \tag{3.47a}$$

$$\text{s.t.} \;\; P_R \leq P_R^{\max}, \tag{3.47b}$$

$$\xi_{HD-AF}^* \geq 1 - \epsilon. \tag{3.47c}$$

By substituting (3.47a) into the step 5 of Algorithm 1, we can then apply Algorithm 1 to solve this optimization problem.

3.2.4 HD-DF Scenario

3.2.4.1 DEP Analysis

In the HD-DF relay system, the expressions of the received signals at W are the same as those in (3.13) and (3.14). Thus, the DEP is the same as in (3.40) from Theorem III.3 of the HD-AF relay system.

3.2.4.2 TOP Analysis

Under the HD-DF scenario, the SNR from S to D is the minimum value of SNR_R and SNR_D based on (3.43) and (3.44). Thus, we can derive the TOP as

$$\begin{aligned} p_{to}^{HD-DF} &= 1 - \left(1 - \int_0^{\gamma_{th}^{HD}} \frac{1}{\gamma_{SR}} e^{-\frac{1}{\gamma_{SR}}x} dx\right)\left(1 - \int_0^{\gamma_{th}^{HD}} \frac{1}{\gamma_{RD}} e^{-\frac{1}{\gamma_{RD}}y} dy\right) \\ &= 1 - e^{-\frac{\gamma_{th}^{HD}(\gamma_{RD}+\gamma_{SR})}{\gamma_{SR}\gamma_{RD}}}. \end{aligned} \tag{3.48}$$

3.2.4.3 CT Maximization

By substituting (3.48) into (3.20), the maximal CT T_{HD-DF}^* under the HD-DF scenario can be formulated as the following optimization problem

$$T_{HD-DF}^* = \max_{P_R, r_t} \; r_t \, e^{-\frac{\gamma_{th}^{HD}(\gamma_{RD}+\gamma_{SR})}{\gamma_{SR}\gamma_{RD}}}, \tag{3.49a}$$

$$\text{s.t.} \;\; P_R \leq P_R^{\max}, \tag{3.49b}$$

$$\xi_{HD-DF}^* \geq 1 - \epsilon. \tag{3.49c}$$

By substituting (3.49a) into the step 5 in Algorithm 1, we can then apply Algorithm 1 to solve this optimization problem.

3.3 Joint Transmission/Forwarding Mode Selection

In a fixed-parameter system, we further propose a joint transmission/forwarding mode selection scheme to determine the maximal CT T^*. Here, we apply the Traversal Searching Algorithm to devise the following Algorithm 2 for solving the optimization problem.

Algorithm 2: Maximum Covert Throughput Traversal Searching Algorithm under Joint Transmission/Forwarding Mode Selection Mode

Input: Transmit power of S P_S, relay transmit power P_R, self-interference channel gain $|h_{RR}|^2$ and covert requirement ϵ;

Output: Maximum covert throughput T^*, best mode combination and corresponding target transmission rate r_t ;

Initialize $r_t^1 = 0$, $T_{FD-AF}(P_R^*, r_t^1) = 0$ and $\epsilon = 0.1$;

Set the length L for r_t, the iteration index $m \in \{1, 2, \ldots, M\}$ and $r_t^{m+1} = r_t^m + L$;

Compute $\xi_{FD-AF}^*(P_S, P_R)$ according to (3.24);

if $\xi_{FD-AF}^* \geq 1 - \epsilon$ **then**

  Compute $T_{FD-AF}^*(P_R, r_t^{*,FD-AF})$, $T_{FD-DF}^*(P_R, r_t^{*,FD-DF})$, $T_{HD-AF}^*(P_R, r_t^{*,HD-AF})$ and $T_{HD-DF}^*(P_R, r_t^{*,HD-DF})$ according to (3.34), (3.37), (3.47) and (3.49), respectively;

  Note the $T_{FD-AF}^*(P_R, r_t^{*,FD-AF}) < T_{FD-DF}^*(P_R, r_t^{*,FD-DF})$ and $T_{HD-AF}^*(P_R, r_t^{*,HD-AF}) < T_{HD-DF}^*(P_R, r_t^{*,HD-DF})$;

  if $T_{FD-DF}^*(P_R, r_t^{*,FD-DF}) \leq T_{HD-DF}^*(P_R, r_t^{*,HD-DF})$ **then**

    Return $T^* = T_{HD-DF}^*(P_R, r_t^{*,HD-DF})$, best mode combination is HD-DF, $r_t^* = r_t^{*,HD-DF}$;

  else

    Return $T^* = T_{FD-DF}^*(P_R, r_t^{*,FD-DF})$, best mode combination is FD-DF, $r_t^* = r_t^{*,FD-DF}$;

  end

else

  The covert relay communication cannot be achieved;

end

3.4 Numerical Results

In this section, we provide numerical results to illustrate the performance of our proposed four relay scenarios in terms of DEP ξ, TOP p_{to}, and CT T. Unless otherwise stated, the related parameters in the numerical results are set as $P_S = 1\text{W}$, $P_R = 10\text{W}$, $r_t = 0.5$ bits per channel use, and $\sigma_R^2 = \sigma_D^2 = \sigma_W^2 = 1\text{W}$.

3.4.1 DEP Performance

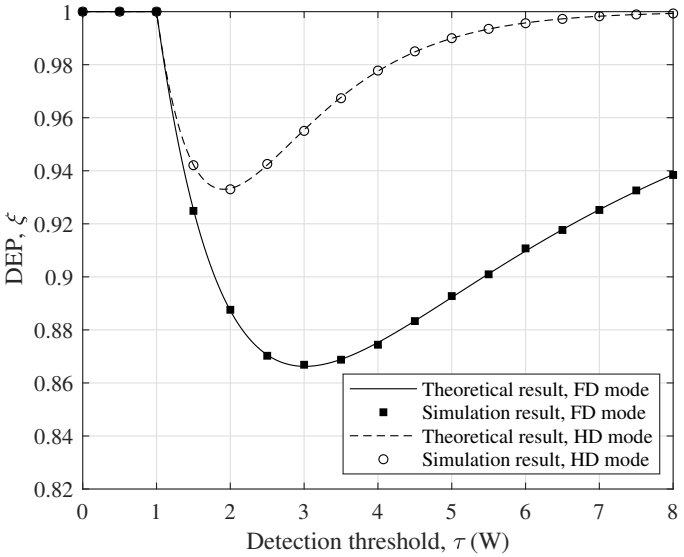

Figure 3.2: DEP ξ vs. detection threshold τ.

We show in Fig. 3.2 the simulation and theoretical results for ξ vs. τ under FD and HD modes to validate our theoretical models on DEP. We can observe from Fig. 3.2 that the simulation results match well with the results evaluated by the proposed theoretical models, indicating that our theoretical models can accurately depict the DEP performance of the concerned system. We can find that for a fixed mode, as τ increases, ξ first decreases and then increases, indicating the existence of an optimal τ that leads to the minimum ξ. The results can be explained as follows. Note that ξ in (3.16) is the sum of p_{FA} and p_{MD}, where p_{FA} decreases with the increase of τ

while p_{MD} increases with the increase of τ. Thus, as τ is relatively small, the p_{FA} dominates ξ, leading to the decrease of ξ with τ. However, as τ further increases, the p_{MD} dominates ξ, leading to the increase of ξ. In addition, we can also see that ξ in FD scenario is smaller than that in HD scenario for a given detection threshold τ. This is because covert message transmission using FD relay requires only one time slot, which means that the total power received at W in FD scenario is larger than that in HD scenario, leading to a smaller ξ.

3.4.2 TOP Performance

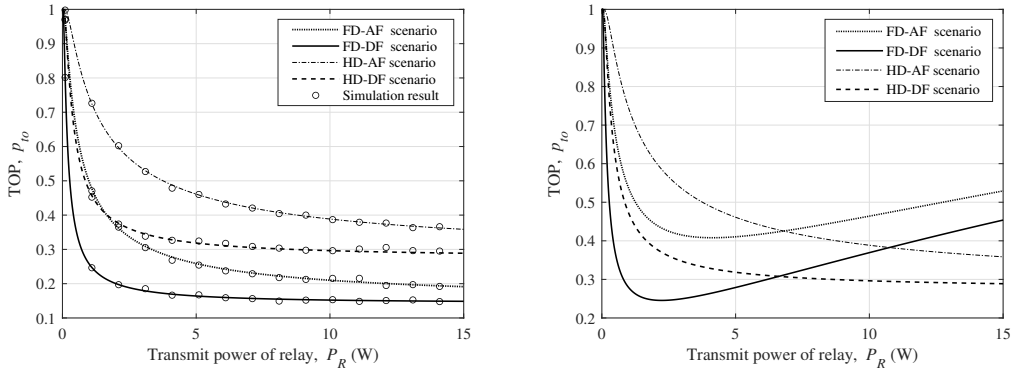

(a) Self-interference channel gain, $|h_{RR}|^2 = 0.001$

(b) Self-interference channel gain, $|h_{RR}|^2 = 0.2$

Figure 3.3: TOP p_{to} vs. transmit power of relay P_R.

We first show in Fig. 3.3(a) both the theoretical and simulation results for TOP p_{to} vs. target transmission rate r_t. From Fig. 3.3(a), we can see that the simulation results agree well with the theoretical ones, so our theoretical models can accurately describe the TOP performance of the concerned system. We show in Fig. 3.3 the impact of relay transmit power P_R on the TOP p_{to} under the four scenarios, where $P_R^{\max} = 15$W and $|h_{RR}|^2 = \{0.001, 0.2\}$. We can see from Fig. 3.3(a) that when $|h_{RR}|^2 = 0.001$, p_{to} decreases as P_R increases under the four scenarios. This is due to the fact that as P_R increases, the channel capacity becomes larger, leading to a reduced p_{to}. We can also see from Fig. 3.3(b) that under $|h_{RR}|^2 = 0.2$, as P_R increases,

p_{to} in the FD scenario first decreases and then increases. This is because when P_R is small, the effect of self-interference is negligible in the FD mode, leading to a higher spectrum efficiency and a lower p_{to}.

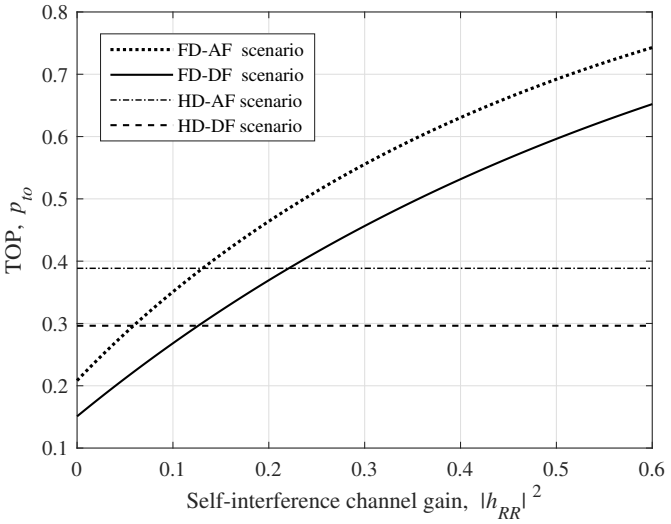

Figure 3.4: TOP p_{to} vs. self-interference channel gain $|h_{RR}|^2$.

We then show in Fig. 3.4 the impact of the self-interference channel gain $|h_{RR}|^2$ on the TOP p_{to} under the four relay scenarios. We can observe from Fig. 3.4 that as $|h_{RR}|^2$ increases, p_{to} in the FD mode increases, while p_{to} in the HD mode remains unchanged. This is due to the fact that there is no self-interference in the HD mode, whereas in the FD mode, a stronger self-interference results in a smaller SINR at D, leading to a larger p_{to}. We also see from Fig. 3.4 that as $|h_{RR}|^2$ increases, p_{to}^{FD} is first smaller than p_{to}^{HD} and then becomes larger than p_{to}^{HD}. This observation further proves that the performance of p_{to} in the FD mode is greatly affected by self-interference. In addition, we can see from Fig. 3.4 that under a fixed $|h_{RR}|^2$, the p_{to} in the DF mode is smaller than that in the AF mode under either FD or HD modes. This is because the capacity from S to D in the DF mode is larger than that in the AF mode.

We further investigate the impact of target transmission rate r_t on the TOP p_{to} under the four scenarios and summarize in Fig. 3.5 how p_{to} varies with r_t under the

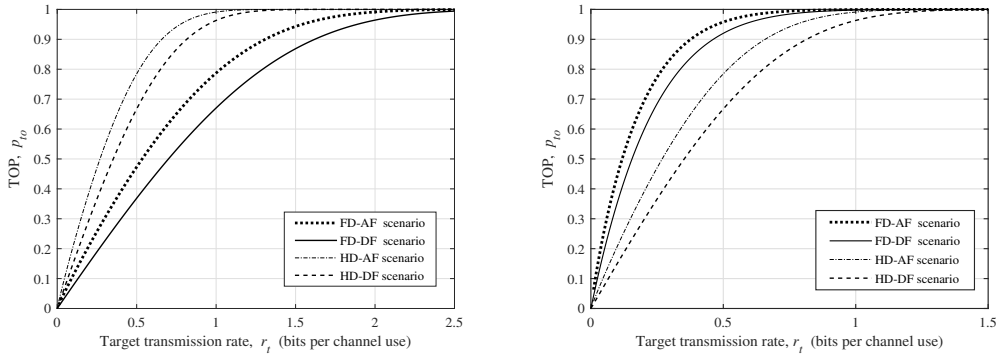

(a) Self-interference channel gain, $|h_{RR}|^2 = 0.001$

(b) Self-interference channel gain, $|h_{RR}|^2 = 0.5$

Figure 3.5: TOP p_{to} vs. target transmission rate r_t.

setting of $|h_{RR}|^2 = \{0.001, 0.5\}$. We can see from Fig. 3.5 that for a fixed $|h_{RR}|^2$, p_{to} first increases with r_t and then remains unchanged. The reason is that when the target transmission rate becomes larger, the receiver cannot decode the signals timely, leading to more transmission outage events and thus a larger p_{to}. We further observe from Fig. 3.5(a) that when $|h_{RR}|^2$ is relatively small (e.g., $|h_{RR}|^2 = 0.0001$), $p_{to}^{HD-AF} > p_{to}^{HD-DF} > p_{to}^{FD-AF} > p_{to}^{FD-DF}$. We also observe from Fig. 3.5(b) that when $|h_{RR}|^2$ is relatively large (e.g., $|h_{RR}|^2 = 0.5$), $p_{to}^{FD-AF} > p_{to}^{FD-DF} > p_{to}^{HD-AF} > p_{to}^{HD-DF}$. The reasons behind these observations are similar to those illustrated in Fig. 3.4.

3.4.3 MCT Performance

We continue to investigate the impact of self-interference channel gain $|h_{RR}|^2$ on the MCT T^* and summarize in Fig. 3.6 how the MCT T^* varies with self-interference channel gain $|h_{RR}|^2$ under the four scenarios. We can observe from Fig. 3.6 that T^* decreases with the $|h_{RR}|^2$ in FD mode, while T^* remains unchanged in HD mode. This is because as $|h_{RR}|^2$ in the FD mode increases, the SINR at R decreases and thus the channel capacity between S and D decreases, leading to a lower T^*. We can also see that T^* in the FD-AF scenario is the largest when $|h_{RR}|^2$ is smaller, but as $|h_{RR}|^2$ increases, T^* in HD-DF scenario then becomes the largest one. This implies

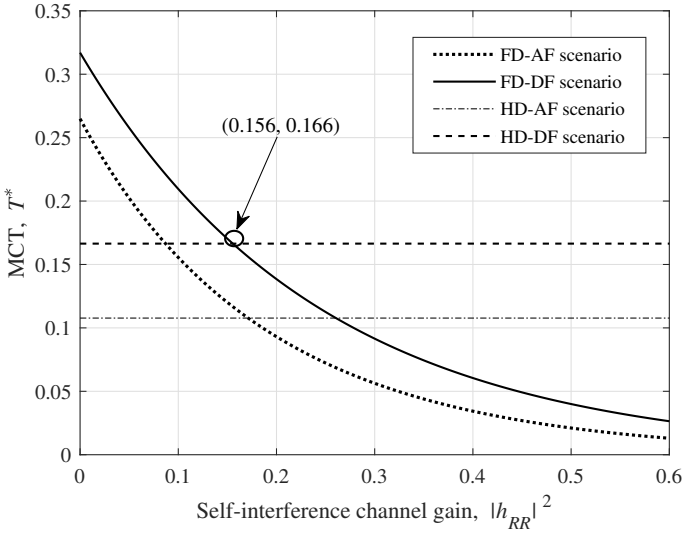

Figure 3.6: MCT T^* vs. self-interference channel gain $|h_{RR}|^2$.

that the FD-AF scenario is the best relay scenario when $|h_{RR}|^2$ is small. Otherwise, the best one is the HD-DF scenario.

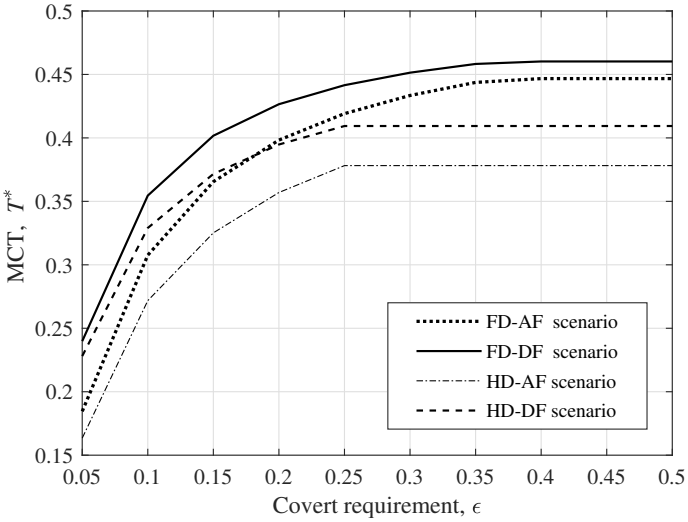

Figure 3.7: MCT T^* vs. covert requirement ϵ.

We then investigate the impact of the covert requirement ϵ on MCT T^* and summarize in Fig. 3.7 how the T^* varies with ϵ under the four scenarios. We can see from Fig. 3.7 that for a fixed P_R, as ϵ increases, T^* first increases and then keeps unchanged. This is because when ϵ increases, P_S increases, leading to a larger T^*.

Since P_S cannot be larger than P_R, T^* keeps unchanged when ϵ increases further.

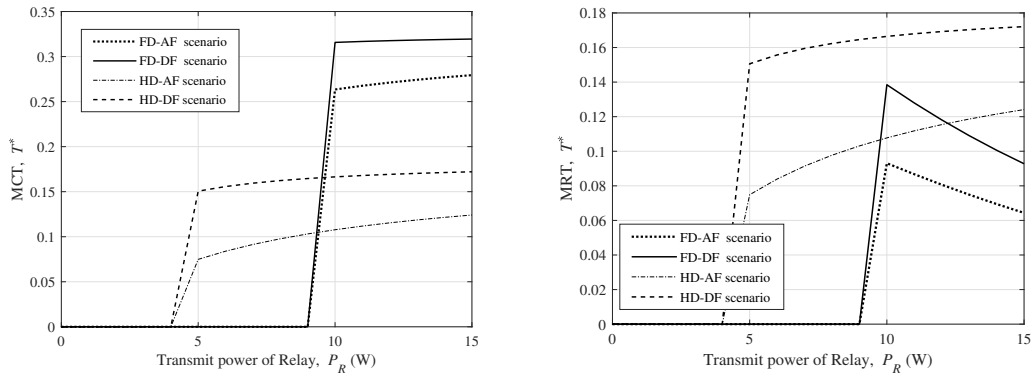

(a) Self-interference channel gain, $|h_{RR}|^2 = 0.001$ (b) Self-interference channel gain, $|h_{RR}|^2 = 0.2$

Figure 3.8: MCT T^* vs. transmit power of relay P_R.

We further explore the impact of the relay transmit power P_R on the MCT T^* and summarize in Fig. 3.8 how the T^* varies with P_R under the settings of $|h_{RR}|^2 = \{0.001, 0.2\}$ and $\epsilon = 0.0775$. It can be seen from Fig. 3.8(a) that when $|h_{RR}|^2$ is relatively small (e.g., $|h_{RR}|^2 = 0.001$), as P_R increases, T^* is first zero and then increases. This can be explained as follows. When P_R is relatively small, the covert constraint cannot be ensured, which means that S cannot send signals covertly to D, so T^* is zero. When P_R increases further beyond a threshold, T^* then increases with P_R. It can be seen from Fig. 3.8(b) that under FD-AF/DF scenarios, when $|h_{RR}|^2$ is relatively large (e.g., $|h_{RR}|^2 = 0.2$), T^* is first zero, then increases to reach its maximum value and then decreases. This means that under FD-AF or FD-DF scenarios, when P_R increases beyond a threshold, the effect of self-interference becomes larger, leading to a reduced T^*.

3.5 Summary

This chapter explored the performance comparison and mode selection among different combinations of transmission modes and forwarding modes for covert re-

lay communication in a single-relay system. The results in this chapter indicate that different mode combinations behave quite differently with the variation of system settings. For a given system setting mainly determined by target transmission rate, self-interference coefficient of FD, constraints of DEP and upper bound on relay transmit power, we can always identify a best combination of transmission modes and forwarding modes to achieve the MCT in the system.

CHAPTER IV

Joint Mode/Relay Selection in Multi-Relay Systems

This chapter considers covert relay communication in a multi-relay system consisting of one transmitter, multiple relays, one receiver, one friendly jammer and one warden, where each relay with AF forwarding mode can switch between the HD and FD transmission modes. For the scenarios when all relays work in either the fixed HD or FD mode, we develop the corresponding relay selection schemes for covert relay communication in the system. For the scenario when all relays work in the hybrid HD/FD transmission mode where each relay can switch between HD and FD transmission modes, we propose a joint mode/relay selection scheme for covert relay communication in the system. Under either scheme, we develop related theoretical models for performance analysis, and also explore the optimal designs of transmit power, jamming power and target transmission rate for CT maximization, subjecting to the constraints of covertness requirement, transmit power and jamming power. Finally, we provide extensive numerical results to illustrate the impact of joint mode/relay selection on covert relay communication in the multi-relay system.

4.1 System Model and Performance Metrics

4.1.1 Communication Scenario and Assumptions

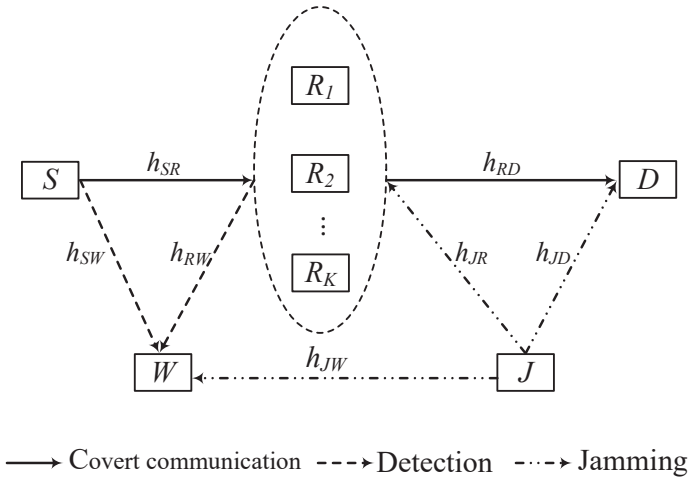

Figure 4.1: System model.

As shown in Fig. 4.1, we consider a two-hop multi-relay system consisting of one source S, K AF relays $R_1, R_2, \ldots, R_K$, one destination D, one friendly jammer J, and one warden W. The source S pre-shares with relays and the destination D a secret Gaussian codebook unknown to the warden W [51, 63], and the source S desires to send covert messages to the destination D with the assistance of one optimally selected relay R^* subject to the detection of the warden W. We assume that each of S, D, J, and W is equipped with a single omnidirectional antenna and operates in the HD mode, while each relay is equipped with a pair of transmit-receive antennas so that it can adopt the HD or FD modes. We focus on three scenarios when all relays work under either the HD, FD or hybrid HD/FD mode, respectively. In the scenario when all relays work under the HD mode, the selected relay receives the signal in one time slot from S and then forwards the signal to D in the next time slot. In the scenario when all relays work under the FD mode, the selected relay can receive and forward signals simultaneously, but it suffers from self-interference. In the scenario

when all relays work under the hybrid HD/FD mode, the selected relay can select between the HD and FD modes to transmit the received signal to D. We apply the common assumption in [74–76] that J sends Gaussian jamming signals in all time slots, which is known to R^* and D but unknown to W. Thus, R^* and D are able to cancel out the effect of jamming signals while W experiences interference from such jamming signals.

We consider the quasi-static Rayleigh fading channel model, where the channel coefficient of a link remains constant in one slot but changes independently and randomly from one slot to another. We denote the channel coefficient from node A to B as h_{AB}, which is a zero-mean circularly symmetric complex Gaussian random variable with variance $E[|h_{AB}|^2] = \lambda_{AB}$. We consider the scenario where S, R and J send public pilot signals so the instantaneous CSI of h_{SR}, h_{RD}, h_{JR} and h_{JD} are known by R and D. W knows only the statistical CSI of h_{SW}, h_{RW} and h_{JW}.

4.1.2 Transmission Process

4.1.2.1 HD mode

In the HD mode, the transmission from S to D is divided into two time slots, i.e., $S \to R^*$ transmission and $R^* \to D$ transmission.

$S \to R^*$ transmission: S encodes the signal into n symbols $(x_S(1), \ldots, x_S(i), \ldots, x_S(n))$ and transmits them to R^*, where each symbol $x_S(i)(i = 1, 2, \ldots, n)$ satisfies the unit power constraint $E[|x_S(i)|^2] = 1$. Here, $E[\cdot]$ denotes the expected value of a random variable. Thus, the i-th symbol $y_{R^*}^{(1)}(i)$ received at R^* in the first time slot is given by

$$y_{R^*}^{(1)}(i) = \sqrt{P} h_{SR^*} x_S(i) + n_{R^*}(i), \tag{4.1}$$

where P denotes the transmit power of S subject to the maximum transmit power

constraint $P^{\max}$; $n_{R^*}(i)$ is the AWGN at R with zero mean and variance σ_R^2, i.e., $n_{R^*}(i) \sim \mathcal{CN}(0, \sigma_{R^*}^2)$. Note that R^* operates in the AF mode, R amplifies its received symbol $y_{R^*}^{(1)}(i)$ by an amplification factor G_{HD} and then forwards to D. Thus, the corresponding symbol $x_{R^*}(i)$ transmitted by R^* is determined as

$$x_{R^*}(i) = G_{HD} y_{R^*}^{(1)}(i), \tag{4.2}$$

where $G_{HD} = \sqrt{\frac{1}{P|h_{SR^*}|^2 + \sigma_{R^*}^2}}$, which ensures that $E[|x_{R^*}(i)|^2] = 1$.

$R^* \rightarrow D$ transmission: R^* forwards the linearly amplified symbol $x_{R^*}(i)$ with transmit power P, so the symbol $y_D^{(2)}(i)$ received at D in the second time slot is given by

$$y_D^{(2)}(i) = \sqrt{P} h_{R^*D} x_{R^*}(i) + n_D(i), \tag{4.3}$$

where $n_D(i)$ is the AWGN at D with zero mean and variance σ_D^2, i.e., $n_D(i) \sim \mathcal{CN}(0, \sigma_D^2)$.

4.1.2.2 FD mode

In the FD mode, the transmission between S and D can be implemented in one time slot, in which S transmits n symbols to R^* while R^* amplifies and forwards the received signals to D simultaneously. Since R^* suffers the self-interference in the FD mode, the i-th symbol $y_{R^*}(i)$ received at R^* is given by

$$y_{R^*}(i) = \sqrt{P} h_{SR^*} x_S(i) + \sqrt{P} h_{R^*R^*} x_{R^*}(i) + n_{R^*}(i), \tag{4.4}$$

Here, $x_{R^*}(i)$ is the transmitted symbol from R^*, which is given by

$$x_{R^*}(i) = G_{FD} y_{R^*}(i), \tag{4.5}$$

where the amplification factor G_{FD} is determined as $G_{FD} = \sqrt{\frac{1}{P|h_{SR^*}|^2+P|h_{R^*R^*}|^2+\sigma^2_{R^*}}}$, which guarantees the power constraint of $E[x_{R^*}(i)x^{\dagger}_{R^*}(i)] = 1$ at R^*.

Finally, the symbol $y_D(i)$ received at D is given by

$$y_D(i) = \sqrt{P}h_{R^*D}x_{R^*}(i) + n_D(i). \tag{4.6}$$

4.1.3 Detection at Warden

In the considered system, we assume that W adopts a radiometer as the detector to decide whether S or R^* has transmitted or not [11, 61]. As such, W faces a binary hypothesis testing problem. The null hypothesis $\mathcal{H}_0$ means that S or R^* does not conduct transmission, while the alternative hypothesis $\mathcal{H}_1$ means that they conduct transmission.

4.1.3.1 HD mode

The detection in HD mode takes place in two time slots. In the first time slot, when S does not transmit (i.e., $\mathcal{H}_0$ is true), W only receives the jamming signal $(x_J(1), \ldots, x_J(i), \ldots, x_J(n))$ with transmit power P_J, where $x_J(i)$ is the transmitted symbol in i-th channel use with the constraint of $E[|x_J(i)|^2] = 1, i = 1, 2, \ldots, n$. While S transmits (i.e., $\mathcal{H}_1$ is true), W receives both the covert signal from S and the jamming signal from J. Thus, the signal $y^{(1)}_W(i)$ received at W in the first time slot is determined as

$$y^{(1)}_W(i) = \begin{cases} \sqrt{P_J}h_{JW}x_J(i) + n_W(i), & \mathcal{H}_0, \\ \sqrt{P}h_{SW}x_S(i) + \sqrt{P_J}h_{JW}x_J(i) + n_W(i), & \mathcal{H}_1, \end{cases} \tag{4.7}$$

where $n_W(i)$ is the AWGN at W with zero mean and variance σ^2_W, i.e., $n_W(i) \sim \mathcal{CN}(0, \sigma^2_W)$. Similarly, when R^* does not transmit, W receives only the jamming signal. When R^* forwards the normalized signal $x_{R^*}(i)$, W receives both the signal

from R^* and the jamming signal from J. Thus, the signal $y_W^{(2)}(i)$ received at W in the second time slot can be determined as

$$y_W^{(2)}(i) = \begin{cases} \sqrt{P_J} h_{JW} x_J(i) + n_W(i), & \mathcal{H}_0, \\ \sqrt{P} h_{R^*W} x_{R^*}(i) + \sqrt{P_J} h_{JW} x_J(i) + n_W(i), & \mathcal{H}_1. \end{cases} \tag{4.8}$$

To conduct a detection, W uses the total received power in one time slot to decide whether the covert communication exists or not. The decision rule in one time slot is given by

$$\bar{P}_W \triangleq \frac{1}{n} \sum_{i=1}^{n} |y_W^a(i)|^2 \underset{\mathcal{D}_0}{\overset{\mathcal{D}_1}{\gtrless}} \tau, \tag{4.9}$$

where $a \in \{(1), (2)\}$; τ is the detection threshold for the average power of received signals $\bar{P}_W$; $\mathcal{D}_0$ and $\mathcal{D}_1$ are the binary decisions that denote W makes a decision when he accepts $\mathcal{H}_0$ and $\mathcal{H}_1$, respectively.

4.1.3.2 FD mode

In the FD mode, the detection at W takes place in one time slot. When $\mathcal{H}_0$ is true, W receives only the jamming signal. When $\mathcal{H}_1$ is true, W receives the signal from S, the amplified signal in (4.5) from R^* and the jamming signal in the time slot. Thus, the signal received at W is

$$y_W(i) = \begin{cases} \sqrt{P_J} h_{JW} x_J(i) + n_W(i), & \mathcal{H}_0, \\ \sqrt{P} h_{SW} x_S(i) + \sqrt{P} h_{R^*W} x_{R^*}(i) + \sqrt{P_J} h_{JW} x_J(i) + n_W(i), & \mathcal{H}_1. \end{cases} \tag{4.10}$$

Thus, under the FD mode, we can obtain the DEP ξ_{FD} by applying the rule in (4.9) to decide on the received signal in (4.10).

4.1.4 Performance Metrics

The performance metrics adopted in this study are DEP, TOP, and MCT. The DEP involves two types of detection errors in W's hypothesis test, i.e., FA and MD. FA means that W's decision is $\mathcal{D}_1$ while $\mathcal{H}_0$ is true, and MD means that W's decision is $\mathcal{D}_0$ while $\mathcal{H}_1$ is true. We use p_{FA} and p_{MD} to denote the probability of FA and MD, respectively. Then $p_{FA} = \mathbb{P}(\mathcal{D}_1|\mathcal{H}_0)$ and $p_{MD} = \mathbb{P}(\mathcal{D}_0|\mathcal{H}_1)$, and DEP ξ is given by

$$\xi = p_{FA} + p_{MD} = \mathbb{P}(\mathcal{D}_1|\mathcal{H}_0) + \mathbb{P}(\mathcal{D}_0|\mathcal{H}_1). \tag{4.11}$$

When the target transmission rate r_t is greater than the channel capacity C between S and D, transmission outage happens in the sense that D cannot recover the messages reliably [37]. We use p_{to} to denote the TOP, which is determined as

$$p_{to} = \mathbb{P}\left\{C < r_t\right\}. \tag{4.12}$$

We use the MCT T^* to depict the covert performance of our system, which is defined as

$$\begin{aligned} T^* = \max_{P,P_J,r_t} \quad & r_t\,(\,1 - p_{to}\,), && \text{(4.13a)} \\ \text{s.t.} \quad & \xi^* \geq 1 - \epsilon, && \text{(4.13b)} \\ & 0 \leq P \leq P^{\max}, && \text{(4.13c)} \\ & 0 \leq P_J \leq P_J^{\max}, && \text{(4.13d)} \end{aligned}$$

where ϵ denotes the covertness requirement, and $P^{\max}$ and $P_J^{\max}$ represent the maximum transmit power and the maximum jamming power, respectively.

4.2 Covert Performance under HD Mode

In this section, we first present the optimal relay selection scheme in the scenario when all relays work under the HD mode and then provide the evaluations of DEP, TOP and MCT in this scenario.

4.2.1 Relay Selection Scheme

For the scenario when all relays work under the HD mode, we consider an optimal relay selection scheme where the relay that leads to the largest S-to-D capacity is selected for signal forwarding. We use γ_{SR_k} and γ_{R_kD} to denote the SNR for the $S \to R_k$ and $R_k \to D$ links, and use γ_{S-R_k-D} and $C_{R_k}^{HD}$ to denote the end-to-end SNR and channel capacity of $S - R_k - D$, respectively. Then we have

$$\gamma_{S-R_k-D} = \frac{\gamma_{SR_k}\gamma_{R_kD}}{\gamma_{SR_k} + \gamma_{R_kD} + 1}, \tag{4.14}$$

$$C_{R_k}^{HD} = \frac{1}{2}\log_2(1 + \gamma_{S-R_k-D}). \tag{4.15}$$

Thus, the optimal relay R^* in this scenario can be determined as

$$R^* = \arg \max_{R_k \in \{R_1,\ldots,R_K\}} \left\{C_{R_k}^{HD}\right\}. \tag{4.16}$$

4.2.2 DEP Analysis

Notice that the DEP defined in (4.11) describes the detection performance in one time slot, but the detection of W in HD relay system involves two consecutive time slots. Thus, the DEP ξ_{HD} under the HD mode can be determined as

$$\xi_{HD} = \xi_{HD}^{(1)}\xi_{HD}^{(2)}, \tag{4.17}$$

where $\xi_{HD}^{(1)}$ and $\xi_{HD}^{(2)}$ denotes the DEP in the first time and second time slots, respectively.

We first derive the DEP $\xi_{HD}^{(1)}$ in the first time. From the decision rule in (4.9), a FA occurs when S does not transmit but W makes decision of $\mathcal{D}_1$ by $\bar{P}_W \geq \tau$. Based on the received signal (4.7) at W in the first time, we can see that the probability $p_{FA}^{(1)}$ of FA in the first time slot is given by

$$\begin{aligned} p_{FA}^{(1)} &= \mathbb{P}\{(P_J|h_{JW}|^2 + \sigma_W^2)\frac{\chi_{2n}^2}{n} \geq \tau \,|\, \mathcal{H}_0\} \\ &= \mathbb{P}\{(P_J|h_{JW}|^2 + \sigma_W^2) \geq \tau \,|\, \mathcal{H}_0\} \\ &= \begin{cases} e^{-\frac{(\tau-\sigma_W^2)}{P_J\lambda_{JW}}}, & \sigma_W^2 < \tau, \\ 1, & \sigma_W^2 \geq \tau, \end{cases} \end{aligned} \tag{4.18}$$

where χ_{2n}^2 is a chi-squared random variable with $2n$ degrees of freedom. From the Strong Law of Large Numbers and Lebesgue's Dominated Convergence Theorem [70] we know $\frac{\chi_{2n}^2}{n}$ can be approximated with 1 when $n \to \infty$.

From the decision rule in (4.9), a MD occurs when S transmits but W makes decision of $\mathcal{D}_0$ by $\bar{P}_W < \tau$. Thus, the probability $p_{MD}^{(1)}$ of MD in the first time slot is given by

$$\begin{aligned} p_{MD}^{(1)} &= \mathbb{P}\{(P|h_{SW}|^2 + P_J|h_{JW}|^2 + \sigma_W^2) < \tau \,|\, \mathcal{H}_1\} \\ &= \begin{cases} 1 + \frac{P\lambda_{SW}e^{-\frac{(\tau-\sigma_W^2)}{P\lambda_{SW}}} - P_J\lambda_{JW}e^{-\frac{(\tau-\sigma_W^2)}{P_J\lambda_{JW}}}}{P_J\lambda_{JW} - P\lambda_{SW}}, & \sigma_W^2 < \tau, \\ 0, & \sigma_W^2 \geq \tau. \end{cases} \end{aligned} \tag{4.19}$$

By substituting $p_{FA}^{(1)}$ in (4.18) and $p_{MD}^{(1)}$ in (4.19) into (4.11), we can obtain the

DEP $\xi_{HD}^{(1)}$ in the first time slot as

$$\xi_{HD}^{(1)} = \begin{cases} 1 + \frac{P\lambda_{SW}\left(e^{-\frac{(\tau-\sigma_W^2)}{P\lambda_{SW}}} - e^{-\frac{(\tau-\sigma_W^2)}{P_J\lambda_{JW}}}\right)}{P_J\lambda_{JW}-P\lambda_{SW}}, & \sigma_W^2 < \tau, \\ 1, & \sigma_W^2 \geq \tau. \end{cases} \tag{4.20}$$

Based on similar analysis as that in the first time slot, we can see that the probability $p_{FA}^{(2)}$ of FA in the second time slot is the same as that in (4.18), and the probability $p_{MD}^{(2)}$ of MD in the second time slot is given by

$$\begin{aligned} p_{MD}^{(2)} &= \mathbb{P}\{(P|h_{R^*W}|^2 + P_J|h_{JW}|^2 + \sigma_W^2) < \tau \,|\, \mathcal{H}_1\} \\ &= \begin{cases} 1 + \frac{P\lambda_{R^*W}e^{-\frac{(\tau-\sigma_W^2)}{P\lambda_{R^*W}}} - P_J\lambda_{JW}e^{-\frac{(\tau-\sigma_W^2)}{P_J\lambda_{JW}}}}{P_J\lambda_{JW}-P\lambda_{R^*W}}, & \sigma_W^2 < \tau, \\ 0, & \sigma_W^2 \geq \tau. \end{cases} \end{aligned} \tag{4.21}$$

By substituting $p_{FA}^{(1)}$ in (4.18) and $p_{MD}^{(2)}$ in (4.21) into ξ in (4.11), the DEP $\xi_{HD}^{(2)}$ in the second time slot is determined as

$$\xi_{HD}^{(2)}(\tau) = \begin{cases} 1 + \frac{P\lambda_{R^*W}\left(e^{-\frac{(\tau-\sigma_W^2)}{P\lambda_{R^*W}}} - e^{-\frac{(\tau-\sigma_W^2)}{P_J\lambda_{JW}}}\right)}{P_J\lambda_{JW}-P\lambda_{R^*W}}, & \sigma_W^2 < \tau, \\ 1, & \sigma_W^2 \geq \tau. \end{cases} \tag{4.22}$$

In this work, we consider the worst-case communication scenario where W can achieve the minimum DEP by adopting the optimal detection thresholds in each time slot.

Theorem IV.1 *Consider the covert communication in an HD relay system with transmit power P for S and R^*, transmit power P_J for J. If we denote the variance of the channel coefficients h_{SW}, h_{JW} and h_{R^*W} as $\lambda_{SW}, \lambda_{JW}$, and λ_{R^*W}, respectively,*

then the minimum DEP ξ_{HD}^* in the system is determined as

$$\xi_{HD}^* = \left(1 - (\frac{P\lambda_{SW}}{P_J\lambda_{JW}})^{\frac{P_J\lambda_{JW}}{P_J\lambda_{JW}-P\lambda_{SW}}}\right)\left(1-(\frac{P\lambda_{R^*W}}{P_J\lambda_{JW}})^{\frac{P_J\lambda_{JW}}{P_J\lambda_{JW}-P\lambda_{R^*W}}}\right). \tag{4.23}$$

Proof 4 *Similar to the proof of Proposition 1 in [62], we can take the first derivate of the $\xi_{HD}^{(1)}$ in (4.20) to determine the minimum DEP $\xi_{HD}^{(1),*}$ in the first time slot. We can see that the optimal detection threshold τ_1^* in the first time slot can be obtained as*

$$\tau_1^* = \frac{P\lambda_{SW}P_J\lambda_{JW}\ln\frac{P\lambda_{SW}}{P_J\lambda_{JW}}}{P\lambda_{SW}-P_J\lambda_{JW}} + \sigma_W^2. \tag{4.24}$$

We can easily prove that $\xi_{HD}^{(1)}$ decreases with τ when $\tau \in (0, \tau_1^*)$ while increases when $\tau \in (\tau_1^*, \infty)$. Thus, the minimum DEP $\xi_{HD}^{(1),*}$ is achieved when $\tau = \tau_1^*$, which is determined as

$$\xi_{HD}^{(1),*} = \xi_{HD}^{(1)}(\tau_1^*) = 1 - \left(\frac{P\lambda_{SW}}{P_J\lambda_{JW}}\right)^{\frac{P_J\lambda_{JW}}{P_J\lambda_{JW}-P\lambda_{SW}}}. \tag{4.25}$$

Based on the same analysis as $\xi_{HD}^{(1),*}$, we can prove that the optimal detection threshold τ_2^* and the minimum DEP $\xi_{HD}^{(2),*}$ in the second time slot are determined as

$$\tau_2^* = \frac{P\lambda_{R^*W}P_J\lambda_{JW}\ln\frac{P\lambda_{R^*W}}{P_J\lambda_{JW}}}{P\lambda_{R^*W}-P_J\lambda_{JW}} + \sigma_W^2, \tag{4.26}$$

$$\xi_{HD}^{(2),*} = \xi_{HD}^{(2)}(\tau_2^*) = 1 - \left(\frac{P\lambda_{R^*W}}{P_J\lambda_{JW}}\right)^{\frac{P_J\lambda_{JW}}{P_J\lambda_{JW}-P\lambda_{R^*W}}}. \tag{4.27}$$

By substituting $\xi_{HD}^{(1),*}$ in (4.25) and $\xi_{HD}^{(2),*}$ in (4.27) into ξ_{HD} in (4.17), we complete the proof.

4.2.3 TOP Analysis

Regarding the TOP performance in the scenario when all relays work under the HD mode, we have the following theorem.

Theorem IV.2 *For the concerned system with K relays, target transmission rate r_t, transmit power P for S and R^*, and transmit power P_J for J, its TOP p_{to}^{HD} under the relay selection (4.16) is evaluated as*

$$p_{to}^{HD} = \prod_{k=1}^{K} \left(1 - \eta_3 K_{-1}(\zeta_3)\right), \tag{4.28}$$

where $\eta_3 = 2\sqrt{\mu\nu\gamma_{th}^{HD}(\gamma_{th}^{HD}+1)}e^{-\gamma_{th}^{HD}(\mu+\nu)}$, $\zeta_3 = 2\sqrt{\mu\nu\gamma_{th}^{HD}(\gamma_{th}^{HD}+1)}$, $\mu = \frac{\sigma_{R_k}^2}{P\lambda_{SR_k}}$, $\nu = \frac{\sigma_D^2}{P\lambda_{R_kD}}$, and $\gamma_{th}^{HD} = 2^{2r_t} - 1$. $K_{-1}(\zeta_1) = \frac{1}{\zeta_1}\int_0^\infty e^{(-(t+\frac{\zeta_1^2}{4t}))}dt$ is the modified Bessel function of the second kind with the -1-th order [72, 73].

Proof 5 *When we apply (4.16) to select the optimal relay R^* in the concerned HD relay system, the capacity $C_{R^*}^{HD}$ from S to D is determined as*

$$\begin{aligned} C_{R^*}^{HD} &= \frac{1}{2}\log_2(1+\gamma_{S-R^*-D}) \\ &= \frac{1}{2}\log_2(1+\frac{\gamma_{SR^*}\gamma_{R^*D}}{\gamma_{SR^*}+\gamma_{R^*D}+1}). \end{aligned} \tag{4.29}$$

Based on (4.12) and (4.29), the p_{to}^{HD} can be formulated as

$$p_{to}^{HD} = \mathbb{P}\left\{\gamma_{S-R^*-D} < \gamma_{th}^{HD}\right\}. \tag{4.30}$$

Since γ_{S-R^*-D} is the maximum random variable of the K independent distributed ordered random variables $\gamma_{S-R_1-D}, \gamma_{S-R_2-D}, \ldots, \gamma_{S-R_K-D}$, the p_{to}^{HD} can be determined

by using the order statistics in [77, 78]. Then, we have

$$p_{to}^{HD} = \prod_{k=1}^{K} \mathbb{P}\left\{\gamma_{S-R_k-D} < \gamma_{th}^{HD}\right\}, \tag{4.31}$$

where

$$\begin{aligned}
&\mathbb{P}\left\{\gamma_{S-R_k-D} < \gamma_{th}^{HD}\right\} \\
=&\int_0^{\infty} \mathbb{P}\left(\frac{\gamma_{SR_k} y}{\gamma_{SR_k} + y + 1} < \gamma_{th}^{HD}\right) f_{\gamma_{R_k D}}(y) dy \\
=&\int_0^{\gamma_{th}^{HD}} \int_0^{\infty} f_{\gamma_{SR_k}}(x) f_{\gamma_{R_k D}}(y) dx dy \\
&+ \int_{\gamma_{th}^{HD}}^{\infty} \int_0^{\frac{\gamma_{th}^{HD}(y+1)}{y-\gamma_{th}^{HD}}} f_{\gamma_{SR_k}}(x) f_{\gamma_{R_k D}}(y) dx dy \\
=&1 - \eta_3 K_{-1}(\zeta_3),
\end{aligned} \tag{4.32}$$

$f_{\gamma_{SR_k}}(\cdot)$ and $f_{\gamma_{R_k D}}(\cdot)$ denote the PDF of the random variables γ_{SR_k} and $\gamma_{R_k D}$, respectively. Finally, we can obtain the (4.28) by substituting (4.32) into (4.31).

4.2.4 MCT Analysis

We use T_H^* to denote the MCT in the concerned scenario. From (4.13) we can see that T_H^* is related to ξ_{HD}^* and p_{to}^{HD}, while ξ_{HD}^* is a function of P and P_J and p_{to}^{HD} is a function of P and r_t. Notice that ξ_{HD}^* is independent of r_t and p_{to}^{HD} is independent of P_J, so the optimization in (4.13) can be conducted with the following two steps.

Step 1: We first optimize the transmit power P and jamming power P_J according to (4.23). We can see from (4.23) that the minimum DEP is related to the ratio of P and P_J. Similar to works in [65] and [62], ξ_{HD}^* increases with P_J and decreases with P. If $\frac{P^{\max}}{\xi_{HD}^{*,-1}(\epsilon)} \leq P_J^{\max}$, the optimal transmit power and jamming power are $P^* = P^{\max}$ and $P_J^* = \frac{P^{\max}}{\xi_{HD}^{*,-1}(\epsilon)}$, where $\xi_{HD}^{*,-1}(\epsilon)$ denotes the inverse function of $\xi_{HD}^*(\frac{P}{P_J})$. Otherwise, the optimal transmit power and jamming

power are $P^* = P_J^{\max}\xi_{HD}^{*,-1}(\epsilon)$ and $P_J^* = P_J^{\max}$.

Step 2: Since the optimal transmit power P^* (and thus P_J^*) is obtained in Step 1, this step aims to optimize the target transmission rate r_t to achieve the MCT. Notice it is hard to directly determine the optimal r_t due to complicated relation between the p_{to}^{HD} and r_t. However, we can easily see that a larger $T_H = r_t(1 - p_{to}^{HD})$ is achievable when r_t is too small or too large, so we can apply a searching algorithm to determine the optimal r_t.

Based on the above analysis, we devise the following Algorithm 3 for solving the optimization problem (4.13) and the evaluation of T_H^*.

Algorithm 3: Maximum Covert Throughput Searching Algorithm

Input: Maximum transmit power $P^{\max}$, maximum jamming power $P_J^{\max}$, covert requirement ϵ;

Output: Maximum covert throughput T_H^*, the corresponding optimal transmit power P^*, optimal jamming power P_J^* and optimal target transmission rate r_t^*;

Initialize $r_t = 0$, $T_H^1(P^*, r_t) = T_H^0(P^*, r_t) = 0$ and $\epsilon = 0.1$;
Set the length L for r_t, the iteration index $m = 0$ and the maximum number of iterations $m^{\max}$;
Calculate $\xi_{HD}^{*,-1}(\epsilon)$ according to (4.23) and obtain the $\frac{P}{P_J}$;
if $\frac{P^{\max}}{\xi_{HD}^{*,-1}(\epsilon)} \leq P_J^{\max}$ **then**
    $P^* = P^{\max}$ and $P_J^* = \frac{P^{\max}}{\xi_{HD}^{*,-1}(\epsilon)}$;
else
    $P_J^* = P_J^{\max}$ and $P^* = P_J^{\max}\xi_{HD}^{*,-1}(\epsilon)$;
end
for $m = 2$; $T_H^{m-1}(P^*, r_t) \geq T_H^{m-2}(P^*, r_t)$ and $m \leq m^{\max}$; $m++$ **do**
    $r_t = r_t + L$;
    Calculate $T_H^m(P^*, r_t)$ by substituting (4.28) into $r_t(1 - p_{to}^{HD})$;
end
Obtain the $T_H^* = T_H^{m-2}(P^*, r_t)$ and $r_t^* = T_H^{*,-1}(P^*)$;
return T_H^*, P^*, P_J^* and r_t^*;

4.3 Covert Performance under FD Mode

This section deals with the optimal relay selection and related performance analysis in terms of DEP, TOP and MCT in the scenario when all relays work under the FD mode.

4.3.1 Relay Selection Scheme

When all relays work under the FD mode, we also consider an optimal relay selection scheme where the relay that leads to the largest S-to-D capacity is selected for signal forwarding. However, we need to takes into account the self-interference issue in the relay selection. We use $\gamma_{R_kR_k}$ and $C_{R_k}^{FD}$ to denote the SNR for the self-interference link of $R_k \to R_k$ and end-to-end channel capacity of S-R_k-D, respectively. Then the end-to-end SINR from S to D γ_{S-R_k-D} and $C_{R_k}^{FD}$ are given by

$$\gamma_{S-R_k-D} = \frac{\frac{\gamma_{SR_k}}{\gamma_{R_kR_k}+1}\gamma_{R_kD}}{\frac{\gamma_{SR_k}}{\gamma_{R_kR_k}+1} + \gamma_{R_kD} + 1}, \tag{4.33}$$

$$C_{R_k}^{FD} = \log_2(1 + \gamma_{S-R_k-D}). \tag{4.34}$$

Thus, the optimal relay R^* in this scenario can be determined as

$$R^* = \arg \max_{R_k \in \{R_1,\ldots,R_K\}} \left\{C_{R_k}^{FD}\right\}. \tag{4.35}$$

4.3.2 DEP Analysis

When all relays adopt the FD mode, the transmission between S and D takes only one time slot. We can see from (4.7) and (4.10) that under hypothesis $\mathcal{H}_0$, the received signals at W are the same for both FD and HD modes, so the probability of FA here is the same as that in (4.18). On the other hand, the probability of MD in

the system can be determined as

$$\begin{aligned} p_{MD} &= \mathbb{P}\{(P|h_{SW}|^2 + P|h_{R^*W}|^2 + P_J|h_{JW}|^2 + \sigma_W^2) < \tau \mid \mathcal{H}_1\} \\ &= \begin{cases} \int_0^{\tau-\sigma_W^2} \int_0^{\tau-\sigma_W^2-y} f_{P_J|h_{JW}|^2}(x) f_Y(y) dx dy, & \sigma_W^2 < \tau, \\ 0, & \sigma_W^2 \geq \tau, \end{cases} \end{aligned} \tag{4.36}$$

where $Y = P|h_{SW}|^2 + P|h_{R^*W}|^2$. We notice that the channel gains of λ_{SW} and λ_{R^*W} are same, so the PDF of the random variables $P|h_{SW}|^2$ and $P|h_{R^*W}|^2$ are same, which is given by

$$f_{P|h_{SW}|^2}(x) = \frac{1}{P\lambda_{SW}} e^{-\frac{1}{P\lambda_{SW}}x}, \text{if } 0 < x < \infty. \tag{4.37}$$

By applying the convolution theorem, the PDF of Y is determined as

$$f_Y(y) = \frac{1}{P^2\lambda_{SW}^2} y e^{-\frac{1}{P\lambda_{SW}}y}, \text{if } 0 < y < \infty. \tag{4.38}$$

Thus, the probability of MD can be rewritten as

$$\begin{aligned} p_{MD} &= \mathbb{P}\{(P|h_{SW}|^2 + P|h_{R^*W}|^2 + P_J|h_{JW}|^2 + \sigma_W^2) < \tau \mid \mathcal{H}_1\} \\ &= \begin{cases} \int_0^{\tau-\sigma_W^2} \frac{1}{P^2\lambda_{SW}^2} y e^{-\frac{y}{P\lambda_{SW}}} (1 - e^{-\frac{\tau-\sigma_W^2-y}{P_J\lambda_{JW}}}) dy, & \sigma_W^2 < \tau, \\ 0, & \sigma_W^2 \geq \tau. \end{cases} \end{aligned} \tag{4.39}$$

By substituting the p_{FA} in (4.18) and p_{MD} in (4.39) into (4.11), the DEP of the

FD relay system is given by

$$\xi_{FD}(\tau) = \begin{cases} \int_0^{\tau-\sigma_W^2} y e^{-\frac{y}{P\lambda_{SW}}}(1-e^{-\frac{\tau-\sigma_W^2-y}{P_J\lambda_{JW}}})dy \times \frac{1}{P^2\lambda_{SW}^2} + e^{-\frac{\tau-\sigma_W^2}{P_J\lambda_{JW}}}, & \sigma_W^2 < \tau, \\ 1, & \sigma_W^2 \geq \tau. \end{cases} \tag{4.40}$$

We proceed to analyze the minimum DEF ξ_{FD}^* in the concerned FD system. We can see from (4.40) that $\xi_{FD} = 1$ when $\sigma_W^2 \geq \tau$, so W cannot detect the transmission from $S - R^* - D$ in this case. Hence, we only need to consider the case of $\sigma_W^2 < \tau$. To understand the monotonicity of the DEP, we take the first-order derivation of the ξ_{FD} in (4.40) with respect to τ as

$$\begin{aligned} \frac{\partial \xi_{FD}}{\partial \tau} &= \int_0^{\tau-\sigma_W^2} \frac{y e^{-\frac{y}{P\lambda_{SW}}} e^{-\frac{\tau-\sigma_W^2-y}{P_J\lambda_{JW}}}}{P^2\lambda_{SW}^2 P_J\lambda_{JW}} dy - \frac{e^{-\frac{\tau-\sigma_W^2}{P_J\lambda_{JW}}}}{P_J\lambda_{JW}} \\ &= \frac{e^{-\frac{\tau-\sigma_W^2}{P_J\lambda_{JW}}}}{P_J\lambda_{JW}} \left(\int_0^{\tau-\sigma_W^2} \frac{y e^{-\frac{(P_J\lambda_{JW}-P\lambda_{SW})y}{P\lambda_{SW}P_J\lambda_{JW}}}}{P^2\lambda_{SW}^2} dy - 1 \right). \end{aligned} \tag{4.41}$$

From (4.41) we can determine a detection threshold τ_1 such that when $\tau = \tau_1$ we have $\int_0^{\tau-\sigma_W^2} \frac{y e^{-\frac{(P_J\lambda_{JW}-P\lambda_{SW})y}{P\lambda_{SW}P_J\lambda_{JW}}}}{P^2\lambda_{SW}^2} dy = 1$ and thus $\frac{\partial \xi^{FD}}{\partial \tau} = 0$. We can further see that when $\tau \in (0, \tau_1)$, $\int_0^{\tau-\sigma_W^2} \frac{y e^{-\frac{(P_J\lambda_{JW}-P\lambda_{SW})y}{P\lambda_{SW}P_J\lambda_{JW}}}}{P^2\lambda_{SW}^2} dy < 1$ and $\frac{\partial \xi_{FD}}{\partial \tau} < 0$; when $\tau \in (\tau_1, \infty)$, $\int_0^{\tau-\sigma_W^2} \frac{y e^{-\frac{(P_J\lambda_{JW}-P\lambda_{SW})y}{P\lambda_{SW}P_J\lambda_{JW}}}}{P^2\lambda_{SW}^2} dy > 1$ and $\frac{\partial \xi_{FD}}{\partial \tau} > 0$. Thus, we conclude that ξ_{FD} decrease with τ when $\tau \in (0, \tau_1)$ while ξ_{FD} increase with τ when $\tau \in (\tau_1, \infty)$, so the optimal detection threshold as $\tau^* = \tau_1$ and the corresponding minimum DEP as $\xi_{FD}^* = \xi_{FD}(\tau^*)$.

4.3.3 TOP Analysis

About the TOP of the FD relay system, we have the following theorem.

Theorem IV.3 *For the concerned system with K relays, target transmission rate r_t,*

transmit power P for S and R^*, and transmit power P_J for J, its TOP p_{to}^{FD} under the relay selection (4.35) is evaluated as

$$p_{to}^{FD} = \prod_{k=1}^{K} \left(1 - \int_{\gamma_{th}^{FD}}^{\infty} \eta_4 \nu e^{-\nu y} dy \right), \tag{4.42}$$

where $\eta_4 = \frac{e^{-\frac{\mu(y+1)\gamma_{th}^{FD}}{y-\gamma_{th}^{FD}}}}{1+\frac{\lambda_{R_k R_k}(y+1)\gamma_{th}^{FD}}{\lambda_{SR_k}(y-\gamma_{th}^{FD})}}$ *and* $\gamma_{th}^{FD} = 2^{r_t} - 1$.

Proof 6 *Based on the end-to-end SINR in (4.33), the p_{to}^{FD} can be expressed as*

$$p_{to}^{FD} = \mathbb{P}\{\gamma_{S-R^*-D} < \gamma_{th}^{FD}\}, \tag{4.43}$$

Similar to the analysis of p_{to}^{HD} in (4.31), the p_{to}^{FD} can be determined as

$$p_{to}^{FD} = \prod_{k=1}^{K} \mathbb{P}\{\gamma_{S-R_k-D} < \gamma_{th}^{FD}\}, \tag{4.44}$$

where

$$\begin{aligned}
&\mathbb{P}\{\gamma_{S-R_k-D} < \gamma_{th}^{FD}\} \\
=& \int_0^{\infty} \mathbb{P}\left(\frac{\frac{\gamma_{SR_k}}{\gamma_{R_k R_k}+1} y}{\frac{\gamma_{SR_k}}{\gamma_{R_k R_k}+1} + y + 1} < \gamma_{th}^{FD} \right) f_{\gamma_{R_k D}}(y) dy \\
=& \int_{\gamma_{th}^{FD}}^{\infty} \int_0^{\infty} \int_0^{(s+1)x} f_{\gamma_{SR_k}}(x) f_{\gamma_{R_k R_k}}(s) f_{\gamma_{R_k D}}(y) dx ds dy \\
&+ \int_0^{\gamma_{th}^{FD}} f_{\gamma_{R_k D}}(y) dy \\
=& \int_{\gamma_{th}^{FD}}^{\infty} (1-\eta_4) \nu e^{-\nu y} dy + 1 - e^{-\nu \gamma_{th}^{FD}} \\
=& 1 - \int_{\gamma_{th}^{FD}}^{\infty} \eta_4 \nu e^{-\nu y} dy,
\end{aligned} \tag{4.45}$$

$f_{\gamma_{R_k R_k}}(\cdot)$ denotes the PDF of the random variable $\gamma_{R_k R_k}$.

We then obtain the (4.42) by substituting (4.45) into (4.44).

4.3.4 MCT Analysis

We use T_F^* to denote the MCT in the concerned scenario. Similar to the HD scenario, the optimization in (4.13) in the FD scenario can be also conducted with the following two steps.

Step 1: Similar to the HD scenario, we optimize the parameters of P and P_J based on (4.40) and (4.41). From (4.41) we can obtain τ^* by exploiting the function fsolve() in MATLAB such that $\frac{\partial \xi_{FD}}{\partial \tau} = 0$, and then obtain ξ_{FD}^* by substituting τ^* into ξ_{FD} in (4.40). If $\xi_{FD}^{*,-1}(\epsilon, P^{\max}) \leq P_J^{\max}$, the optimal transmit power and jamming power are $P^* = P^{\max}$ and $P_J^* = \xi_{FD}^{*,-1}(\epsilon, P^{\max})$, where $\xi_{FD}^{*,-1}(\cdot)$ denotes the inverse function of $\xi_{FD}^*(\cdot)$. Otherwise, the optimal transmit power and jamming power are $P^* = \xi_{FD}^{*,-1}(\epsilon, P_J^{\max})$ and $P_J^* = P_J^{\max}$.

Step 2: Similar to the HD scenario, this step aims to determine the optimal target transmission rate r_t^* for achieving the MCT. Since the complicated relation between the TOP p_{to}^{FD} and r_t, it is difficult to directly determine the optimal r_t. However, we can easily find that a larger $T_F = r_t(1 - p_{to}^{FD})$ is achievable when r_t is too small or too large, so we can apply a searching algorithm to obtain the optimal target transmission rate r_t^*.

Based on the above analysis, we can identify P^* and P_J^* by devising the following Algorithm 4 and identify r_t^* by substituting $T_F = r_t(1 - p_{to}^{FD})$ into the steps 9-13 in Algorithm 3, then we complete the optimization problem (4.13) and the evaluation of T_F^*.

4.4 Joint Mode/Relay Selection

This section focuses on the hybrid HD/FD mode scenario where relay can flexibly switch between the HD and FD modes, and present the related optimal relay selection and performance analysis in terms of DEP, TOP and MCT.

Algorithm 4: Optimization Algorithm for Optimal Transmit Power and Jamming Power

Input: Maximum transmit power $P^{\max}$, maximum jamming power $P_J^{\max}$, covert requirement ϵ;

Output: Optimal transmit power P^* and optimal jamming power P_J^*;

Initialize $\epsilon = 0.1$;

Calculate τ^* according to $\frac{\partial \xi_{FD}}{\partial \tau} = 0$ by exploiting the MATLAB function fsolve() and obtain the ξ_{FD}^*;

Calculate $\xi_{FD}^{*,-1}(\epsilon, P^{\max})$ and obtain the corresponding P_J;

if $\xi_{FD}^{*,-1}(\epsilon, P^{\max}) \leq P_J^{\max}$ **then**

  $P^* = P^{\max}$ and $P_J^* = \xi_{FD}^{*,-1}(\epsilon, P^{\max})$;

else

  $P^* = \xi_{FD}^{*,-1}(\epsilon, P_J^{\max})$ and $P_J^* = P_J^{\max}$;

end

return P^* and P_J^* ;

4.4.1 Joint Mode/Relay Selection Scheme

Under the hybrid HD/FD mode, we need to jointly select the optimal relay R^* and its optimal mode M^* for signal forwarding. Based on the same principle of optimal relay in both HD and FD modes, the joint relay and mode selection can be determined as

$$(R^*, M^*) = \arg \max_{R_k \in \{R_1, \ldots, R_K\}} \arg \max_{M \in \{HD, FD\}} \left\{C_{R_k}^{HD}, C_{R_k}^{FD}\right\}. \tag{4.46}$$

4.4.2 DEP Analysis

To ensure the covertness under the hybrid HD/FD mode, we consider the optimal DEP as the minimum one between the minimum DEP in the HD and the minimum DEP in the FD mode. Thus, the minimum DEP $\xi_{H.F}$ under the hybrid HD/FD mode is determined as

$$\xi_{H.F}^* = \min\{\xi_{HD}^*, \xi_{FD}^*\}. \tag{4.47}$$

4.4.3 TOP Analysis

Regarding the TOP under the hybrid HD/FD mode, we have the following theorem.

Theorem IV.4 *For the concerned system with K relays, target transmission rate r_t, transmit power P for S and R^*, and transmit power P_J for J, its TOP $p_{to}^{H.F}$ under the relay selection (4.46) can be evaluated as*

$$p_{to}^{H.F} = \prod_{k=1}^{K}(1 - \eta_5 - \zeta_4 - \psi_2), \tag{4.48}$$

where $\eta_5 = \int_{\gamma_{th}^{FD}}^{\gamma_{th}^{HD}} \frac{\rho\nu e^{-\frac{\mu\gamma_{th}^{FD}(y+1)}{y-\gamma_{th}^{FD}}-\nu y}}{\rho+\frac{\mu\gamma_{th}^{FD}(y+1)}{y-\gamma_{th}^{FD}}} dy$, $\zeta_4 = \int_{\gamma_{th}^{HD}}^{\infty} \rho\nu e^{-\frac{\mu\gamma_{th}^{FD}(y+1)}{y-\gamma_{th}^{FD}}-\nu y} \left(\frac{1-e^{-\left(\frac{\mu\gamma_{th}^{FD}(y+1)}{y-\gamma_{th}^{FD}}+\rho\right)\phi_2}}{\rho+\frac{\mu\gamma_{th}^{FD}(y+1)}{y-\gamma_{th}^{FD}}} \right) dy$ *and* $\psi_2 = \int_{\gamma_{th}^{HD}}^{\infty} \nu e^{-\frac{\mu\gamma_{th}^{HD}(y+1)}{y-\gamma_{th}^{HD}}-\rho\phi_2-\nu y} dy$.

Proof 7 *Based on (4.12) and (4.46), the $p_{to}^{H.F}$ under the hybrid HD/FD mode can be given by*

$$p_{to}^{H.F} = \prod_{k=1}^{K} \mathbb{P}\left\{\max\left\{C_{R_k}^{HD}, C_{R_k}^{FD}\right\} \leq r_t\right\}, \tag{4.49}$$

where

$$
\begin{aligned}
&\mathbb{P}\left\{\max\left(C_{R_k}^{HD}, C_{R_k}^{FD}\right) \le r_t\right\} \\
=&\mathbb{P}\left\{\max\left(\sqrt{1+\frac{\gamma_{SR_k}\gamma_{R_kD}}{\gamma_{SR_k}+\gamma_{R_kD}+1}},\right.\right. \\
&\left.\left.\quad 1+\frac{\frac{\gamma_{SR_k}}{\gamma_{R_kR_k}+1}\gamma_{R_kD}}{\frac{\gamma_{SR_k}}{\gamma_{R_kR_k}+1}+\gamma_{R_kD}+1}\right) \le 2^{r_t}\right\}, \\
=&\mathbb{P}\left\{\underbrace{\gamma_{SR_k}\left(\gamma_{R_kD}-\gamma_{th}^{HD}\right) \le \gamma_{th}^{HD}(\gamma_{R_kD}+1)}_{E_1},\right. \\
&\left.\underbrace{\frac{\gamma_{SR_k}(\gamma_{R_kD}-\gamma_{th}^{FD})}{\gamma_{R_kR_k}+1} \le \gamma_{th}^{FD}(\gamma_{R_kD}+1)}_{E_2}\right\}. \qquad (4.50)
\end{aligned}
$$

Notice that the probability in (4.50) can be divided into three sub-probabilities p_1*,* p_2 *and* p_3 *according to* $\gamma_{R_kD} < \gamma_{th}^{FD}$*,* $\gamma_{th}^{FD} \le \gamma_{R_kD} \le \gamma_{th}^{HD}$*, and* $\gamma_{R_kD} > \gamma_{th}^{HD}$*, respectively. Therefore, we have*

$$\mathbb{P}\left\{\max\left(C_{R_k}^{HD}, C_{R_k}^{FD}\right) \le r_t\right\} = p_1 + p_2 + p_3. \qquad (4.51)$$

When $\gamma_{R_kD} < \gamma_{th}^{FD}$*, we have both* E_1 *and* E_2 *are true, and thus the* p_1 *is calculated as*

$$p_1 = 1 - e^{-\nu\gamma_{th}^{FD}}. \qquad (4.52)$$

When $\gamma_{th}^{FD} \le \gamma_{R_kD} \le \gamma_{th}^{HD}$ *and* $\gamma_{SR_k} \le \frac{\gamma_{th}^{FD}(\gamma_{R_kD}+1)(\gamma_{R_kR_k}+1)}{\gamma_{R_kD}-\gamma_{th}^{FD}}$*, the inequalities of* E_1

and E_2 are true. Thus, the p_2 is calculated as

$$p_2 = \int_{\gamma_{th}^{FD}}^{\gamma_{th}^{HD}} \int_0^{\infty} \int_0^{\frac{\gamma_{th}^{FD}(y+1)(s+1)}{y-\gamma_{th}^{FD}}} f_{\gamma_{SR_k}}(x) f_{\gamma_{R_k R_k}}(s) f_{\gamma_{R_k D}}(y) dx ds dy$$
$$= e^{-\nu\gamma_{th}^{FD}} - e^{-\nu\gamma_{th}^{HD}} - \int_{\gamma_{th}^{FD}}^{\gamma_{th}^{HD}} \frac{\rho\nu e^{-\frac{\mu\gamma_{th}^{FD}(y+1)}{y-\gamma_{th}^{FD}} - \nu y}}{\rho + \frac{\mu\gamma_{th}^{FD}(y+1)}{y-\gamma_{th}^{FD}}} dy. \tag{4.53}$$

When $\gamma_{R_k D} > \gamma_{th}^{HD}$, $\gamma_{SR_k} \leq \frac{\gamma_{th}^{HD}(\gamma_{R_k D}+1)}{\gamma_{R_k D}-\gamma_{th}^{HD}}$ and $\gamma_{SR_k} \leq \frac{\gamma_{th}^{FD}(\gamma_{R_k D}+1)(\gamma_{R_k R_k}+1)}{\gamma_{R_k D}-\gamma_{th}^{FD}}$, we then calculate p_3 as

$$p_3 = \int_{\gamma_{th}^{HD}}^{\infty} \int_0^{\phi_2} \int_0^{\frac{\gamma_{th}^{FD}(y+1)(s+1)}{y-\gamma_{th}^{FD}}} f_{\gamma_{SR_k}}(x) f_{\gamma_{R_k R_k}}(s) f_{\gamma_{R_k D}}(y) dx ds dy$$
$$+ \int_{\gamma_{th}^{HD}}^{\infty} \int_{\phi_2}^{\infty} \int_0^{\frac{\gamma_{th}^{HD}(y+1)}{y-\gamma_{th}^{HD}}} f_{\gamma_{SR_k}}(x) f_{\gamma_{R_k R_k}}(s) f_{\gamma_{R_k D}}(y) dx ds dy, \tag{4.54}$$

where $\phi_2 = \frac{(\gamma_{th}^{HD}-\gamma_{th}^{FD})y}{\gamma_{th}^{FD}(y-\gamma_{th}^{HD})}$. We can see from (4.54), the p_3 can be divided into two parts. The first part Q_3 can be expressed as

$$Q_3 = e^{-\nu\gamma_{th}^{HD}} - \int_{\gamma_{th}^{HD}}^{\infty} \nu e^{-\rho\phi_2 - \nu y} dy - \int_{\gamma_{th}^{HD}}^{\infty} \rho\nu e^{-\frac{\mu\gamma_{th}^{FD}(y+1)}{y-\gamma_{th}^{FD}} - vy}$$
$$\times \left(\frac{1 - e^{-\left(\frac{\mu\gamma_{th}^{FD}(y+1)}{y-\gamma_{th}^{FD}} + \rho\right)\phi_2}}{\rho + \frac{\mu\gamma_{th}^{FD}(y+1)}{y-\gamma_{th}^{FD}}} \right) dy, \tag{4.55}$$

and the second part Q_4 can be expressed as

$$Q_4 = \int_{\gamma_{th}^{HD}}^{\infty} \nu e^{-\rho\phi_2 - \nu y} dy - \int_{\gamma_{th}^{HD}}^{\infty} \nu e^{-\frac{\mu\gamma_{th}^{HD}(y+1)}{y-\gamma_{th}^{HD}} - \rho\phi_2 - \nu y} dy. \tag{4.56}$$

Combining (4.55) and (4.56), we obtain the p_3. Thus, we can complete the derivation of $p_{to}^{H.F}$ in (4.49) based on $\mathbb{P}\left\{\max\left(C_{R_k}^{HD}, C_{R_k}^{FD}\right) \leq r_t\right\}$ in (4.51), p_1 in (4.52), p_2 in (4.53) and p_3.

4.4.4 MCT Analysis

To identify the optimal transmit power P^*, optimal jamming power P_J^* and optimal target transmission rate r_t^*, the optimization problem on $T_{H.F}^*$ involves two sub-optimization problems. According to (4.47), the minimum DEP of this considered relay system with hybrid HD/FD mode is the minimum of ξ_{HD}^* and ξ_{FD}^*. Therefore, the P^* and P_J^* are determined using steps 3-8 in Algorithm 3 or using Algorithm 4. We then analyze the monotonicity of the $p_{to}^{H.F}$ in (4.48) with respect of r_t. We note that the expression in (4.48) is too complex to obtain the closed-form solutions. Hence, we can solve this optimization problem by substituting $T_{H.F} = r_t(1 - p_{to}^{H.F})$ into the steps 9-13 in Algorithm 3.

4.5 Numerical Results

This section provides extensive numerical results to validate our theoretical models as well as to illustrate the impacts of system parameters on DEP ξ, TOP p_{to}, and MCT T^*. For comparison, in addition to the optimal relay selection (ORS) for fixed FD or HD mode and the joint relay/mode selection concerned in this paper, we also consider the random relay selection (RRS) with random transmission (RT) mode as benchmark. Unless otherwise stated, in the numerical results, the related parameters are set as $P^{\max} = 1\text{W}$, $P_J^{\max} = 10\text{W}$, $\sigma_R^2 = \sigma_D^2 = \sigma_W^2 = 10^{-4}\text{W}$, $\lambda_{AB} = 1$ and $\lambda_{R_k R_k} = 1$.

4.5.1 DEP Performance

We can see from (4.47) the DEP for the joint HD/FD mode is determined by the minimum of the DEPs in the HD and FD modes, so we show in Fig. 4.2 the simulation and theoretical results for ξ vs. τ under HD and FD modes to validate our theoretical models on DEP. We can observe from Fig. 4.2 that the simulation

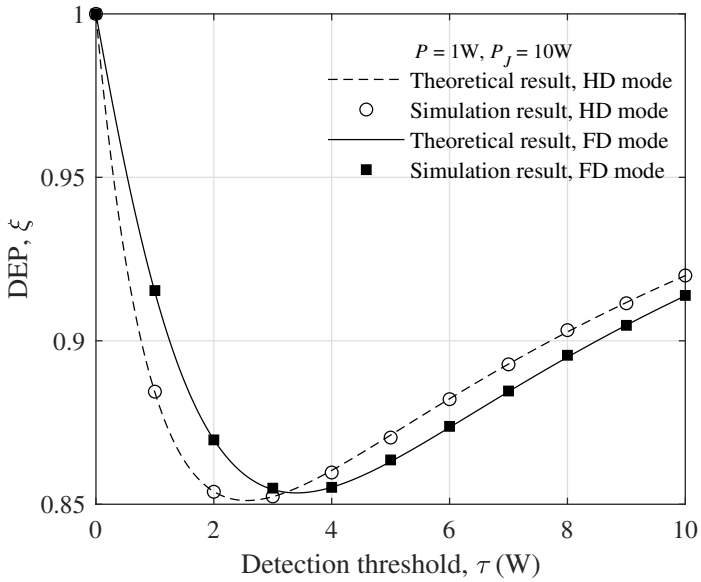

Figure 4.2: DEP ξ vs. detection threshold τ.

results match well with the results evaluated by the proposed theoretical models, indicating that our theoretical models can accurately depict the DEP performance of the concerned system. We can find that for fixed mode, as τ increases, ξ first decreases and then increases, and an optimal τ exists that leads to the minimum ξ. The results can be explained as follows. Note that ξ in (4.11) is the sum of p_{FA} and p_{MD}, where p_{FA} decreases with the increase of τ while p_{MD} increases with the increase of τ. Thus, as τ is relatively small, the p_{FA} dominates ξ, leading to the decrease of ξ with τ. However, as τ further increases, the p_{MD} dominates ξ, leading to the increase of ξ.

4.5.2 TOP Performance

We show in Fig. 4.3 both the theoretical and simulation results for TOP p_{to} vs. target transmission rate r_t under the settings of $P = 0.5$W and $K = 4$. From Fig. 4.3, we can see that the simulation results agree well with the theoretical ones, so our theoretical models can accurately describe the TOP performance of the concerned

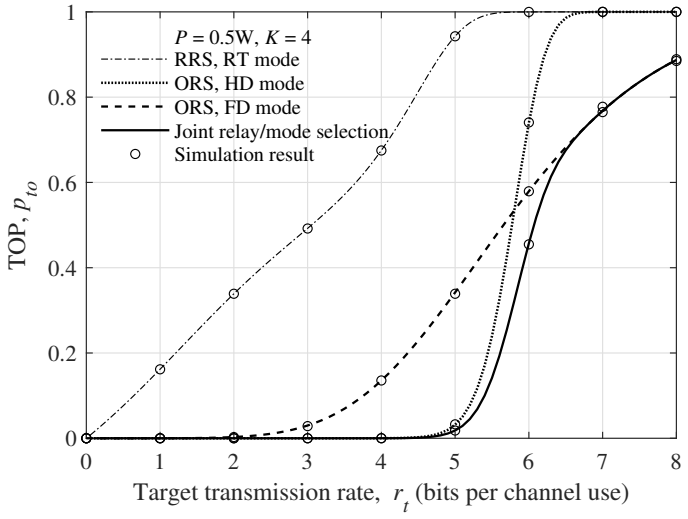

Figure 4.3: TOP p_{to} vs. target transmission rate r_t.

system. We can also observe from Fig. 4.3 that p_{to} increases as r_t increases. The reason is that when r_t becomes larger, D cannot decode all the received signals reliably, leading to an increased p_{to}. From Fig. 4.3 we can further observe that p_{to}^{HD} is less than p_{to}^{FD} when r_t is relatively small, but when r_t increases beyond a threshold, then p_{to}^{HD} becomes greater than p_{to}^{FD}. This is because when the instantaneous channel capacity between S and D is relatively small, the capacity reduction from the self-interference in the FD mode becomes significant, leading to a higher TOP in the FD mode than that in the HD mode. However, when the instantaneous channel capacity between S and D is relatively large, the impact of the self-interference on the capacity in the FD mode is less significant, so the overall capacity between S and D in the FD mode will be larger than that in the HD mode, resulting that $p_{to}^{FD} < p_{to}^{HD}$.

We then show in Fig. 4.4 how p_{to} varies with P under the settings of $r_t = 5$ bits per channel use and $K = 4$. It can be seen from Fig. 4.4 that p_{to} decreases as P increases. The reason is that as P increases, the channel capacity between S and D becomes larger, leading to a reduced p_{to}. From Fig. 4.4 we can further observe that p_{to}^{HD} is higher than p_{to}^{FD} when P is relatively small, but as P increases then p_{to}^{HD}

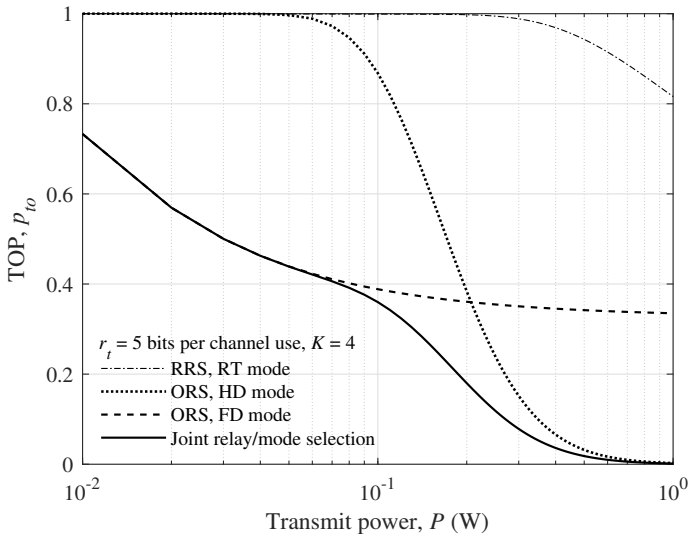

Figure 4.4: TOP p_{to} vs. transmission power P.

tends to be lower than p_{to}^{FD}. This is because as P increases, the self-interference effect in FD mode becomes stronger, which will result in a reduced channel capacity of S-to-D, and thus a higher p_{to}^{FD}. The results in Fig. 4.3 and Fig. 4.4 also indicate that the RRS with the RT mode always achieves the worst TOP performance, and ORS under FD outperforms that under HD in some cases (e.g., when r_t is relatively large or when P is relatively small) and then becomes opposite in other cases. However, the joint relay/mode selection, which takes the advantages of both relay selection and mode selection, always leads to the best TOP performance and thus can significantly improve the overall transmission performance for the covert relay communication between S and D.

4.5.3 MCT Performance

We summarize in Fig. 4.5 and Fig. 4.6 how the MCT T^* varies with the covertness requirement and jamming power. We can see from Fig. 4.5 that as ϵ increases, T^* first increases and then keeps unchanged. The reason is that P increases when ϵ increases, leading to a larger T^*. Since P cannot be larger than $P^{\max}$, the T^* keeps unchanged

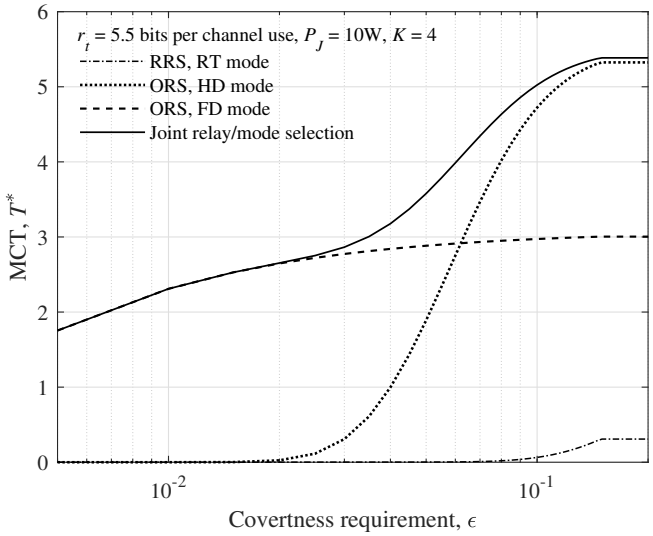

Figure 4.5: MCT T^* vs. covertness requirement ϵ.

when ϵ increases further. We can also observe from Fig. 4.5 that as ϵ increases, T_F^* is first larger than T_H^* and then becomes smaller than T_H^*. The reasons behind these observations are similar to those illustrated in Fig. 4.4. In addition, From Fig. 4.6 we can also notice that as P_J increases, T^* first increases and then keeps unchanged. The reason for this phenomenon is that a higher P_J will increase the uncertainty of W'detection and also lead to a larger P, thus result in a larger T^*. Since P cannot be larger than $P^{\max}$, the T^* remains constant as P_J increases further.

Fig. 4.7 illustrates the impact of r_t on MCT T^* under the settings of $P_J = 10$W, $\epsilon = 0.1$ and $K = 4$. We can see from Fig. 4.7 that as r_t increases, T^* first increases and then remains unchanged. This is due to the fact that the effects of r_t on T^* in (4.13) are two-fold. When r_t is in the region smaller than the channel capacity, there will be no transmission outage event and T^* increases as r_t increases. However, when r_t increases to be in the region larger than the channel capacity, p_{to} increases as r_t increases, leading to a lower $r_t(1 - p_{to})$. We can also see from Fig. 4.7 that there for each scenario, there exists an optimal setting of r_t to achieve T^*, beyond which T^* cannot be further improved. Again, the results in Fig. 4.5-Fig. 4.7 indicate clearly

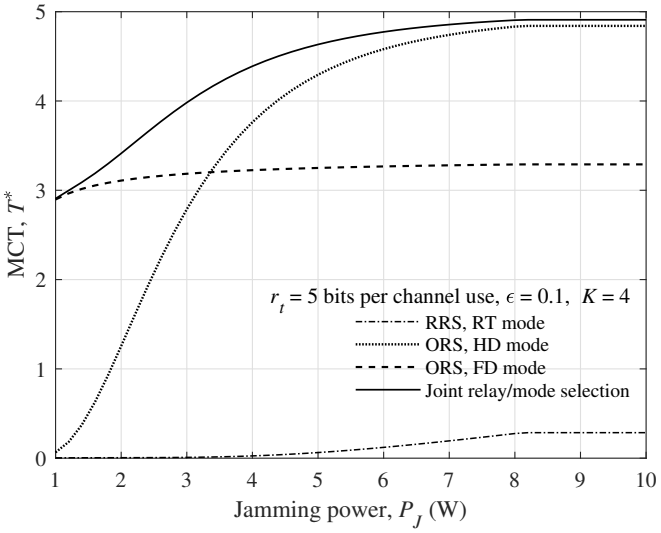

Figure 4.6: MCT T^* vs. jamming power P_J.

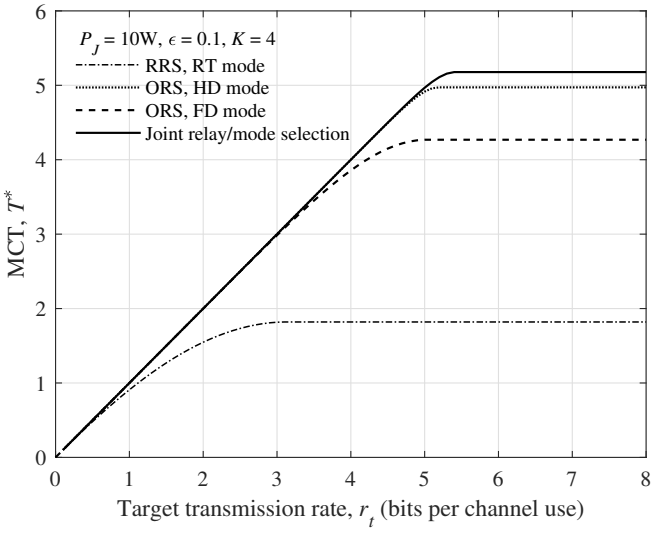

Figure 4.7: MCT T^* vs. target transmission rate r_t.

that compared to the simple RRS with RT mode, the ORS under fixed HD mode or FD mode can lead to a significant improvement in MCT, and such improvement can be further enhanced by adopting the joint relay/mode selection.

4.6 Summary

This chapter investigated the relay selection under fixed HD or FD mode, and further the joint mode/relay selection in an AF wireless relay system with multiple relays. The related performance modeling and optimal parameter setting issues are addressed as well. Our results in this chapter indicate although the covert relay communication performance in the system can be significantly improved by applying the optimal relay selection under fixed HD or FD mode, such improvement can be further enhanced from the joint mode/relay selection. It is expected this work can shed lights on the performance enhancement for covert relay communication in wireless systems.

CHAPTER V

Joint Mode/Relay Selection in Buffer-Aided Multi-Relay Systems

This chapter further considers covert relay communication in a buffer-aided multi-relay system consisting of one source, multiple relays, one destination, one friendly jammer and one warden, where each relay with DF forwarding mode is equipped with an infinite buffer. For the scenarios when all relays work in either fixed HD or FD transmission mode, we develop the corresponding relay selection schemes for covert relay communication in the system. For the scenario when all relays work in the hybrid HD/FD transmission mode, we propose a joint mode/relay selection scheme for covert relay communication in the system. We also develop related theoretical models for performance analysis under each scheme, and explore the optimal designs of transmit power, jamming power and target transmission rate for CT maximization. Finally, we provide extensive numerical results to illustrate the impact of joint mode/relay selection on covert relay communication in such a buffer-aided multi-relay system.

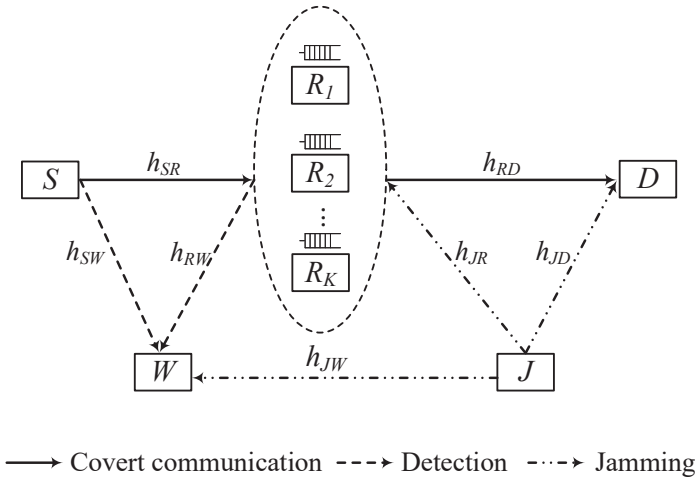

Figure 5.1: System model.

5.1 System Model and Performance Metrics

5.1.1 Communication Scenario and Assumptions

As shown in Fig. 5.1, we consider a two-hop buffer-aided multi-relay system consisting of one source S, K DF buffer-aided relays $R_1, R_2, \ldots, R_K$, one destination D, one friendly jammer J, and one warden W. We assume that there is no direct link between S and D so that the communication from S to D is established via relays subject to the detection of the warden W. Following [79, 80], R_k is assumed to have an infinite buffer for storing packets. Here, the buffer size is defined by the number of packets. For simplicity, each relay is assumed to store sufficient packets to ensure the buffer is not empty. All packets in the buffer follow the First-In-First-Out (FIFO) discipline. We assume that each of S, D, J and W is equipped with a single omnidirectional antenna and operates in the HD mode, while each relay is equipped with a pair of transmit-receive antennas so that it can adopt the HD or FD modes. We focus on three scenarios when all relays work under either the HD, FD or hybrid HD/FD mode, respectively. In the scenario when all relays work under the HD mode, one relay is selected to receive and store the signal from S in one time slot and

one relay is selected to forward a signal to D in the next time slot. In the scenario when all relays work under the FD mode, relays are selected to receive and forward signals simultaneously, but it suffers from self-interference. In the scenario when all relays work under the hybrid HD/FD mode, the selected relays can select between the HD and FD modes to transmit the received signal to D. We apply the common assumption in [74–76] that J sends Gaussian jamming signals using a pseudo-random sequence in all time slots, which is known to all nodes except W. Thus, only W experiences interference from jamming signals while other nodes can cancel out the jamming signal from the received signals.

We consider the quasi-static Rayleigh fading channel model, where the channel coefficient of a link remains constant in one slot but changes independently and randomly from one slot to another. We denote the channel coefficient from node A to B as h_{AB}, which is a zero-mean circularly symmetric complex Gaussian random variable with variance $E[|h_{AB}|^2] = \lambda_{AB}$. We consider the scenario that S, R_k and J send public pilot signals so the instantaneous CSI of h_{SR_k} and h_{R_kD} are known by R_k and D. W knows only the statistical CSI of h_{SW}, h_{RW} and h_{JW}.

5.1.2 Transmission Process

5.1.2.1 HD mode

In the HD mode, the transmission from S to D needs two time slots. In the first time slot, S encodes the signal into n symbols $\mathbf{x}_S(n)$ and transmits them to the selected relay R^{br}, where each symbol $x_S(i)(i = 1, 2, \ldots, n)$ satisfies the unit power constraint $E[|x_S(i)|^2] = 1$. Here, $E[\cdot]$ denotes the expected value of a random variable. In the next time slot, the selected relay R^{bt} forwards the re-encoded symbol $x_{R^{bt}}(i)$ in its buffer, where each symbol $x_{R^{bt}}(i)(i = 1, 2, \ldots, n)$ satisfies the unit power constraint $E[|x_{R^{bt}}(i)|^2] = 1$. Thus, the i-th symbols received at R^{br} and D are given

by

$$y_{R^{br}}(i) = \sqrt{P} h_{SR^{br}} x_S(i) + n_{R^{br}}(i), \tag{5.1}$$

$$y_D(i) = \sqrt{P} h_{R^{bt}D} x_{R^{bt}}(i) + n_D(i), \tag{5.2}$$

where P denotes the transmit power of S and R^{bt} subject to the maximum transmit power constraint $P^{\max}$; $n_{R^{br}}(i)$ and $n_D(i)$ are the AWGN at R^{br} and D with zero mean and variance $\sigma^2_{R^{br}}$ and σ^2_D, respectively, i.e., $n_{R^{br}}(i) \sim \mathcal{CN}(0, \sigma^2_{R^{br}})$ and $n_D(i) \sim \mathcal{CN}(0, \sigma^2_D)$.

5.1.2.2 FD mode

In the FD mode, the transmission between S and D can be implemented in one time slot, in which S transmits and stores n symbols to R^{br} while R^{bt} simultaneously forwards the received signals in its buffer to D. R^{br} and R^{bt} can be the same relay. Thus, we note that the expressions of the received symbols at D is the same as those in (5.2). The i-th symbol received at R^{br} is given by

$$y_{R^{br}}(i) = \sqrt{P} h_{SR^{br}} x_S(i) + \sqrt{P} h_{R^{br}R^{bt}} x_{R^{bt}}(i) + n_{R^{br}}(i). \tag{5.3}$$

5.1.3 Detection at Warden

To conduct the detection, we assume that W uses a radiometer as a detector to determine whether S or R^{bt} has transmitted or not [11, 61]. In the binary hypothesis testing problem faced by W, the null hypothesis $\mathcal{H}_0$ states that S or R^{bt} did not conduct transmission, while the alternative hypothesis $\mathcal{H}_1$ states that they conducted transmission.

5.1.3.1 HD mode

In the first time slot, when $\mathcal{H}_0$ is true, W only receives the jamming signal with transmit power P_J following a continuous uniform distribution over the interval $[0, P_J^{\max}]$, having a PDF given by

$$f_{P_J}(x) = \begin{cases} \frac{1}{P_J^{\max}}, & 0 \leq P_J \leq P_J^{\max}, \\ 0, & otherwise. \end{cases} \tag{5.4}$$

While $\mathcal{H}_1$ is true, W receives both the covert signal from S and the jamming signal from J. Thus, the signal $y_W^{(1)}(i)$ received at W in the first time slot is determined as

$$y_W^{(1)}(i) = \begin{cases} \sqrt{P_J} h_{JW} x_J(i) + n_W(i), & \mathcal{H}_0, \\ \sqrt{P} h_{SW} x_S(i) + \sqrt{P_J} h_{JW} x_J(i) + n_W(i), & \mathcal{H}_1, \end{cases} \tag{5.5}$$

where $x_J(i)$ is the transmitted symbol in the i-th channel use with the constraint of $E[|x_J(i)|^2] = 1$, $i = 1, 2, \ldots, n$; $n_W(i)$ is the AWGN at W with zero mean and variance σ_W^2, i.e., $n_W(i) \sim \mathcal{CN}(0, \sigma_W^2)$. Similar to $y_W^{(1)}(i)$, the signal $y_W^{(2)}(i)$ received at W in the second time slot can be determined as

$$y_W^{(2)}(i) = \begin{cases} \sqrt{P_J} h_{JW} x_J(i) + n_W(i), & \mathcal{H}_0, \\ \sqrt{P} h_{R^{bt}W} x_{R^{bt}}(i) + \sqrt{P_J} h_{JW} x_J(i) + n_W(i), & \mathcal{H}_1. \end{cases} \tag{5.6}$$

To conduct a detection, W uses the total received power in one time slot to decide whether the covert communication exists or not. The decision rule in one time slot is given by

$$\bar{P}_W \triangleq \frac{1}{n} \sum_{i=1}^{n} |y_W^a(i)|^2 \underset{\mathcal{D}_0}{\overset{\mathcal{D}_1}{\gtrless}} \tau, \tag{5.7}$$

where $a \in \{(1), (2)\}$; τ is the detection threshold for the average power of received

signals $\bar{P}_W$; $\mathcal{D}_0$ and $\mathcal{D}_1$ are the binary decisions that denote W makes a decision when he accepts $\mathcal{H}_0$ and $\mathcal{H}_1$, respectively.

5.1.3.2 FD mode

When $\mathcal{H}_0$ is true, W receives only the jamming signal. When $\mathcal{H}_1$ is true, W receives the signal from S, the re-encoded signal from R^{bt} and the jamming signal in one time slot. Thus, the signal received at W is

$$y_W(i) = \begin{cases} \sqrt{P_J} h_{JW} x_J(i) + n_W(i), & \mathcal{H}_0, \\ \sqrt{P} h_{SW} x_S(i) + \sqrt{P} h_{R^{bt}W} x_{R^{bt}}(i) + \sqrt{P_J} h_{JW} x_J(i) + n_W(i), & \mathcal{H}_1. \end{cases} \tag{5.8}$$

Thus, under the FD mode, we can obtain the DEP ξ_{FD} by applying the rule in (5.7) to decide on the received signal in (5.8).

5.1.4 Performance Metrics

The performance metrics adopted in this study are DEP, TOP, and MCT. The DEP involves two types of detection errors in W's hypothesis test, i.e., FA and MD. FA means that W's decision is $\mathcal{D}_1$ while $\mathcal{H}_0$ is true, and MD means that W's decision is $\mathcal{D}_0$ while $\mathcal{H}_1$ is true. We use p_{FA} and p_{MD} to denote the probability of FA and MD, respectively. Then $p_{FA} = \mathbb{P}(\mathcal{D}_1|\mathcal{H}_0)$ and $p_{MD} = \mathbb{P}(\mathcal{D}_0|\mathcal{H}_1)$, and DEP ξ is given by

$$\xi = p_{FA} + p_{MD} = \mathbb{P}(\mathcal{D}_1|\mathcal{H}_0) + \mathbb{P}(\mathcal{D}_0|\mathcal{H}_1). \tag{5.9}$$

When the target transmission rate r_t is greater than the channel capacity C between S and D, transmission outage happens in the sense that D cannot recover the messages reliably [37]. We use p_{to} to denote the TOP, which is determined as

$$p_{to} = \mathbb{P}\left\{C < r_t\right\}. \tag{5.10}$$

We use the MCT T^* to depict the covert performance of our system, which is defined as

$$T^* = \max_{P,P_J,r_t} \quad r_t\,(\,1 - p_{to}\,), \tag{5.11a}$$

$$\text{s.t.} \quad \xi^* \geq 1 - \epsilon, \tag{5.11b}$$

$$0 \leq P \leq P^{\max}, \tag{5.11c}$$

$$0 \leq P_J \leq P_J^{\max}, \tag{5.11d}$$

where ϵ denotes the covertness requirement, and $P^{\max}$ and $P_J^{\max}$ represent the maximum allowed transmit power and the maximum allowed jamming power, respectively.

5.2 Covert Performance under HD Mode

In this section, we first present the relay selection scheme in the HD mode and then provide the evaluations of DEP, TOP and MCT in this scenario.

5.2.1 Relay Selection Scheme

When all relays are equipped with buffers, they can store the signal received from S and do not have to re-transmit them immediately in the next time slot. We consider the relay selection scheme where the relay with the best $S-R$ link for reception and the relay with the best $R-D$ link for transmission. We use γ_{SR_k} and γ_{R_kD} to denote the SNR for the $S \to R_k$ and $R_k \to D$ links, respectively. Thus, the best relay R^{br} for reception and the best relay R^{bt} for transmission in this scenario can be determined as

$$R^{br} = \arg \max_{R_k \in \{R_1,\ldots,R_K\}} \{\gamma_{SR_k}\}, \tag{5.12}$$

$$R^{bt} = \arg \max_{R_k \in \{R_1,\ldots,R_K\}} \{\gamma_{R_k D}\}. \tag{5.13}$$

5.2.2 DEP Analysis

Notice that the DEP defined in (5.9) describes the detection performance in one time slot, but the detection of W in HD relay system involves two consecutive time slots. Thus, the DEP ξ_{HD} under the HD mode can be determined as

$$\xi_{HD} = \xi_{HD}^{(1)} \xi_{HD}^{(2)}, \tag{5.14}$$

where $\xi_{HD}^{(1)}$ and $\xi_{HD}^{(2)}$ denote the DEP in the first time and second time slots, respectively.

We first derive the DEP $\xi_{HD}^{(1)}$ in the first time slot. From the decision rule in (5.7), a FA occurs when S does not transmit but W makes decision of $\mathcal{D}_1$ by $\bar{P}_W \geq \tau$. Based on the received signal in (5.5) at W, we can see that the probability $p_{FA}^{(1)}$ of FA in the first time slot is given by

$$\begin{aligned} p_{FA}^{(1)} &= \mathbb{P}\{(P_J|h_{JW}|^2 + \sigma_W^2)\frac{\chi_{2n}^2}{n} \geq \tau \,|\, \mathcal{H}_0\} \\ &= \mathbb{P}\{(P_J|h_{JW}|^2 + \sigma_W^2) \geq \tau \,|\, \mathcal{H}_0\} \\ &= \begin{cases} 1, & \tau \leq \sigma_W^2, \\ 1 - \frac{\tau - \sigma_W^2}{P_J^{\max}|h_{JW}|^2}, & \sigma_W^2 < \tau \leq \rho_1, \\ 0, & \tau > \rho_1, \end{cases} \end{aligned} \tag{5.15}$$

where $\rho_1 = P_J^{\max}|h_{JW}|^2 + \sigma_W^2$; χ_{2n}^2 is a chi-squared random variable with $2n$ degrees of freedom. From the Strong Law of Large Numbers and Lebesgue's Dominated Convergence Theorem [70] we know $\frac{\chi_{2n}^2}{n}$ can be approximated with 1 when $n \to \infty$.

From the decision rule in (5.7), an MD occurs when S transmits but W makes decision of $\mathcal{D}_0$ by $\bar{P}_W < \tau$. Thus, the probability $p_{MD}^{(1)}$ of MD in the first time slot is

given by

$$p_{MD}^{(1)} = \mathbb{P}\{(P|h_{SW}|^2 + P_J|h_{JW}|^2 + \sigma_W^2) < \tau \,|\, \mathcal{H}_1\}$$
$$= \begin{cases} 0, & \tau \leq \rho_2, \\ \frac{\tau - \rho_2}{P_J^{\max}|h_{JW}|^2}, & \rho_2 < \tau \leq \rho_3, \\ 1, & \tau > \rho_3, \end{cases} \tag{5.16}$$

where $\rho_2 = P|h_{SW}|^2 + \sigma_W^2$; $\rho_3 = P|h_{SW}|^2 + P_J^{\max}|h_{JW}|^2 + \sigma_W^2$.

By substituting $p_{FA}^{(1)}$ in (5.15) and $p_{MD}^{(1)}$ in (5.16) into (5.9), we can obtain the DEP $\xi_{HD}^{(1)}$ in the first time slot. We note that the value of ρ_1 in $p_{FA}^{(1)}$ and ρ_2 in $p_{MD}^{(1)}$ brings two cases (i.e., $\rho_1 < \rho_2$ and $\rho_1 \geq \rho_2$) to determine the $\xi_{HD}^{(1)}$. When $\rho_1 < \rho_2$, the $\xi_{HD}^{(1)}$ is determined as

$$\xi_{HD}^{(1)} = \begin{cases} 1, & \tau \leq \sigma_W^2, \\ 1 - \frac{\tau - \sigma_W^2}{P_J^{\max}|h_{JW}|^2}, & \sigma_W^2 < \tau \leq \rho_1, \\ 0, & \rho_1 < \tau \leq \rho_2, \\ \frac{\tau - \rho_2}{P_J^{\max}|h_{JW}|^2}, & \rho_2 < \tau \leq \rho_3, \\ 1, & \tau > \rho_3. \end{cases} \tag{5.17}$$

We can see from (5.17) that as τ increases, $\xi_{HD}^{(1)}$ decreases when $\tau \in (\sigma_W^2, \rho_1]$ and $\xi_{HD}^{(1)}$ increases when $\tau \in (\rho_2, \rho_3]$. Thus, the minimum DEP $\xi_{HD}^{(1),*} = 0$ with the optimal

detection threshold $\tau_1^* \in [\rho_1, \rho_2]$. When $\rho_1 \geq \rho_2$, the $\xi_{HD}^{(1)}$ is determined as

$$\xi_{HD}^{(1)} = \begin{cases} 1, & \tau \leq \sigma_W^2, \\ 1 - \frac{\tau - \sigma_W^2}{P_J^{\max}|h_{JW}|^2}, & \sigma_W^2 < \tau \leq \rho_2, \\ 1 - \frac{P|h_{SW}|^2}{P_J^{\max}|h_{JW}|^2}, & \rho_2 < \tau \leq \rho_1, \\ \frac{\tau - \rho_2}{P_J^{\max}|h_{JW}|^2}, & \rho_1 < \tau \leq \rho_3, \\ 1, & \tau > \rho_3. \end{cases} \tag{5.18}$$

Following (5.18), we note that when $\tau \in (\sigma_W^2, \rho_2]$, $\xi_{HD}^{(1)}$ decreases with τ and when $\tau \in (\rho_1, \rho_3]$, $\xi_{HD}^{(1)}$ increases with τ. Thus, the minimum DEP $\xi_{HD}^{(1),*} = 1 - \frac{P|h_{SW}|^2}{P_J^{\max}|h_{JW}|^2}$ with $\tau_1^* \in [\rho_2, \rho_1]$. Then, the minimum DEP in the first time slot is given by

$$\xi_{HD}^{(1),*} = \begin{cases} 0, & \rho_1 < \rho_2, \\ 1 - \frac{P|h_{SW}|^2}{P_J^{\max}|h_{JW}|^2}, & \rho_1 \geq \rho_2. \end{cases} \tag{5.19}$$

Since S and J do not know the instantaneous channel coefficient h_{SW} and h_{JW}, we consider the expected value of minimum DEP at W. Let $\bar{\xi}^*$ denote the average minimum DEP, which is given in the following theorem.

Theorem V.1 *Consider the covert communication in an HD relay system with transmit power P for S, transmit power P_J for J. If we denote the variance of the channel coefficients h_{SW} and h_{JW} as λ_{SW} and λ_{JW}, respectively, then the minimum DEP $\bar{\xi}_{HD}^{(1),*}$ in the first time slot is determined as*

$$\bar{\xi}_{HD}^{(1),*} = \frac{P_J^{\max}\lambda_{JW}}{P_J^{\max}\lambda_{JW} + P\lambda_{SW}} \left[1 - \frac{P\lambda_{SW}}{P_J^{\max}\lambda_{JW}} \left[\ln\left(\frac{P_J^{\max}\lambda_{JW}}{P\lambda_{SW}} + 1\right) - \frac{P_J^{\max}\lambda_{JW}}{P_J^{\max}\lambda_{JW} + P\lambda_{SW}}\right]\right]. \tag{5.20}$$

Proof 8 *We know that $|h_{SW}|^2$ and $|h_{JW}|^2$ follow exponential distributions with ex-*

pected values λ_{SW} and λ_{JW}. Based on (5.19), we have

$$\begin{aligned}\bar{\xi}_{HD}^{(1),*} &= \mathbb{E}[\xi_{HD}^{(1),*}] \\ &= \mathbb{P}\{\rho_1 < \rho_2\}\mathbb{E}[0|\rho_1 < \rho_2] + \mathbb{P}\{\rho_1 \geq \rho_2\}\mathbb{E}[1 - \frac{P|h_{SW}|^2}{P_J^{\max}|h_{JW}|^2}|\rho_1 \geq \rho_2] \\ &= \mathbb{P}\{\rho_1 \geq \rho_2\}\mathbb{E}[1 - \frac{P|h_{SW}|^2}{P_J^{\max}|h_{JW}|^2}|\rho_1 \geq \rho_2], \end{aligned} \tag{5.21}$$

where

$$\begin{aligned}\mathbb{P}\{\rho_1 \geq \rho_2\} &= \mathbb{P}\{P_J^{\max}|h_{JW}|^2 > P|h_{SW}|^2\} \\ &= \int_0^{\infty}\int_0^{\frac{P_J^{\max}y}{P}} f_{|h_{SW}|^2}(x)f_{|h_{JW}|^2}(y)dxdy \\ &= \frac{P_J^{\max}\lambda_{JW}}{P_J^{\max}\lambda_{JW} + P\lambda_{SW}} \end{aligned} \tag{5.22}$$

and

$$\begin{aligned}&\mathbb{E}\left[1 - \frac{P|h_{SW}|^2}{P_J^{\max}|h_{JW}|^2}|\rho_1 \geq \rho_2\right] \\ &= 1 - \mathbb{E}\left[\frac{P|h_{SW}|^2}{P_J^{\max}|h_{JW}|^2}|\rho_1 \geq \rho_2\right] \\ &= 1 - \frac{P}{P_J^{\max}}\int_0^{\infty}\int_0^{\frac{P_J^{\max}y}{P}} \frac{x}{y} f_{|h_{SW}|^2}(x)f_{|h_{JW}|^2}(y)dxdy \\ &= 1 - \frac{P\lambda_{SW}}{P_J^{\max}\lambda_{JW}}\left[\ln\left(\frac{P_J^{\max}\lambda_{JW}}{P\lambda_{SW}} + 1\right) - \frac{P_J^{\max}\lambda_{JW}}{P_J^{\max}\lambda_{JW} + P\lambda_{SW}}\right]. \end{aligned} \tag{5.23}$$

Substituting (5.22) and (5.23) into (5.21), we can obtain (5.20).

Based on similar analysis as that in the first time slot, we can see that the probability $\xi_{HD}^{(2)}$ is similar to $\xi_{HD}^{(1)}$. Thus, the minimum DEP in the second time slot is

given by

$$\xi_{HD}^{(2),*} = \begin{cases} 0, & \rho_1 < \rho_4, \\ 1 - \frac{P|h_{R^{bt}W}|^2}{P_J^{\max}|h_{JW}|^2}, & \rho_1 \geq \rho_4. \end{cases} \tag{5.24}$$

where $\rho_4 = P|h_{R^{bt}W}|^2 + \sigma_W^2$ and $\rho_5 = P|h_{R^{bt}W}|^2 + P_J^{\max}|h_{JW}|^2 + \sigma_W^2$. Based on similar analysis as that in (V.1), the minimum DEP $\bar{\xi}_{HD}^{(2),*}$ in the second time slot is determined as

$$\bar{\xi}_{HD}^{(2),*} = \frac{P_J^{\max}\lambda_{JW}}{P_J^{\max}\lambda_{JW} + P\lambda_{R^{bt}W}}\left[1 - \frac{P\lambda_{R^{bt}W}}{P_J^{\max}\lambda_{JW}}\left[\ln\left(\frac{P_J^{\max}\lambda_{JW}}{P\lambda_{R^{bt}W}} + 1\right) - \frac{P_J^{\max}\lambda_{JW}}{P_J^{\max}\lambda_{JW} + P\lambda_{R^{bt}W}}\right]\right]. \tag{5.25}$$

In this work, we consider the worst-case communication scenario where W can achieve the minimum DEP by adopting the optimal detection thresholds in each time slot. By substituting $\bar{\xi}_{HD}^{(1),*}$ in (5.20) and $\bar{\xi}_{HD}^{(2),*}$ in (5.25) into ξ_{HD} in (5.14), the DEP $\bar{\xi}_{HD}^{*}$ in the system is

$$\begin{aligned} \bar{\xi}_{HD}^{*} =& \frac{P_J^{\max}\lambda_{JW}}{P_J^{\max}\lambda_{JW} + P\lambda_{R^{bt}W}}\left[1 - \frac{P\lambda_{R^{bt}W}}{P_J^{\max}\lambda_{JW}}\left[\ln\left(\frac{P_J^{\max}\lambda_{JW}}{P\lambda_{R^{bt}W}} + 1\right) - \frac{P_J^{\max}\lambda_{JW}}{P_J^{\max}\lambda_{JW} + P\lambda_{R^{bt}W}}\right]\right] \\ & \times \frac{P_J^{\max}\lambda_{JW}}{P_J^{\max}\lambda_{JW} + P\lambda_{SW}}\left[1 - \frac{P\lambda_{SW}}{P_J^{\max}\lambda_{JW}}\left[\ln\left(\frac{P_J^{\max}\lambda_{JW}}{P\lambda_{SW}} + 1\right) - \frac{P_J^{\max}\lambda_{JW}}{P_J^{\max}\lambda_{JW} + P\lambda_{SW}}\right]\right]. \end{aligned} \tag{5.26}$$

5.2.3 TOP Analysis

Regarding the TOP performance in the scenario when all relays work under the HD mode, we have the following theorem.

Theorem V.2 *For the concerned system with K relays, target transmission rate r_t, transmit power P for S and R^{bt}, and transmit power P_J for J, its TOP p_{to}^{HD} under*

the relay selection (5.12) and (5.13) is evaluated as

$$p_{to}^{HD} = 1 - \left[1 - \prod_{k=1}^{K}(1 - e^{-\frac{\gamma_{th}^{HD}}{\gamma_{SR_k}}})\right]\left[1 - \prod_{k=1}^{K}(1 - e^{-\frac{\gamma_{th}^{HD}}{\gamma_{R_kD}}})\right], \tag{5.27}$$

where $\gamma_{th}^{HD} = 2^{2r_t} - 1$.

Proof 9 *When we apply (5.12) and (5.13) to select the optimal relay* R^{br} *and* R^{bt} *in the concerned HD relay system, the capacity* C_{HD} *from* S *to* D *is determined as*

$$C_{HD} = \frac{1}{2}\log_2(1 + \min\{\gamma_{SR^{br}}, \gamma_{R^{bt}D}\}). \tag{5.28}$$

Based on (5.10) and (5.28), the p_{to}^{HD} *can be formulated as*

$$p_{to}^{HD} = \mathbb{P}\left\{\min\{\gamma_{SR^{br}}, \gamma_{R^{bt}D}\} < \gamma_{th}^{HD}\right\}. \tag{5.29}$$

Thus, the p_{to}^{HD} *can be determined as*

$$\begin{aligned}
p_{to}^{HD} &= 1 - \left[1 - \mathbb{P}\{\gamma_{SR^{br}} < \gamma_{th}^{HD}\}\right]\left[1 - \mathbb{P}\{\gamma_{R^{bt}D} < \gamma_{th}^{HD}\}\right] \\
&= 1 - \left[1 - \prod_{k=1}^{K}\mathbb{P}\{\gamma_{SR_k} < \gamma_{th}^{HD}\}\right]\left[1 - \prod_{k=1}^{K}\mathbb{P}\{\gamma_{R_kD} < \gamma_{th}^{HD}\}\right] \\
&= 1 - \left[1 - \prod_{k=1}^{K}\int_0^{\gamma_{th}^{HD}} f_{\gamma_{SR_k}}(x)dx\right]\left[1 - \prod_{k=1}^{K}\int_0^{\gamma_{th}^{HD}} f_{\gamma_{R_kD}}(y)dy\right] \\
&= 1 - \left[1 - \prod_{k=1}^{K}(1 - e^{-\frac{\gamma_{th}^{HD}}{\gamma_{SR_k}}})\right]\left[1 - \prod_{k=1}^{K}(1 - e^{-\frac{\gamma_{th}^{HD}}{\gamma_{R_kD}}})\right],
\end{aligned} \tag{5.30}$$

where $f_{\gamma_{SR_k}}(\cdot)$ *and* $f_{\gamma_{R_kD}}(\cdot)$ *denote the PDF of the random variables* γ_{SR_k} *and* γ_{R_kD}*, respectively.* $\gamma_{SR_k} = \frac{P\lambda_{SR_k}}{\sigma_{R_k}^2}$ *and* $\gamma_{R_kD} = \frac{P\lambda_{R_kD}}{\sigma_D^2}$*. Finally, we can complete the proof.*

5.2.4 MCT Analysis

We use T_H^* to denote the MCT in the concerned scenario. From (5.11) we can see that T_H^* is related to $\bar{\xi}_{HD}^*$ and p_{to}^{HD}, while $\bar{\xi}_{HD}^*$ is a function of P and P_J and p_{to}^{HD} is a function of P and r_t. Based on the above analysis, we devise the following Algorithm 5 for solving the optimization problem (5.11) and the evaluation of T_H^*.

Algorithm 5: Maximum Covert Throughput Searching Algorithm

Input: Maximum transmit power $P^{\max}$, maximum jamming power $P_J^{\max}$, covert requirement ϵ;

Output: Maximum covert throughput T_H^*, the corresponding optimal transmit power P^*, optimal jamming power P_J^* and optimal target transmission rate r_t^*;

Initialize $r_t = 0$, $T_H^1(P^*, r_t) = T_H^0(P^*, r_t) = 0$ and $\epsilon = 0.1$;
Set the length L for r_t, the iteration index $m = 0$ and the maximum number of iterations $m^{\max}$;
Calculate $\bar{\xi}_{HD}^{*,-1}(\epsilon, P_J^{\max})$ according to (5.26);
if $\bar{\xi}_{HD}^{*,-1}(\epsilon, P_J^{\max}) \leq P^{\max}$ **then**
    $P^* = \bar{\xi}_{HD}^{*,-1}(\epsilon, P_J^{\max})$;
else
    $P^* = P^{\max}$;
end
for $m = 2$; $T_H^{m-1}(P^*, r_t) \geq T_H^{m-2}(P^*, r_t)$ and $m \leq m^{\max}$; $m++$ **do**
    $r_t = r_t + L$;
    Calculate $T_H^m(P^*, r_t)$ by substituting (4.28) into $r_t(1 - p_{to}^{HD})$;
end
Obtain the $T_H^* = T_H^{m-2}(P^*, r_t)$ and $r_t^* = T_H^{*,-1}(P^*)$;
return T_H^*, P^*, P_J^* and r_t^*;

5.3 Covert Performance under FD Mode

This section deals with the relay selection and related performance analysis in terms of DEP, TOP and MCT in the scenario when all relays work under the FD mode.

5.3.1 Relay Selection Scheme

When all relays equipped with buffers, the selected relay for receiving the signal from S and the selected relay for transmitting the signal to D can be different. When all relays work under the FD mode, the transmission from S to D needs one time slot, and we need to take into account the self-interference issue in the relay selection. We consider the relay selection scheme where the relay with the best $S-R$ link for reception and the relay with the best $R-D$ link for transmission. We use $\gamma_{R_kR_k}$ to denote the SNR for the R_k. Thus, the best relay R^{br} for reception and the best relay R^{bt} for transmission in this scenario can be determined as

$$R^{br} = \arg \max_{R_k \in \{R_1,\ldots,R_K\}} \left\{ \frac{\gamma_{SR_k}}{\gamma_{R_kR_k}+1} \right\}, \tag{5.31}$$

$$R^{bt} = \arg \max_{R_k \in \{R_1,\ldots,R_K\}} \left\{ \gamma_{R_kD} \right\}. \tag{5.32}$$

5.3.2 DEP Analysis

We can see from (5.5) and (5.8) that under hypothesis $\mathcal{H}_0$, the received signals at W are the same for both FD and HD modes, so the probability of FA here is the same as that in (5.15). On the other hand, the probability of MD in the system can be determined as

$$\begin{aligned} p_{MD} &= \mathbb{P}\{(P|h_{SW}|^2 + P|h_{R^{bt}W}|^2 + P_J|h_{JW}|^2 + \sigma_W^2) < \tau \,|\, \mathcal{H}_1\} \\ &= \begin{cases} 0, & \tau \le \rho_6, \\ \frac{\tau-\rho_6}{P_J^{\max}|h_{JW}|^2}, & \rho_6 < \tau \le \rho_6 + P_J^{\max}|h_{JW}|^2, \\ 1, & \tau > \rho_6 + P_J^{\max}|h_{JW}|^2. \end{cases} \end{aligned} \tag{5.33}$$

where $\rho_6 = P|h_{SW}|^2 + P|h_{R^{bt}W}|^2 + \sigma_W^2$.

By substituting $p_{FA}^{(1)}$ in (5.15) and $p_{MD}^{(1)}$ in (5.33) into (5.9), we can obtain the DEP ξ_{FD}. We note that the value of ρ_1 in $p_{FA}^{(1)}$ and ρ_6 in p_{MD} brings two cases (i.e., $\rho_1 < \rho_6$ and $\rho_6 \geq \rho_1$) to determine the ξ_{FD}. When $\rho_1 < \rho_6$, the ξ_{FD} is determined as

$$\xi_{FD} = \begin{cases} 1, & \tau \leq \sigma_W^2, \\ 1 - \frac{\tau - \sigma_W^2}{P_J^{\max}|h_{JW}|^2}, & \sigma_W^2 < \tau \leq \rho_1, \\ 0, & \rho_1 < \tau \leq \rho_6, \\ \frac{\tau - \rho_6}{P_J^{\max}|h_{JW}|^2}, & \rho_6 < \tau \leq \rho_6 + P_J^{\max}|h_{JW}|^2, \\ 1, & \tau > \rho_6 + P_J^{\max}|h_{JW}|^2. \end{cases} \tag{5.34}$$

We can see from (5.34) that as τ increases, ξ_{FD} decreases when $\tau \in (\sigma_W^2, \rho_1]$ and ξ_{FD} increases when $\tau \in (\rho_6, \rho_6 + P_J^{\max}|h_{JW}|^2]$. Thus, the minimum DEP $\xi_{FD}^* = 0$ with the optimal detection threshold $\tau^* \in [\rho_1, \rho_6]$. When $\rho_1 \geq \rho_6$, the ξ_{FD} is determined as

$$\xi_{FD} = \begin{cases} 1, & \tau \leq \sigma_W^2, \\ 1 - \frac{\tau - \sigma_W^2}{P_J^{\max}|h_{JW}|^2}, & \sigma_W^2 < \tau \leq \rho_6, \\ 1 - \frac{\rho_6 - \sigma_W^2}{P_J^{\max}|h_{JW}|^2}, & \rho_6 < \tau \leq \rho_1, \\ \frac{\tau - \rho_6}{P_J^{\max}|h_{JW}|^2}, & \rho_1 < \tau \leq \rho_6 + P_J^{\max}|h_{JW}|^2, \\ 1, & \tau > \rho_6 + P_J^{\max}|h_{JW}|^2. \end{cases} \tag{5.35}$$

Following (5.35), we note that when $\tau \in (\sigma_W^2, \rho_6]$, ξ_{FD} decreases with τ and when $\tau \in (\rho_1, \rho_6 + P_J^{\max}|h_{JW}|^2]$, ξ_{FD} increases with τ. Thus, the minimum DEP $\xi_{FD}^* = 1 - \frac{\rho_6 - \sigma_W^2}{P_J^{\max}|h_{JW}|^2}$ with $\tau^* \in [\rho_6, \rho_1]$. Then, the minimum DEP in the first time slot is

given by

$$\xi_{FD}^{*}=\begin{cases}0, & \rho_1<\rho_6,\\ 1-\frac{\rho_6-\sigma_W^2}{P_J^{\max}|h_{JW}|^2}, & \rho_1\geq\rho_6.\end{cases} \tag{5.36}$$

Since S, R^{bt} and J do not know the instantaneous channel coefficient h_{SW}, $h_{R^{bt}W}$ and h_{JW}, we consider the expected value of minimum DEP at W. Let $\bar{\xi}_{FD}^{*}$ denote the average minimum DEP, which is given in the following theorem.

Theorem V.3 *Consider the covert communication in an FD relay system with transmit power P for S and R^{br}, transmit power P_J for J. If we denote the variance of the channel coefficients h_{SW}, $h_{R^{br}W}$ and h_{JW} as λ_{SW},$\lambda_{R^{br}W}$ and λ_{JW}, respectively, then the minimum DEP $\bar{\xi}_{FD}^{*}$ in the first time slot is determined as*

$$\bar{\xi}_{FD}^{*}=\frac{(P_J^{\max}\lambda_{JW})^2}{(P_J^{\max}\lambda_{JW}+P\lambda_{SW})(P_J^{\max}\lambda_{JW}+P\lambda_{R^{bt}W})}\left[1-\frac{1}{P_J^{\max}\lambda_{JW}(\lambda_{SW}-\lambda_{RW})}\right.$$
$$\left.\left[P\lambda_{SW}^2\ln(1+\frac{P_J^{\max}\lambda_{JW}}{P\lambda_{SW}})-\int_0^{\infty}\frac{P\lambda_{RW}^2}{y}e^{-\frac{1}{\lambda_{JW}}y}dy-\frac{P_J^{\max}\lambda_{JW}P\lambda_{SW}^2}{(P_J^{\max}\lambda_{JW}+P\lambda_{SW})}\right]\right] \tag{5.37}$$

Proof 10 *We know that $|h_{SW}|^2$ and $|h_{JW}|^2$ follow exponential distributions with expected values λ_{SW} and λ_{JW}. Based on (5.19), we have*

$$\begin{aligned}\bar{\xi}_{FD}^{*}&=\mathbb{E}[\xi_{FD}^{*}]\\ &=\mathbb{P}\{\rho_1<\rho_6\}\mathbb{E}[0|\rho_1<\rho_6]+\mathbb{P}\{\rho_1\geq\rho_6\}\mathbb{E}\left[1-\frac{\rho_6-\sigma_W^2}{P_J^{\max}|h_{JW}|^2}|\rho_1\geq\rho_6\right]\\ &=\mathbb{P}\{\rho_1\geq\rho_6\}\mathbb{E}\left[1-\frac{\rho_6-\sigma_W^2}{P_J^{\max}|h_{JW}|^2}|\rho_1\geq\rho_6\right],\end{aligned} \tag{5.38}$$

where

$$\begin{aligned}\mathbb{P}\{\rho_1 \geq \rho_6\} &= \mathbb{P}\{P_J^{\max}|h_{JW}|^2 \geq P|h_{SW}|^2 + P|h_{R^{bt}W}|^2\} \\ &= \int_0^\infty \int_0^\infty \int_0^{\frac{P_J^{\max} y - Pz}{P}} f_{|h_{SW}|^2}(x) f_{|h_{JW}|^2}(y) f_{|h_{R^{bt}W}|^2}(z) dxdydz \\ &= \frac{(P_J^{\max}\lambda_{JW})^2}{(P_J^{\max}\lambda_{JW} + P\lambda_{SW})(P_J^{\max}\lambda_{JW} + P\lambda_{R^{bt}W})} \end{aligned} \tag{5.39}$$

and

$$\begin{aligned}&\mathbb{E}[1 - \frac{P|h_{SW}|^2 + P|h_{RW}|^2}{P_J^{\max}|h_{JW}|^2}|\rho_1 \geq \rho_6] \\ &= 1 - \mathbb{E}[\frac{P|h_{SW}|^2 + P|h_{RW}|^2}{P_J^{\max}|h_{JW}|^2}|\rho_1 \geq \rho_6] \\ &= 1 - \int_0^\infty \int_0^\infty \int_0^{\frac{P_J^{\max} y - Pz}{P}} \frac{Px + Pz}{P_J^{\max} y} f_{|h_{SW}|^2}(x) f_{|h_{RW}|^2}(z) f_{|h_{JW}|^2}(y) dxdzdy \\ &= 1 - \int_0^\infty \frac{1}{P_J^{\max} y} \left[P\lambda_{SW} + P\lambda_{RW} - \frac{(P_J^{\max} y + P\lambda_{SW})\lambda_{SW}}{\lambda_{SW} - \lambda_{RW}} e^{-\frac{P_J^{\max}}{P\lambda_{SW}} y} \right] \frac{1}{\lambda_{JW}} e^{-\frac{1}{\lambda_{JW}} y} dy \\ &= 1 - \frac{1}{P_J^{\max}\lambda_{JW}(\lambda_{SW} - \lambda_{RW})} \left[P\lambda_{SW}^2 \ln(1 + \frac{P_J^{\max}\lambda_{JW}}{P\lambda_{SW}}) - \int_0^\infty \frac{P\lambda_{RW}^2}{y} e^{-\frac{1}{\lambda_{JW}} y} dy \right. \\ &\qquad \left. - \frac{P_J^{\max}\lambda_{JW} P\lambda_{SW}^2}{(P_J^{\max}\lambda_{JW} + P\lambda_{SW})} \right]. \end{aligned} \tag{5.40}$$

Substituting (5.39) and (5.40) into (5.38), we can obtain (5.37).

5.3.3 TOP Analysis

About the TOP of the FD relay system, we have the following theorem.

Theorem V.4 *For the concerned system with K relays, target transmission rate r_t, transmit power P for S and R^{bt}, and transmit power P_J for J, its TOP p_{to}^{FD} under the relay selection (5.31) is evaluated as*

$$p_{to}^{FD} = 1 - \left[1 - \prod_{k=1}^{K} (1 - \frac{\gamma_{SR_k}}{\gamma_{th}^{FD}\gamma_{R_k R_k} + \gamma_{SR_k}} e^{-\frac{\gamma_{th}^{FD}}{\gamma_{SR_k}}}) \right] \left[1 - \prod_{k=1}^{K} (1 - e^{-\frac{\gamma_{th}^{FD}}{\gamma_{R_k D}}}) \right], \tag{5.41}$$

where $\gamma_{th}^{FD} = 2^{r_t} - 1$.

Proof 11 *When we apply (5.31) to select the optimal relay* R^* *in the concerned FD relay system, the capacity* C_{FD} *from* S *to* D *is determined as*

$$C_{FD} = \log_2(1 + \min\{\frac{\gamma_{SR^{br}}}{\gamma_{R^{br}R^{bt}} + 1}, \gamma_{R^{bt}D}\}). \tag{5.42}$$

Based on (5.10) and (5.42), the p_{to}^{FD} *can be formulated as*

$$p_{to}^{FD} = \mathbb{P}\left\{\min\{\frac{\gamma_{SR^{br}}}{\gamma_{R^{br}R^{bt}} + 1}, \gamma_{R^{bt}D}\} < \gamma_{th}^{FD}\right\}. \tag{5.43}$$

Thus, the p_{to}^{FD} *can be determined as*

$$\begin{aligned}
p_{to}^{FD} &= 1 - \left[1 - \mathbb{P}\{\frac{\gamma_{SR^{br}}}{\gamma_{R^{br}R^{bt}} + 1} < \gamma_{th}^{FD}\}\right]\left[1 - \mathbb{P}\{\gamma_{R^{bt}D} < \gamma_{th}^{FD}\}\right] \\
&= 1 - \left[1 - \prod_{k=1}^{K}\mathbb{P}\{\frac{\gamma_{SR_k}}{\gamma_{R_kR_k} + 1} < \gamma_{th}^{FD}\}\right]\left[1 - \prod_{k=1}^{K}\mathbb{P}\{\gamma_{R_kD} < \gamma_{th}^{FD}\}\right] \\
&= 1 - \left[1 - \prod_{k=1}^{K}\int_0^{\infty}\int_0^{\gamma_{th}^{FD}(s+1)} f_{\gamma_{SR_k}}(x) f_{\gamma_{R_kR_k}}(s) dx ds\right]\left[1 - \prod_{k=1}^{K}\int_0^{\gamma_{th}^{FD}} f_{\gamma_{R_kD}}(y) dy\right] \\
&= 1 - \left[1 - \prod_{k=1}^{K}(1 - \frac{\gamma_{SR_k}}{\gamma_{th}^{FD}\gamma_{R_kR_k} + \gamma_{SR_k}} e^{-\frac{\gamma_{th}^{FD}}{\gamma_{SR_k}}})\right]\left[1 - \prod_{k=1}^{K}(1 - e^{-\frac{\gamma_{th}^{FD}}{\gamma_{R_kD}}})\right],
\end{aligned} \tag{5.44}$$

where $f_{\gamma_{SR_k}}(\cdot)$ *and* $f_{\gamma_{R_kD}}(\cdot)$ *denote the PDF of the random variables* γ_{SR_k} *and* γ_{R_kD}*, respectively.* $\gamma_{SR_k} = \frac{P\lambda_{SR_k}}{\sigma_{R_k}^2}$ *and* $\gamma_{R_kD} = \frac{P\lambda_{R_kD}}{\sigma_D^2}$. $f_{\gamma_{R_kR_k}}(\cdot)$ *denotes the PDF of the random variable* $\gamma_{R_kR_k} = \frac{P\lambda_{R_kR_k}}{\sigma_{R_k}^2}$. *We then obtain the (5.41).*

5.3.4 MCT Analysis

We use T_F^* to denote the MCT in the concerned scenario. Based on the above analysis, we can identify P^* and P_J^* by substituting $\bar{\xi}_{FD}^*$ (5.37) into the steps 3-5 in Algorithm 5 and identify r_t^* by substituting $T_F = r_t(1 - p_{to}^{FD})$ into the steps 9-13 in Algorithm 5, then we complete the optimization problem (5.11) and the evaluation

of T_F^*.

5.4 Joint Mode/Relay Selection

This section focuses on the hybrid HD/FD mode scenario where relay can flexibly switch between the HD and FD modes, and presents the related optimal relay selection and performance analysis in terms of DEP, TOP and MCT.

5.4.1 Joint Mode/Relay Selection Scheme

Under the hybrid HD/FD mode, we need to jointly select the optimal relay combination $R_{k_1K_2}$ and its optimal mode M^* for signal forwarding. Based on the same principle of optimal relay in both HD and FD modes, the joint relay and mode selection can be determined as

$$(R^{br,*}, R^{bt,*}, M^*) = \arg \max_{R^{br}R^{bt} \in \{R_1,\ldots,R_K\}} \arg \max_{M \in \{HD,FD\}} \left\{ C^{HD}_{R^{br}R^{bt}}, C^{FD}_{R^{br}R^{bt}} \right\}. \quad (5.45)$$

5.4.2 DEP Analysis

To ensure the covertness under the hybrid HD/FD mode, we consider the optimal DEP as the minimum one between the minimum DEP in the HD and the minimum DEP in the FD mode. Thus, the minimum DEP $\xi_{H.F}$ under the hybrid HD/FD mode is determined as

$$\bar{\xi}^*_{H.F} = \min\{\bar{\xi}^*_{HD}, \bar{\xi}^*_{FD}\} \quad (5.46)$$

5.4.3 TOP Analysis

Regarding the TOP under the hybrid HD/FD mode, we have the following theorem.

Theorem V.5 *For the concerned system with K relays, target transmission rate r_t, transmit power P for S and R^{rt}, and transmit power P_J for J, its TOP $p_{to}^{H.F}$ under the relay selection (5.45) can be evaluated as*

$$p_{to}^{H.F} = \prod_{k=1}^{K^2}(1 - e^{-\frac{\gamma_{th}^{HD}}{\gamma_{SR_k}}} e^{-\frac{\gamma_{th}^{HD}}{\gamma_{R_kD}}})(1 - \frac{\gamma_{SR_k}}{\gamma_{th}^{FD}\gamma_{R_kR_k} + \gamma_{SR_k}} e^{-\frac{\gamma_{th}^{FD}}{\gamma_{SR_k}}} e^{-\frac{\gamma_{th}^{FD}}{\gamma_{R_kD}}}). \tag{5.47}$$

Proof 12 *Based on (5.10) and (5.45), the $p_{to}^{H.F}$ under the joint HD/FD mode can be given by*

$$p_{to}^{H.F} = \prod_{k=1}^{K^2} \mathbb{P}\left\{\max\left\{C_{R^{br}R^{bt}}^{HD}, C_{R^{br}R^{bt}}^{FD}\right\} \leq r_t\right\}. \tag{5.48}$$

where

$$\begin{aligned}
&\mathbb{P}\left\{\max\left(C_{R^{br}R^{bt}}^{HD}, C_{R^{br}R^{bt}}^{FD}\right) \leq r_t\right\} \\
=&\mathbb{P}\left\{\max\left(\frac{1}{2}\log_2(1+\min\{\gamma_{SR^{br}}, \gamma_{R^{bt}D}\}), \log_2(1+\min\{\frac{\gamma_{SR^{br}}}{\gamma_{R^{br}R^{bt}}+1}, \gamma_{R^{bt}D}\})\right) \leq r_t\right\}, \\
=&\mathbb{P}\left\{\max\left(\sqrt{1+\min\{\gamma_{SR^{br}}, \gamma_{R^{bt}D}\}}, 1+\min\{\frac{\gamma_{SR^{br}}}{\gamma_{R^{br}R^{bt}}+1}, \gamma_{R^{bt}D}\}\right) \leq 2^{r_t}\right\}, \\
=&\mathbb{P}\left\{\min\{\gamma_{SR^{br}}, \gamma_{R^{bt}D}\} \leq \gamma_{th}^{HD}, \min\{\frac{\gamma_{SR^{br}}}{\gamma_{R^{br}R^{bt}}+1}, \gamma_{R^{bt}D}\} \leq \gamma_{th}^{FD}\right\}, \\
=&(1 - e^{-\frac{\gamma_{th}^{HD}}{\gamma_{SR_k}}} e^{-\frac{\gamma_{th}^{HD}}{\gamma_{R_kD}}})(1 - \frac{\gamma_{SR_k}}{\gamma_{th}^{FD}\gamma_{R_kR_k} + \gamma_{SR_k}} e^{-\frac{\gamma_{th}^{FD}}{\gamma_{SR_k}}} e^{-\frac{\gamma_{th}^{FD}}{\gamma_{R_kD}}}).
\end{aligned} \tag{5.49}$$

By substituting $\mathbb{P}\left\{\max\left(C_{R^{br}R^{bt}}^{HD}, C_{R^{br}R^{bt}}^{FD}\right) \leq r_t\right\}$ in (5.49) into $p_{to}^{H.F}$ in (5.48), we complete the proof.

5.4.4 MCT Analysis

To identify the optimal transmit power P^*, optimal jamming power P_J^* and optimal target transmission rate r_t^*, the optimization problem on $T_{H.F}^*$ involves two sub-optimization problems. According to (5.46), the minimum DEP of the wireless

relay system with hybrid HD/FD mode is the minimum of $\bar{\xi}^*_{HD}$ and $\bar{\xi}^*_{FD}$. Therefore, the P^* and P^*_J are determined using steps 3-8 in Algorithm 5. We then analyze the monotonicity of the $p_{to}^{H.F}$ in (5.47) with respect of r_t. We note that the expression in (5.47) is too complex to obtain the closed-form solutions. Hence, we can solve this optimization problem by substituting $T_{H.F} = r_t(1 - p_{to}^{H.F})$ into the steps 9-13 in Algorithm 5.

5.5 Numerical Results

This section provides extensive numerical results to validate our theoretical models as well as to illustrate the impacts of system parameters on DEP ξ, TOP p_{to}, and MCT T^*. Unless otherwise stated, in the numerical results, the related parameters are set as $P^{\max} = 2$W, $P_J^{\max} = 20$W, $\sigma_R^2 = \sigma_D^2 = \sigma_W^2 = 10^{-4}$W, $\lambda_{AB} = 1$.

5.5.1 DEP Performance

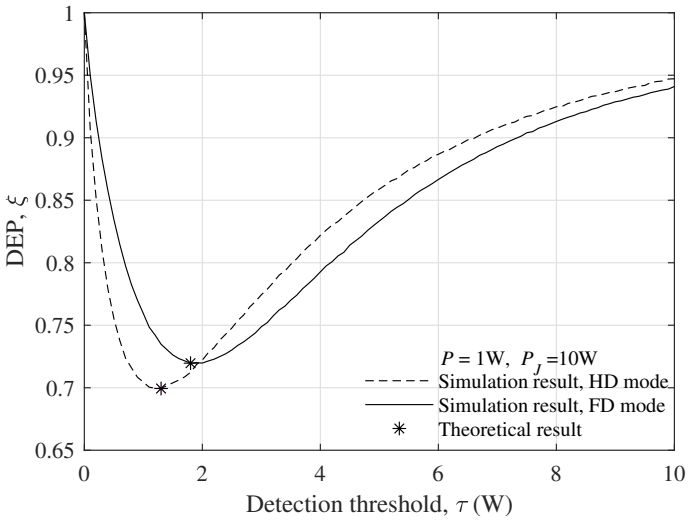

Figure 5.2: DEP ξ vs. detection threshold τ.

We can see from (5.46) the DEP for the hybrid HD/FD mode is determined by the minimum of the DEPs in the HD and FD modes, so we show in Fig. 5.2 the

simulation and theoretical results for ξ vs. τ under HD and FD modes to validate our theoretical models on DEP. We can observe from Fig. 5.2 that the simulation results match well with the results evaluated by the proposed theoretical models, indicating that our theoretical models can accurately depict the DEP performance of the concerned system. We can find that for fixed mode, as τ increases, ξ first decreases and then increases, and an optimal τ exists that leads to the minimum ξ. The results can be explained as follows. Note that ξ in (5.9) is the sum of p_{FA} and p_{MD}, where p_{FA} decreases with the increase of τ while p_{MD} increases with the increase of τ. Thus, as τ is relatively small, the p_{FA} dominates ξ, leading to the decrease of ξ with τ. However, as τ further increases, the p_{MD} dominates ξ, leading to the increase of ξ.

5.5.2 TOP Performance

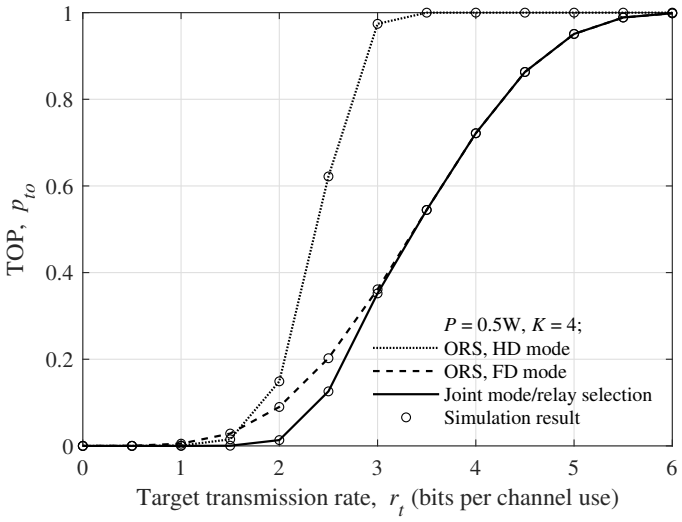

Figure 5.3: TOP p_{to} vs. target transmission rate r_t.

We show in Fig. 5.3 both the theoretical and simulation results for TOP p_{to} vs. target transmission rate r_t under the settings of $P = 0.5$W and $K = 4$. From Fig. 5.3, we can see that the simulation results agree well with the theoretical ones, so our

theoretical models can accurately describe the TOP performance of the concerned system. We can also observe from Fig. 5.3 that p_{to} increases as r_t increases. The reason is that when r_t becomes larger, D cannot decode all the received signals reliably, leading to an increased p_{to}. From Fig. 5.3 we can further observe that p_{to}^{HD} is less than p_{to}^{FD} when r_t is relatively small, but when r_t increases beyond a threshold, then p_{to}^{HD} becomes greater than p_{to}^{FD}. This is because when the instantaneous channel capacity between S and D is relatively small, the capacity reduction from the self-interference in the FD mode becomes significant, leading to a higher TOP in the FD mode than that in the HD mode. However, when the instantaneous channel capacity between S and D is relatively large, the impact of the self-interference on the capacity in the FD mode is less significant, so the overall capacity between S and D in the FD mode will be larger than that in the HD mode, resulting in $p_{to}^{FD} < p_{to}^{HD}$.

5.5.3 MCT Performance

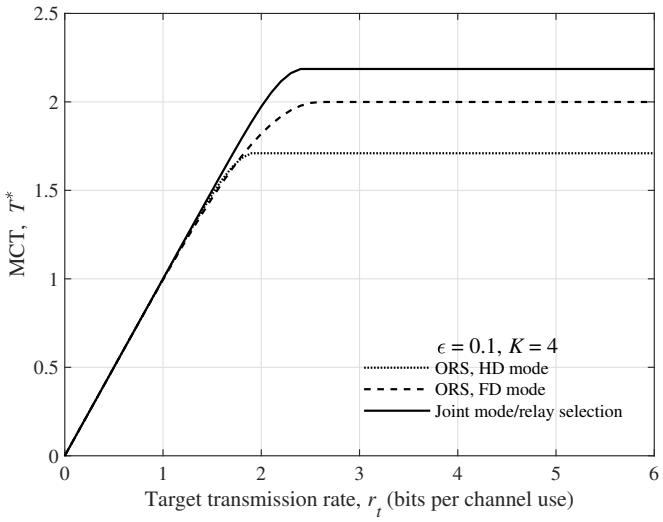

Figure 5.4: MCT T^* vs. target transmission rate r_t.

Fig. 5.4 illustrates the impact of r_t on MCT T^* under the settings of $\epsilon = 0.1$ and $K = 4$. We can see from Fig. 5.4 that as r_t increases, T^* first increases and then

remains unchanged. This is due to the fact that the effects of r_t on T^* in (5.11) are two-fold. When r_t is in the region smaller than the channel capacity, there will be no transmission outage event and T^* increases as r_t increases. However, when r_t increases to be in the region larger than the channel capacity, p_{to} increases as r_t increases, leading to a lower $r_t(1 - p_{to})$. We can also see from Fig. 5.4 that there for each scenario, there exists an optimal setting of r_t to achieve T^*, beyond which T^* cannot be further improved. Again, the results in Fig. 5.4 indicate clearly that compared to the ORS under fixed HD mode or FD mode, joint mode/relay selection can lead to a significant improvement in MCT.

5.6 Summary

This chapter investigated the relay selection under fixed HD or FD mode, and further the joint mode/relay selection in a DF wireless system with multiple buffer-aided relays. The related performance modeling and optimal parameter setting issues are addressed as well. Our results in this chapter indicate although the covert relay communication performance in the system can be significantly improved by applying the optimal relay selection under fixed HD or FD mode, such improvement can be further enhanced from the joint mode/relay selection. It is expected this work can shed lights on the performance enhancement for covert relay communication in wireless systems.

CHAPTER VI

Conclusion

In this thesis, we explored the joint transmission/forwarding mode selection and joint mode/relay selection for efficient covert relay communication in wireless systems. We first studied the mode selection issue for covert relay communication in a single-relay system. We then explored the joint mode/relay selection for covert relay communication in a multi-relay system with AF forwarding mode. Finally, we extended our investigation to the joint mode/relay selection for covert relay communication in a buffer-aided multi-relay system with DF forwarding mode.

In Chapter III, we studied the performance and the joint transmission/forwarding mode selection for covert relay communication in a single-relay system consisting of a source, a relay, a destination and a warden, where the relay can flexibly select between the transmission modes of FD/HD as well as between the forwarding modes of AF/DF. We first developed theoretical models to show the system covert throughput performance under different combinations between transmission modes of FD/HD and forwarding modes of AF/DF. Based on these models, we further proposed a joint transmission/forwarding mode selection scheme to achieve the maximal CT among all mode combinations in the system. The main results in Chapter III showed that different mode combinations behave quite differently with the variation of system settings. For a given system setting mainly determined by target transmission rate,

self-interference coefficient of FD, constraints of DEP and upper bound on relay transmit power, we can always identify the best combination of transmission modes and forwarding modes to achieve the maximal CT in the system.

In Chapter IV, we explored the joint mode/relay selection scheme for covert relay communication in a multi-relay system consisting of one source, multiple relays, one destination, one friendly jammer and one warden, where each relay with AF forwarding mode can switch between the HD and FD transmission modes. We developed the corresponding relay selection schemes for covert relay communication in the system when all relays work in either fixed HD or FD mode, and then developed a joint transmission mode/relay selection scheme when each relay works in the hybrid HD/FD transmission mode. Under either scheme, we developed related theoretical models for performance analysis and optimization. The main results in Chapter IV indicated that although the covert relay communication performance in the system can be significantly improved by applying relay selection under fixed HD or FD mode, such improvement can be further enhanced from joint mode/relay selection.

In Chapter V, we extended the joint mode/relay selection investigation to a buffer-aided multi-relay system with DF forwarding mode, where each relay is equipped with an infinite buffer. We developed the corresponding relay selection schemes for covert relay communication in the system when all relays work in either the fixed HD or FD mode, and then developed a joint transmission mode/relay selection scheme when each relay work in the hybrid HD/FD transmission mode. Under either scheme, we developed related theoretical models for performance analysis and optimization. The main results in Chapter V demonstrated that covert relay communication performance in the system can be significantly improved by applying the joint mode/relay selection.

It is notable that this thesis focuses on simplified wireless systems. However, in practical applications, many factors can influence the performance of covert com-

munications in these systems. Therefore, an interesting and important direction for future research is to investigate covert performance under more complex system models, such as those involving multi-antenna nodes, relays with finite buffers and highly variable channels. In the end, we expect that the work of this thesis can shed light on performance enhancement in future covert wireless communications.

BIBLIOGRAPHY

BIBLIOGRAPHY

[1] N. Langhammer and R. Kays, "Performance evaluation of wireless home automation networks in indoor scenarios," *IEEE Transactions on Smart Grid*, vol. 3, no. 4, pp. 2252–2261, Dec. 2012.

[2] Y. Chu and A. Ganz, "WISTA: A wireless telemedicine system for disaster patient care," *Mobile Networks and Applications*, vol. 12, pp. 201–214, Jul. 2007.

[3] Y. Zou, J. Zhu, X. Wang, and L. Hanzo, "A survey on wireless security: Technical challenges, recent advances, and future trends," *Proceedings of the IEEE*, vol. 104, no. 9, pp. 1727–1765, Sep. 2016.

[4] Z. A. Najar and R. N. Mir, "Wi-Fi: WPA2 security vulnerability and solutions," *Wireless Engineering and Technology*, vol. 12, no. 2, pp. 15–22, Apr. 2021.

[5] H. C. Van Tilborg and S. Jajodia, *Encyclopedia of cryptography and security*. Springer Science & Business Media, 2014.

[6] R. Qazi, K. N. Qureshi, F. Bashir, N. U. Islam, S. Iqbal, and A. Arshad, "Security protocol using elliptic curve cryptography algorithm for wireless sensor networks," *Journal of Ambient Intelligence and Humanized Computing*, vol. 12, pp. 547–566, Jan. 2021.

[7] G. Chen, Y. Gong, P. Xiao, and J. A. Chambers, "Physical layer network security in the full-duplex relay system," *IEEE Transactions on Information Forensics and Security*, vol. 10, no. 3, pp. 574–583, Mar. 2015.

[8] Z. Xiang, W. Yang, G. Pan, Y. Cai, and Y. Song, "Physical layer security in cognitive radio inspired NOMA network," *IEEE Journal of Selected Topics in Signal Processing*, vol. 13, no. 3, pp. 700–714, Feb. 2019.

[9] M. Ragheb, S. M. S. Hemami, A. Kuhestani, D. W. K. Ng, and L. Hanzo, "On the physical layer security of untrusted millimeter wave relaying networks: A stochastic geometry approach," *IEEE Transactions on Information Forensics and Security*, vol. 17, pp. 53–68, Nov. 2021.

[10] B. A. Bash, D. Goeckel, and D. Towsley, "Limits of reliable communication with low probability of detection on AWGN channels," *IEEE Journal on Selected Areas in Communications*, vol. 31, no. 9, pp. 1921–1930, Sep. 2013.

[11] B. He, S. Yan, X. Zhou, and H. Jafarkhani, "Covert wireless communication with a Poisson field of interferers," *IEEE Transactions on Wireless Communications*, vol. 17, no. 9, pp. 6005–6017, Sep. 2018.

[12] J. Hu, S. Yan, X. Zhou, F. Shu, and J. Wang, "Covert communications without channel state information at receiver in IoT systems," *IEEE Internet of Things Journal*, vol. 7, no. 11, pp. 11 103–11 114, Nov. 2020.

[13] C. Gao, B. Yang, X. Jiang, H. Inamura, and M. Fukushi, "Covert communication in relay-assisted IoT systems," *IEEE Internet of Things Journal*, vol. 8, no. 8, pp. 6313–6323, Apr. 2021.

[14] Y. Jiang, L. Wang, and H.-H. Chen, "Covert communications in D2D underlaying cellular networks with antenna array assisted artificial noise transmission," *IEEE Transactions on Vehicular Technology*, vol. 69, no. 3, pp. 2980–2992, Mar. 2020.

[15] B. Yang, T. Taleb, Y. Fan, and S. Shen, "Mode selection and cooperative jamming for covert communication in D2D underlaid UAV networks," *IEEE Network*, vol. 35, no. 2, pp. 104–111, Mar. 2021.

[16] S. Feng, X. Lu, S. Sun, D. Niyato, and E. Hossain, "Securing large-scale D2D networks using covert communication and friendly jamming," *IEEE Transactions on Wireless Communications*, vol. 23, no. 1, pp. 592–606, Jan. 2024.

[17] H.-M. Wang, Y. Zhang, X. Zhang, and Z. Li, "Secrecy and covert communications against UAV surveillance via multi-hop networks," *IEEE Transactions on Communications*, vol. 68, no. 1, pp. 389–401, Jan. 2020.

[18] X. Chen, M. Sheng, N. Zhao, W. Xu, and D. Niyato, "UAV-relayed covert communication towards a flying warden," *IEEE Transactions on Communications*, vol. 69, no. 11, pp. 7659–7672, Nov. 2021.

[19] C. Wang, X. Chen, J. An, Z. Xiong, C. Xing, N. Zhao, and D. Niyato, "Covert communication assisted by UAV-IRS," *IEEE Transactions on Communications*, vol. 71, no. 1, pp. 357–369, Jan. 2023.

[20] R. Zhang, X. Chen, M. Liu, N. Zhao, X. Wang, and A. Nallanathan, "UAV relay assisted cooperative jamming for covert communications over Rician fading," *IEEE Transactions on Vehicular Technology*, vol. 71, no. 7, pp. 7936–7941, Jul. 2022.

[21] M. Lin, C. Liu, and W. Wang, "Relay-assisted uplink covert communication in the presence of multi-antenna warden and uninformed jamming," *IEEE Transactions on Communications*, vol. 72, no. 4, pp. 2124–2137, Apr. 2024.

[22] L. Lv, Z. Li, H. Ding, N. Al-Dhahir, and J. Chen, "Achieving covert wireless communication with a multi-antenna relay," *IEEE Transactions on Information Forensics and Security*, vol. 17, pp. 760–773, Feb. 2022.

[23] M. Li, X. Tao, H. Wu, and N. Li, "Joint trajectory and resource optimization for covert communication in UAV-enabled relaying systems," *IEEE Transactions on Vehicular Technology*, vol. 72, no. 4, pp. 5518–5523, Apr. 2023.

[24] L. Jiao, R. Zhang, M. Liu, Q. Hua, N. Zhao, A. Nallanathan, and X. Wang, "Placement optimization of UAV relaying for covert communication," *IEEE Transactions on Vehicular Technology*, vol. 71, no. 11, pp. 12 327–12 332, Nov. 2022.

[25] K. Shahzad, "Relaying via cooperative jamming in covert wireless communications," in *2018 12th International Conference on Signal Processing and Communication Systems (ICSPCS)*. IEEE, 2018, pp. 1–6.

[26] D. Deng, X. Li, S. Dang, M. C. Gursoy, and A. Nallanathan, "Covert communications in intelligent reflecting surface-assisted two-way relaying networks," *IEEE Transactions on Vehicular Technology*, vol. 71, no. 11, pp. 12 380–12 385, Nov. 2022.

[27] J. Hu, S. Yan, X. Zhou, F. Shu, J. Li, and J. Wang, "Covert communication achieved by a greedy relay in wireless networks," *IEEE Transactions on Wireless Communications*, vol. 17, no. 7, pp. 4766–4779, Jul. 2018.

[28] M. Forouzesh, P. Azmi, A. Kuhestani, and P. L. Yeoh, "Covert communication and secure transmission over untrusted relaying networks in the presence of multiple wardens," *IEEE Transactions on Communications*, vol. 68, no. 6, pp. 3737–3749, Jun. 2020.

[29] J. Bai, J. He, Y. Chen, Y. Shen, and X. Jiang, "On covert communication performance with outdated CSI in wireless greedy relay systems," *IEEE Transactions on Information Forensics and Security*, vol. 17, pp. 2920–2935, Aug. 2022.

[30] J. Wang, W. Tang, Q. Zhu, X. Li, H. Rao, and S. Li, "Covert communication with the help of relay and channel uncertainty," *IEEE Wireless Communications Letters*, vol. 8, no. 1, pp. 317–320, Feb. 2019.

[31] Y. Su, H. Sun, Z. Zhang, Z. Lian, Z. Xie, and Y. Wang, "Covert communication with relay selection," *IEEE Wireless Communications Letters*, vol. 10, no. 2, pp. 421–425, Feb. 2021.

[32] J. Jiang, W. Yang, and R. Ma, "Joint relay and jammer selection for covert communication," in *2021 7th International Conference on Computer and Communications (ICCC)*. IEEE, 2021, pp. 131–135.

[33] C. Gao, B. Yang, D. Zheng, X. Jiang, and T. Taleb, "Cooperative jamming and relay selection for covert communications in wireless relay systems," *IEEE Transactions on Communications*, vol. 72, no. 2, pp. 1020–1032, Feb. 2024.

[34] R. Sun, B. Yang, S. Ma, Y. Shen, and X. Jiang, "Covert rate maximization in wireless full-duplex relaying systems with power control," *IEEE Transactions on Communications*, vol. 69, no. 9, pp. 6198–6212, Sep. 2021.

[35] L. Yang, W. Yang, L. Tang, L. Tao, X. Lu, and Z. He, "Covert communication for wireless networks with full-duplex multiantenna relay," *Complexity*, vol. 2022, no. 1, pp. 1–24, Jan. 2022.

[36] H. Wu, Y. Zhang, X. Liao, Y. Shen, and X. Jiang, "On covert throughput performance of two-way relay covert wireless communications," *Wireless Networks*, vol. 26, pp. 3275–3289, Jan. 2020.

[37] T. Riihonen, S. Werner, R. Wichman, and E. B. Zacarias, "On the feasibility of full-duplex relaying in the presence of loop interference," in *2009 IEEE 10th Workshop on Signal Processing Advances in Wireless Communications (SPAWC)*. IEEE, 2009, pp. 275–279.

[38] B. Rankov and A. Wittneben, "Spectral efficient signaling for half-duplex relay channels," in *2005 39th Asilomar Conference on Signals, Systems and Computers (ACSSC)*. IEEE, 2005, pp. 1066–1071.

[39] W.-J. Huang, Y.-W. P. Hong, and C.-C. J. Kuo, "Lifetime maximization for amplify-and-forward cooperative networks," *IEEE Transactions on Wireless Communications*, vol. 7, no. 5, pp. 1800–1805, May. 2008.

[40] T. Wang, A. Cano, G. B. Giannakis, and J. N. Laneman, "High-performance cooperative demodulation with decode-and-forward relays," *IEEE Transactions on communications*, vol. 55, no. 7, pp. 1427–1438, Jul. 2007.

[41] M. Wang, Z. Xu, B. Xia, Y. Guo, and Z. Chen, "DF relay assisted covert communications: Analysis and optimization," *IEEE Transactions on Vehicular Technology*, vol. 72, no. 3, pp. 4073–4078, Mar. 2023.

[42] J. Hu, S. Yan, F. Shu, and J. Wang, "Covert transmission with a self-sustained relay," *IEEE Transactions on Wireless Communications*, vol. 18, no. 8, pp. 4089–4102, Aug. 2019.

[43] R. Sun, B. Yang, Y. Shen, X. Jiang, and T. Taleb, "Covertness and secrecy study in untrusted relay-assisted D2D networks," *IEEE Internet of Things Journal*, vol. 10, no. 1, pp. 17–30, Jan. 2023.

[44] Y. Zou, X. Wang, and W. Shen, "Optimal relay selection for physical-layer security in cooperative wireless networks," *IEEE Journal on Selected Areas in Communications*, vol. 31, no. 10, pp. 2099–2111, Oct. 2013.

[45] P. H. Che, M. Bakshi, and S. Jaggi, "Reliable deniable communication: Hiding messages in noise," in *2013 IEEE International Symposium on Information Theory (ISIT)*. IEEE, 2013, pp. 2945–2949.

[46] L. Wang, G. W. Wornell, and L. Zheng, "Fundamental limits of communication with low probability of detection," *IEEE Transactions on Information Theory*, vol. 62, no. 6, pp. 3493–3503, Apr. 2016.

[47] K. S. K. Arumugam and M. R. Bloch, "Keyless covert communication over multiple-access channels," in *2016 IEEE International Symposium on Information Theory (ISIT)*. IEEE, 2016, pp. 2229–2233.

[48] B. A. Bash, D. Goeckel, and D. Towsley, "LPD communication when the warden does not know when," in *2014 IEEE International Symposium on Information Theory (ISIT)*. IEEE, 2014, pp. 606–610.

[49] B. A. Bash, D. Goeckel, and D. Towsley, "Covert communication gains from adversary's ignorance of transmission time," *IEEE Transactions on Wireless Communications*, vol. 15, no. 12, pp. 8394–8405, Sep. 2016.

[50] K. Shahzad, X. Zhou, and S. Yan, "Covert communication in fading channels under channel uncertainty," in *2017 IEEE 85th Vehicular Technology Conference (VTC Spring)*. IEEE, 2017, pp. 1–5.

[51] L. Sun, T. Xu, S. Yan, J. Hu, X. Yu, and F. Shu, "On resource allocation in covert wireless communication with channel estimation," *IEEE Transactions on Communications*, vol. 68, no. 10, pp. 6456–6469, Oct. 2020.

[52] K. Shahzad and X. Zhou, "Covert wireless communications under quasi-static fading with channel uncertainty," *IEEE Transactions on Information Forensics and Security*, vol. 16, pp. 1104–1116, Oct. 2020.

[53] Z. Cheng, J. Si, Z. Li, L. Guan, Y. Zhao, D. Wang, J. Cheng, and N. Al-Dhahir, "Covert surveillance via proactive eavesdropping under channel uncertainty," *IEEE Transactions on Communications*, vol. 69, no. 6, pp. 4024–4037, Mar. 2021.

[54] M. Forouzesh, P. Azmi, N. Mokari, and D. Goeckel, "Robust power allocation in covert communication: Imperfect CDI," *IEEE Transactions on Vehicular Technology*, vol. 70, no. 6, pp. 5789–5802, Jun. 2021.

[55] S. Lee, R. J. Baxley, M. A. Weitnauer, and B. Walkenhorst, "Achieving undetectable communication," *IEEE Journal of Selected Topics in Signal Processing*, vol. 9, no. 7, pp. 1195–1205, Apr. 2015.

[56] D. Goeckel, B. Bash, S. Guha, and D. Towsley, "Covert communications when the warden does not know the background noise power," *IEEE Communications Letters*, vol. 20, no. 2, pp. 236–239, Dce. 2015.

[57] B. He, S. Yan, X. Zhou, and V. K. Lau, "On covert communication with noise uncertainty," *IEEE Communications Letters*, vol. 21, no. 4, pp. 941–944, Jan. 2017.

[58] L. Tao, W. Yang, S. Yan, D. Wu, X. Guan, and D. Chen, "Covert communication in downlink NOMA systems with random transmit power," *IEEE Wireless Communications Letters*, vol. 9, no. 11, pp. 2000–2004, Nov. 2020.

[59] K. Li, P. A. Kelly, and D. Goeckel, "Optimal power adaptation in covert communication with an uninformed jammer," *IEEE Transactions on Wireless Communications*, vol. 19, no. 5, pp. 3463–3473, May. 2020.

[60] J. Hu, K. Shahzad, S. Yan, X. Zhou, F. Shu, and J. Li, "Covert communications with a full-duplex receiver over wireless fading channels," in *2018 IEEE International Conference on Communications (ICC)*. IEEE, 2018, pp. 1–6.

[61] K. Shahzad, X. Zhou, S. Yan, J. Hu, F. Shu, and J. Li, "Achieving covert wireless communications using a full-duplex receiver," *IEEE Transactions on Wireless Communications*, vol. 17, no. 12, pp. 8517–8530, Dec. 2018.

[62] X. Chen, W. Sun, C. Xing, N. Zhao, Y. Chen, F. R. Yu, and A. Nallanathan, "Multi-antenna covert communication via full-duplex jamming against a warden with uncertain locations," *IEEE Transactions on Wireless Communications*, vol. 20, no. 8, pp. 5467–5480, Aug. 2021.

[63] T. V. Sobers, B. A. Bash, S. Guha, D. Towsley, and D. Goeckel, "Covert communication in the presence of an uninformed jammer," *IEEE Transactions on Wireless Communications*, vol. 16, no. 9, pp. 6193–6206, Sep. 2017.

[64] R. Soltani, D. Goeckel, D. Towsley, B. A. Bash, and S. Guha, "Covert wireless communication with artificial noise generation," *IEEE Transactions on Wireless Communications*, vol. 17, no. 11, pp. 7252–7267, Aug. 2018.

[65] T.-X. Zheng, H.-M. Wang, D. W. K. Ng, and J. Yuan, "Multi-antenna covert communications in random wireless networks," *IEEE Transactions on Wireless Communications*, vol. 18, no. 3, pp. 1974–1987, Mar. 2019.

[66] K.-W. Huang, H. Deng, and H.-M. Wang, "Jamming aided covert communication with multiple receivers," *IEEE Transactions on Wireless Communications*, vol. 20, no. 7, pp. 4480–4494, Jul. 2021.

[67] M. Forouzesh, P. Azmi, A. Kuhestani, and P. L. Yeoh, "Joint information-theoretic secrecy and covert communication in the presence of an untrusted user and warden," *IEEE Internet of Things Journal*, vol. 8, no. 9, pp. 7170–7181, Nov. 2020.

[68] M. Forouzesh, F. S. Khodadad, P. Azmi, A. Kuhestani, and H. Ahmadi, "Simultaneous secure and covert transmissions against two attacks under practical assumptions," *IEEE Internet of Things Journal*, vol. 10, no. 12, pp. 10 160–10 171, Jun. 2023.

[69] H. Wu, Y. Zhang, Y. Shen, X. Jiang, and T. Taleb, "Achieving covertness and secrecy: The interplay between detection and eavesdropping attacks," *IEEE Internet of Things Journal*, vol. 11, no. 1, pp. 3233–3249, Jan. 2024.

[70] A. Browder, *Mathematical analysis: an introduction*. Springer Science & Business Media, 2012.

[71] T. Riihonen, S. Werner, and R. Wichman, "Hybrid full-duplex/half-duplex relaying with transmit power adaptation," *IEEE Transactions on Wireless Communications*, vol. 10, no. 9, pp. 3074–3085, Jul. 2011.

[72] I. S. Gradshteyn and I. M. Ryzhik, *Table of integrals, series, and products*. Academic press, 2014.

[73] Y. Ai, M. Cheffena, A. Mathur, and H. Lei, "On physical layer security of double Rayleigh fading channels for vehicular communications," *IEEE Wireless Communications Letters*, vol. 7, no. 6, pp. 1038–1041, Dec. 2018.

[74] Y. Zou, "Physical-layer security for spectrum sharing systems," *IEEE Transactions on Wireless Communications*, vol. 16, no. 2, pp. 1319–1329, Feb. 2017.

[75] B. Li, Y. Zou, J. Zhou, F. Wang, W. Cao, and Y.-D. Yao, "Secrecy outage probability analysis of friendly jammer selection aided multiuser scheduling for wireless networks," *IEEE Transactions on Communications*, vol. 67, no. 5, pp. 3482–3495, May. 2019.

[76] K. Cao, B. Wang, H. Ding, L. Lv, R. Dong, T. Cheng, and F. Gong, "Improving physical layer security of uplink NOMA via energy harvesting jammers," *IEEE Transactions on Information Forensics and Security*, vol. 16, pp. 786–799, Sep. 2020.

[77] S. S. Soliman and N. C. Beaulieu, "Exact analysis of dual-hop AF maximum end-to-end SNR relay selection," *IEEE Transactions on Communications*, vol. 60, no. 8, pp. 2135–2145, Aug. 2012.

[78] A. Papoulis and S. Unnikrishna Pillai, *Probability, random variables and stochastic processes*. McGraw-Hill, 2002.

[79] A. El Shafie, A. Sultan, and N. Al-Dhahir, "Physical-layer security of a buffer-aided full-duplex relaying system," *IEEE Communications Letters*, vol. 20, no. 9, pp. 1856–1859, Sep. 2016.

[80] J. He, J. Liu, W. Su, Y. Shen, X. Jiang, and N. Shiratori, "Jamming and link selection for joint secrecy/delay guarantees in buffer-aided relay system," *IEEE Transactions on Communications*, vol. 70, no. 8, pp. 5451–5468, Aug. 2022.

Publications

Jounal Articles

[1] Yan Liu, Huihui Wu and Xiaohong Jiang. "Joint Selection of FD/HD and AF/DF for Covert Communication in Two-Hop Relay Systems," *Ad Hoc Networks,* vol. 148, Sep. 2023.

[2] Yan Liu, Huihui Wu, Wei Su, Yulong Shen and Xiaohong Jiang. "Joint Relay and Mode Selection for Covert Communication in Wireless Relay Systems," *IEEE Transactions on Communications*, 2024. (Major Revision)

[3] Yan Liu, Huihui Wu, Wei Su, Yulong Shen and Xiaohong Jiang. "Buffer-Aided Relay Selection for Covert Communication in Wireless Relay Systems," 2024. (In preparation)

Conference Papers

[4] Yan Liu, Huihui Wu, Yulong Shen and Xiaohong Jiang. " Multi-antenna Covert Communications in Random Wireless Networks with Full-Duplex Relay," in Proceedings of the 37th ACM/SIGAPP Symposium on Applied Computing (SAC 2022), Prague City, Czechia, pp. 1960-1966, Apr. 2022.